ENGINEERING
LIBRARY
JUL 20 1948

NUCLEONICS

AN INTERNATIONAL JOURNAL
FOR TECHNIQUES AND APPLICATIONS OF NUCLEAR SCIENCE

July, 1948

NEUTRON DIFFRACTION AND ASSOCIATED STUDIES—I

TOXICITY OF INHALED OR INGESTED RADIOACTIVE PRODUCTS

PARTICLE DETECTION WITH MULTIPLIER TUBES

STUDY ON THE RADIOACTIVE-ELECTRIC CONVERTER

INTERACTION OF ISOTOPIC RADIATION WITH MATTER—II

NUCLEAR PHYSICS OF THE DEUTERON
AND OTHER TWO-PARTICLE PHENOMENA—II

COUNTER DESIGN FOR GASEOUS WEAK BETA EMITTERS

ATOMIC ENERGY COMMISSION DOCUMENTS

A McGraw-Hill Publication

SHERRON

SHERRON CAN DESIGN AND MANUFACTURE

COUNTERS: Maximum count as required. Predetermined setting anywhere within the counting range. Resolution in the micro-second region.

COMPUTERS: Mechanical linkages. Electrical analogues of any complexity. Digital computers.

SERVO-MECHANISMS: Control to any desired accuracy. Power as desired. Linear control, logarithmic control.

AMPLIFIERS: R.F., Video, A.F., D.C. to fit any application. Particular emphasis on high gain, high stability characteristics.

OSCILLATORS: All frequencies.

POWER SUPPLIES: Electronic - Regulation ½% and less.

REGULATORS: Electronic — direct or through servo control. Regulation, drift, etc. to specification.

MEASUREMENT — CONTROL: Devices for measuring and control of all parameters capable of being controlled and producing proportional electrical, optical or measuring displacement. Electronic microammeters, radiation counters.

CONTROL OF ACCELERATOR ACCESSORIES: Grouping of controls, supplementary apparatus, and experimental system into a compact versatile unit.

SHERRON

SHERRON SERVES YOU 3 WAYS IN NUCLEAR RESEARCH

CONTROL . . . MEASUREMENT . . . POWER SOURCES

Where these three requirements are concerned in nuclear explorations, Sherron offers a comprehensive service that is at once custom-ized and confidential.

This service is based on these coordinated factors: an extensive experience in designing and manufacturing electronic equipment . . . a full complement of physicists and electronic engineers . . . thoroughly modern electronic and electro-mechanical laboratories . . . complete manufacturing facilities.

Inquire!

SHERRON ELECTRONICS CO.

Division of Sherron Metallic Corporation

1201 FLUSHING AVE. • BROOKLYN 6, N. Y.

o.

N. Y.

NUCLEONICS

INDEX to VOLUME 3, July–December, 1948

SUBJECT INDEX*

Absorption
Interaction of isotopic radiation with matter. R. G. Fluharty..Part 2 July 46
Abstracts
Chemical, Life Science, and Physical Publications.....July 69
Aug. 68, Sept. 85, Oct. 85, Nov. 81, Dec. 77
Accelerators
Carnegie Tech. cyclotron creates transport problem (*N.E.*).....Dec. 65
G.E. builds mobile betatron for Navy (*N.E.*).....Dec. 66
Production of radionuclides. J. W. Irvine, Jr.....Aug. 5
Stanford University to build 1-Bev electron linear accelerator (*N.E.*) Oct. 79
University of California to build 12-Mev accelerator (*N.E.*).....July 68
Air Force announces details of Rand Corp. (*N.E.*).....Dec. 66
American Chemical Society holds symposium on "nucleonics and analytical chemistry" (*N.E.*).....Aug. 65
American Institute of Electrical Engineers and Institute of Radio Engineers plan nucleonics instrumentation conference (*N.E.*).....Aug. 65, Nov. 77
Americium
Fission of atomic nuclei. B. C. Purkayastha.....Part 1 Nov. 2, Part 2, Dec. 2
Argonne National Laboratory
Reactor meeting held (*N.E.*).....Nov. 75
Westinghouse men to work in laboratory (*N.E.*).....Oct. 7
Associated Universities, Inc., names F. D. Fackenthal its president (*N.E.*)..Dec. 67
Atomic bomb
British role in development (*N.E.*). M. H. L. Pryce.....Dec. 60
Atomic Energy Commission
Awards 18 health physics fellowships (*N.E.*).....Dec. 64
Congressional group reports on budget (*N.E.*).....July 66
Documents and publications lists July 28, Oct. 72, Nov. 71, Dec. 73
D. F. Hays appointed safety director (*N.E.*).....Nov. 78
MIT granted funds to study tracers in metallurgy (*N.E.*).....Sept. 82
New chemical laboratory to be established at New Brunswick, N. J. (*N.E.*) Aug. 66
ONR and AEC to sponsor 19 research projects (*N.E.*).....Nov. 79
Personnel advisory committee established (*N.E.*).....Oct. 79
Personnel changes and reorganization of power development program (*N.E.*) Oct. 77
Atomic Energy Legislation
New legislation to replace the McMahon Act (*Edit.*). W. M. DeCew.....July 2
The transition period (*Edit.*). W. M. DeCew.....Aug. 2

Baruch International Control Plan
British Atomic Scientists issue statement on failure of plan (*N.E.*).....Sept. 79
Beta Rays
Beta- and gamma-ray spectroscopy. G. J. Hine.....Part 1 Dec. 32
Betatrons (See *Accelerators*)
Bethe, Hans A. to teach nuclear physics at Columbia (*N.E.*).....July 68
Bibliographies
Russian literature.....Part 1 Sept. 74
Book Reviews
Advances in biological and medical physics. Edit. by J. H. Lawrence and J. G. Hamilton.....Oct. 84
Atomic energy. K. K. Darrow....Oct. 84
Brain tumors localized by radiodyes. Part 1, Gerald Boyack, G. E. Moore and D. F. Clausen, Oct. 62; Part 2, J. F. Marvin and G. E. Moore...Oct. 63
Brookhaven National Laboratory
Builds weather towers for pile (*N.E.*) Sept. 82
F. D. Fackenthal becomes president of Associated Universities, Inc. (*N.E.*) Dec. 67
Philip M. Morse resigns as head (*N.E.*) Aug. 66

Canada
U. S., Canada, United Kingdom review declassification guide (*N.E.*).....Oct. 80
Cancer
Committee on Growth of the National Research Council to give grants, fellowships (*N.E.*).....Aug. 65
Carnegie Institute of Technology cyclotron creates transport problem (*N.E.*) Dec. 65
Cathode Rays
Effect of high-voltage X-rays and cathode rays on vitamins (niacin). B. E. Proctor and S. A. Goldblith Aug. 32
Chemical process industries and nuclear energy (*Edit.*). W. M. DeCew...Oct. 69
Chemical Publications (Abstracts)...July 69
Aug. 67, Sept. 85, Oct. 85, Nov. 81, Dec. 77
Cobalt
Radioisotopes in nutritional trace element studies. C. L. Comar Part 2 Oct. 30
Cohen, Karl, named director of atomic work at Ferguson (*N.E.*) .....July 65
Coincidence method for determining nuclear disintegration schemes. C. E. Mandeville and M. V. Scherb....Oct. 2
Compton Effect
Interaction of isotopic radiation with matter. R. G. Fluharty..Part 2 July 46
Copper
Concentration of Cu^{62} by countercurrent electromigration.....Oct. 24
Radioisotopes in nutritional trace element studies. C. L. Comar...Part 3 Nov. 34
Cornell University dedicates nuclear studies laboratory (*N.E.*).....Nov. 75
Cosmic Ray Research
Two Soviet scientists discover new particles (*N.E.*).....Aug. 66

* The notation "(*Edit.*)" indicates reference is an editorial. "(*N.E.*)" indicates that reference is an item in *Nucleonic Events* columns.

UNIVERSITY OF MICHIGAN LIBRARIES

Counters
Counter design for gaseous weak beta emitters. J. T. Kummer.....July 27
Nuclear disintegration schemes and the coincidence method. C. E. Mandeville and M. V. Scherb.....Oct. 2
Particle detection with multiplier tubes J. S. Allen.....July 34
Theory and operation of Geiger-Müller counters. S. C. Brown..Part 2 Aug. 50
Part 3 Oct. 46
Counting Circuits
Analysis of scale units. W. L. Buys Nov. 49
Crystallography
Neutron diffraction and associated studies. E. O. Wollan and C. G. Shull.....Part 2 Aug. 17
Curium
Fission of atomic nuclei. B. C. Purkayastha.....Part 1 Nov. 2, Part 2 Dec. 2
Cyclotrons (See *Accelerators*)

Decay Schemes
Nuclear disintegration schemes and the coincidence method. C. E. Mandeville and M. V. Scherb.....Oct. 2
Detectors
Particle detection with multiplier tubes. J. S. Allen.....July 34
Deuterons
Nuclear physics of the deuteron and other two-particle phenomena. M. E. Rose.....Part 2 July 57
Production of radionuclides. J. W. Irvine, Jr.....Aug. 5
Discharge Tubes
Design of an improved-yield discharge tube. Jaroslav Pachner.....Dec. 43
Dosage Calculations
Review of conventions in radiotracer studies. John Schulman, Jr. and Marlene Falkenheim.....Oct. 13
Toxicity of inhaled or ingested radioactive products. W. E. Cohn...July 21

Electron Multiplier
Particle detection with multiplier tubes. J. S. Allen.....July 34
Electrostatic generator construction started at MIT (*N.E.*).....Dec. 63
Elution
Ion-exchangers to separate, concentrate and purify small amounts of ions. W. E. Cohn, G. W. Parker and E. R. Tompkins.....Nov. 22

Fackenthal, F. D. becomes president of Associated Universities, Inc. (*N.E.*) Dec. 67
Films
Measurement of P^{32} and I^{131} radiations with dental film. F. H. Rudenberg, R. F. Cowing and C. K. Spalding..Dec. 52
Stray-radiation measurement with X-ray film. Adair Morrison.....Sept. 46
Filter-cup for collecting and counting active precipitates. E. L. Abers..Oct. 43
Fission
Fission of atomic nuclei. B. C. Purkayastha.....Part 1 Nov. 2, Part 2 Dec. 2
Fission products and their uses. L. Yaffe.....Sept. 68
Liquid-drop model for nuclear fission. R. D. Present.....Sept. 25
Mass spectrometry and nuclear chemistry. H. G. Thode.....Sept. 14
MIT receives grant from Socony-Vacuum Oil Co., Inc., for fission research (*N.E.*) Sept. 82

Gamma Rays
Beta- and gamma-ray spectroscopy. G. J. Hine.....Part 1 Dec. 32
Gamma-ray shielding data.....Oct. 44
Interaction of isotopic radiation with matter. R. G. Fluharty..Part 2 July 46
Geiger-Müller Counters (See *Counters* and *Products and Materials*)
General Electric Company
Builds mobile betatron for Navy (*N.E.*) Dec. 66
Knolls Atomic Power Laboratory site selected (*N.E.*).....Nov. 74
Great Britain
Atomic energy work in Britain (*N.E.*). M. H. L. Pryce.....Dec. 60
Atomic scientists issue statement on failure of Baruch International Control Plan (*N.E.*).....Sept. 79
Harwell research program (*N.E.*)..Dec. 62
Two piles in operation at Harwell (*N.E.*) Sept. 81
U. S., Canada, United Kingdom review declassification guide (*N.E.*).....Oct. 80

Half-lives
Methods of measuring very long and very short half-lives. S. Rowlands...Sept. 2
Harwell, England (See *Great Britain*)
Health Physics (See also *Medical Physics*)
AEC awards 18 health physics fellowships (*N.E.*).....Dec. 64
Health physics. R. E. Lapp and H. L. Andrews.....Sept. 60

India
Atomic energy commission established (*N.E.*).....Oct. 80
Institute of Radio Engineers and American Institute of Electrical Engineers plan nucleonics instrumentation conference (*N.E.*).....Aug. 65, Nov. 77
Instruments (See also *Products and Materials*)
Analysis of scale units. W. L. Buys Nov. 49
An inexpensive filter-cup for collecting and counting active precipitates. E. L. Abers.....Oct. 43
IRE-AIEE to hold conference on nucleonics instruments (*N.E.*).....Aug. 65 Nov. 77
Iodine-131
Localization of brain tumors with radiodyes. Part 1, Gerald Boyack, G. E. Moore and D. F. Clausen.....Oct. 62
Part 2, J. F. Marvin and G. E. Moore Oct. 63
Measurement of P^{32} and I^{131} radiations with dental film. F. H. Rudenberg, R. F. Cowing and C. K. Spalding..Dec. 52
Ion-exchange
Ion-exchangers to separate, concentrate and purify small amounts of ions. W. E. Cohn, G. W. Parker and E. R. Tompkins.....Nov. 22
Isotope Separation
Ion-exchangers to separate, concentrate and purify small amounts of ions. W. E. Cohn, G. W. Parker and E. R. Tompkins.....Nov. 22
Isotopes
Fission products and their uses. L. Yaffe.....Sept. 68
General Electric issues isotope chart (*N.E.*).....Aug. 66

Isotopes (*cont'd*)
Interaction of isotopic radiation with matter. R. G. Fluharty..Part 2 July 46
Measurement of radioactive isotopes Sept. 55
Methods of measuring very long and very short half-lives. S. Rowlands Sept. 2
Oak Ridge Institute to continue isotope technique courses (*N.E.*).....Oct. 79
Radioisotopes in nutritional trace element studies. C. L. Comar
Part 1 Sept. 32
Part 2 Oct. 30
Part 3 Nov. 34
Transuranium elements....Nov. 8, Dec. 12

Knolls Atomic Power Laboratory site selected (*N.E.*).....Nov. 74

Life Science Publications (Abstracts) July 71 Aug. 68, Sept. 87, Oct. 86, Nov. 82, Dec. 78
Liquid-drop model for nuclear fission. R. D. Present.....Sept. 25
Low-temperature phenomena
Nuclear physics and low temperatures. M. E. Rose.....Dec. 23

Manganese
Radioisotopes in nutritional trace element studies. C. L. Comar.....
Part 2 Oct. 30
Manhattan District Declassified Documents (See *Atomic Energy Commission*)
Mass spectrometry and nuclear chemistry. H. G. Thode.....Sept. 14
Massachusetts Inst. of Technology
Construction of 12-Mev electrostatic generator started (*N.E.*).....Dec. 63
Proposed building for nuclear facilities (*N.E.*).....Dec. 66
Receives grants to study tracers in metallurgy and for fission research (*N.E.*) Sept. 82
McMahon Act, new legislation to replace (*Edit.*). W. M. DeCew.....July 2
Measurements
Measurement of P^{32} and I^{131} radiations with dental film. F. H. Rudenberg, R. F. Cowing and C. K. Spalding..Dec. 52
Methods of measuring very long and very short half-lives. S. Rowlands Sept. 2
Medical Physics
Interaction of isotopic radiation with matter. R. G. Fluharty..Part 2 July 46
Localization of brain tumors with radiodyes. Part 1. Gerald Boyack, G. E. Moore and D. F. Clausen.....Oct. 62
Part 2, J. F. Marvin and G. E. Moore Oct. 63
Medical aspects of radiation safety. B. S. Wolf.....Oct. 25
Radioisotopes in nutritional trace element studies. C. L. Comar.....
Part 1 Sept. 32
Part 2 Oct. 30
Part 3 Nov. 34
Review of conventions in radiotracer studies. John Schulman, Jr., and Marlene Falkenheim.....Oct. 13
Toxicity of inhaled or ingested radioactive products. W. E. Cohn.....July 21
Mercury
Concentration of Hg^{204} in countercurrent molecular stills.....Oct. 23
Metabolism
Radioisotopes in nutritional trace element studies. C. L. Comar.....
Part 1 Sept. 32
Part 2 Oct. 30
Part 3 Nov. 34
Metallurgy
MIT gets grant from AEC to study tracers in metallurgy (*N.E.*).....Sept. 82
Neutron diffraction and associated studies. E. O. Wollan and C. G. Shull.....Part 2 Aug. 17
Molybdenum
Radioisotopes in nutritional trace element studies. C. L. Comar.....
Part 3 Nov. 34
Monazite
AEC describes its interest in monazite (*N.E.*).....Nov. 78
Morse, Dr. Philip M., resigns as head of Brookhaven Lab. (*N.E.*).....Aug. 66
Multiplier tubes used for particle detection. J. S. Allen.....July 34

National Academy of Sciences—twenty-nine papers presented (*N.E.*).....Dec. 64
Naval Ordnance Laboratory gets 10-Mev mobile betatron (*N.E.*).....Dec. 66
Neptunium
Fission of atomic nuclei. B. C. Purkayastha.....Part 1 Nov. 2, Part 2 Dec. 2
Neutron diffraction and associated studies. E. O. Wollan and C. G. Shull Part 1 July 8, Part 2 Aug. 17
Neutron Source
Design of an improved-yield discharge tube. Jaroslav Pachner.....Dec. 43
Niacin
Effect of high voltage X-rays and cathode rays on vitamins (niacin). B. E. Proctor and S. A. Goldblith.....Aug. 32
Nobel prize for physics awarded to P. M. S. Blackett (*N.E.*).....Dec. 67
Nuclear Chemistry (See also *Radiochemistry*)
Fission of atomic nuclei. B. C. Purkayastha.....Part 1 Nov. 2, Part 2 Dec. 2
Mass spectroscopy and nuclear chemistry. H. G. Thode.....Sept. 14
Nuclear Development Associates, Inc., name four scientists as advisers (*N.E.*).....Oct. 80
Nuclear energy and chemical process industries. (*Edit.*). W. M. DeCew..Oct. 69
Nuclear Physics
Liquid-drop model for nuclear fission. R. D. Present.....Sept. 25
Neutron diffraction and associated studies. E. O. Wollan and C. G. Shull Part 1 July 8, Part 2 Aug. 17
Nuclear disintegration schemes and the coincidence method. C. E. Mandeville and M. V. Scherb.....Oct. 2
Nuclear physics and low temperatures. M. E. Rose.....Dec. 23
Westinghouse offers charts on atomic science (*N.E.*).....Nov. 79
Nuclear Power
Analysis of future status of nuclear power based on AEC report and statement by Sir John Cockcroft (*N.E.*).....Sept. 79
The future of nuclear power (*Edit.*). W. M. DeCew.....Sept. 76
Kellex Corp. exhibits model of nuclear energy power plant as center of future industrial life (*N.E.*).....Oct. 81
Study on the radioactive-electric converter. Andrew Gemant and H. M. Archer.....July 40
Nuclear Reactors
British operate two piles at Harwell (*N.E.*).....Sept. 81
Fission of atomic nuclei. B. C. Purkayastha.....Part 1 Nov. 2, Part 2 Dec. 2
Meeting concerned with reactors held at Argonne Natl. Lab. (*N.E.*)...Nov. 75
Review of British reactors (*N.E.*)..Dec. 62

UNIVERSITY OF MICHIGAN LIBRARIES

Nuclides
Fission products and their uses. L. Yaffe....Sept. 68
Production of radionuclides. J. W. Irvine, Jr....Aug. 5
Nutritive Elements
Effect of high voltage X-rays and cathode rays on vitamins (niacin). B. E. Proctor and S. A. Goldblith....Aug. 32
Radioisotopes in nutritional trace element studies. C. L. Comar....
Part 1 Sept. 32
Part 2 Oct. 30
Part 3 Nov. 34

Oak Ridge National Laboratory
Holds shielding symposium (*N.E.*)....Nov. 76
Oak Ridge Institute to continue isotope technique courses (*N.E.*)....Oct. 79
Sponsors nuclear physics conference (*N.E.*)....July 68
Office of Naval Research and AEC to sponsor 19 research projects (*N.E.*)..Nov. 79

Pair Production
Interaction of isotopic radiation with matter. R. G. Fluharty..Part 2 July 46
Particle Acceleration
Design of an improved-yield discharge tube. Jaroslav Pachner....Dec. 43
Particles
Nuclear physics of the deuteron and other two-particle phenomena. M. E. Rose....Part 2 July 57
Two Soviet scientists discover new particles (*N.E.*)....Aug. 66
Patents
What can be patented and how. W. R. Ballard....Dec. 70
Phosphorus-32
Measurement of P^{32} and I^{131} radiations with dental film. F. H. Rudenberg, R. F. Cowing and C. K. Spalding..Dec. 52
Photoelectric Effect
Interaction of isotopic radiation with matter. R. G. Fluharty..Part 2 July 46
Photomultiplier Tubes
Particle detection with multiplier tubes. J. S. Allen....July 34
Physical Publications (Abstracts)....July 73
Aug. 72, Sept. 89, Oct. 88, Nov. 84, Dec. 81
Piles (See *Nuclear Reactors*)
Plutonium
Fission of atomic nuclei. B. C. Purkayastha....Part 1 Nov. 2, Part 2 Dec. 2
Poland
Number of atomic scientists increased (*N.E.*)....July 68
Products and Materials
Alpha counter....Oct. 82
Autoscaler....Sept. 84
Battery....Dec. 68
Beta-gamma counter....Dec. 69
Beta-gamma scaler....Dec. 69
Binary scaler....Dec. 69
Electrometer, vibrating reed....Oct. 82
Gage, thickness....Sept. 84
Geiger counters....Sept. 83, Dec. 68
Probe counter....Oct. 83
Resistors, ultra-high....Oct. 83
Scaler....Dec. 68
Survey meter....Dec. 69
Thorium detector....Sept. 83
Thyratron thermostat....Oct. 83
Timer, precision....Sept. 84
Titanium made by Du Pont....Oct. 84
Van de Graaff generator, portable...Oct. 83
Publications (See also *Atomic Energy Commission* and *Book Reviews*)
Announcement of availability of handbook, reports, and circulars on isotopes and atomic energy from OTS and GPO....Dec. 67

Radiation
Interaction of isotopic radiation with matter. R. G. Fluharty..Part 2 July 46
Measurement of P^{32} and I^{131} radiations with dental film. F. H. Rudenberg, R. F. Cowing and C. K. Spalding..Dec. 52
Stray-radiation measurement with X-ray film. Adair Morrison....Sept. 46
Radioactivity
Medical aspects of radiation safety. B. S. Wolf....Oct. 25
Methods of measuring very long and very short half-lives. S. Rowlands...Sept. 2
Radioactivity Converter
Study on the radioactive-electric converter. Andrew Gemant and H. M. Archer....July 40
Radiochemistry (See also *Nuclear Chemistry*)
Ion-exchangers to separate, concentrate and purify small amounts of ions. W. E. Cohn, G. W. Parker and E. R. Tompkins....Nov. 22
Radiodyes used to locate brain tumors. Part 1, Gerald Boyack, G. E. Moore and D. F. Clausen, Oct. 62; Part 2, J. F. Marvin and G. E. Moore,...Oct. 63
Radioisotopes (See *Isotopes*)
Radiological Society of North America holds annual meeting (*N.E.*)....Dec. 64
Radionuclides
Production of radionuclides. J. W. Irvine, Jr....Aug. 5
Radiotracer studies, review of conventions in. John Schulman, Jr., and Marlene Falkenheim....Oct. 13
Rand Corp., a non-profit organization, details announced (*N.E.*)....Dec. 66
Reactors (See *Nuclear Reactors*)
Russia
Bibliography: Russian literature....
Part 1 Sept. 74
Two Soviet scientists discover new particles (*N.E.*)....Aug. 66

Safety
Gamma-ray shielding data....Oct. 44
Medical aspects of radiation safety. B. S. Wolf....Oct. 25
Toxicity of inhaled or ingested radioactive products. W. E. Cohn...July 21
Scaling Circuits
Analysis of scale units. W. L. Buys Nov. 49
Scattering
Neutron diffraction and associated studies. E. O. Wollan and C. G. Shull....Part 1 July 8, Part 2 Aug. 17
Scintillation Counters
Particle detection with multiplier tubes. J. S. Allen....July 34
Separation of Isotopes
Ion-exchangers to separate, concentrate and purify small amounts of ions. W. E. Cohn, G. W. Parker and E. R. Tompkins....Nov. 22
Shielding
Broad and narrow beam attenuation of 500–1400 kv X-rays in lead and concrete. H. O. Wyckoff, R. J. Kennedy and W. R. Bradford....Nov. 62
Oak Ridge Natl. Lab. holds shielding symposium (*N.E.*)....Nov. 76
Shielding data for gamma rays....Oct. 44

Socony-Vacuum Oil Co., Inc.
Grants fund to MIT for fission research (*N.E.*).....Sept. 82
Spectroscopy of beta- and gamma-rays. G. J. Hine.....Part 1 Dec. 32
Spins
Nuclear physics and low temperatures. M. E. Rose.....Dec. 23
Standards and Units
Health physics. R. E. Lapp and H. L. Andrews.....Sept. 60
Measurement of radioactive isotopes Sept. 55
Review of conventions in radiotracer studies. John Schulman, Jr., and Marlene Falkenheim.....Oct. 13
Stanford University to build 1-Bev electron linear accelerator (*N.E.*).....Oct. 79
Synchrotrons (see *Accelerators*)

Temperature, low, and nuclear physics. M. E. Rose.....Dec. 23
Thorium
AEC describes its interest in monazite, the ore from which thorium is obtained (*N.E.*).....Nov. 78
Trace Elements (See *Medical Physics*)
Tracers (See *Isotopes*)
Transuranium Elements
Fission of atomic nuclei. B. C. Purkayastha.....Part 1 Nov. 2, Part 2 Dec. 2
Tubes
Design of an improved-yield discharge tube. Jaroslav Pachner.....Dec. 43

Ultramicrochemistry
Fission of atomic nuclei. B. C. Purkayastha.....Part 1 Nov. 2, Part 2 Dec. 2
U. S., Canada, United Kingdom review declassification guide (*N.E.*).....Oct. 80
Units (See *Standards and Units*)
University of California will give course on nuclear physics in life sciences (*N.E.*) July 68
University of Chicago's Research Program
Bethlehem Steel joins (*N.E.*).....Aug. 66
Crane Co. joins (*N.E.*).....Oct. 80
Uranium
Fission of atomic nuclei. B. C. Purkayastha.....Part 1 Nov. 2, Part 2 Dec. 2

Vitamins
Effect of high voltage X-rays and cathode rays on vitamins (niacin). B. E. Proctor and S. A. Goldblith.....Aug. 32

Waste Disposal
Problems of radioactive waste disposal. Forrest Western.....Aug. 43
Westinghouse Electric Corp.
Forms atomic power division (*N.E.*) Nov. 74
Offers wall charts on atomic science (*N.E.*).....Nov. 79
Westinghouse men to work at Argonne Laboratory (*N.E.*).....Oct. 79

X-rays
Broad and narrow beam attenuation of 500–1400 kv X-rays in lead and concrete. H. O. Wyckoff, R. J. Kennedy and W. R. Bradford.....Nov. 62
Effect of high-voltage X-rays and cathode rays on vitamins (niacin). B. E. Proctor and S. A. Goldblith.....Aug. 32
Interaction of isotopic radiation with matter. R. G. Fluharty..Part 2 July 46
Stray-radiation measurement with X-ray film. Adair Morrison.....Sept. 46

Zinc
Radioisotopes in nutritional trace element studies. C. L. Comar..... Part 3 Nov. 34

Big Capacity Pumps

FOR VACUUMS AS LOW AS ONE-BILLIONTH OF AN ATMOSPHERE

Employment of high vacuum in physical chemistry and nuclear physics is demanding bigger capacity pumps for faster, larger-scale vacuum production.

To this end DPI builds a wide variety of rugged, all-metal diffusion pumps capable of pumping many thousands of cubic feet of air per minute.

The DPI line also includes gauges, recorders, controls, chambers and accessories used in high-vacuum applications including cyclotrons, synchrotrons and betatrons. The special Bale-Haven immersion type counter tube is also available from DPI. Write:

Vacuum Equipment Division

DISTILLATION PRODUCTS, INC.
781 Ridge Road West • Rochester 13, N. Y.
570 Lexington Ave. • New York 22, N. Y.
135 So. LaSalle Street • Chicago 3, Ill.

Manufacturers of Molecular Stills and High-Vacuum Equipment; Distillers of Oil-Soluble Vitamins and Other Concentrates for Science and Industry

UNIVERSITY OF MICHIGAN LIBRARIES

AUTHOR INDEX

Abers, Elliott L. An inexpensive filter-cup for collecting and counting active precipitates.....Oct. 43
Allen, James S. Particle detection with multiplier tubes.....July 34
Andrews, H. L. and R. E. Lapp. Health physics.....Sept. 60
Archer, Hugh M. and Andrew Gemant. Study on the radioactive-electric converter.....July 40
Ballard, William R. What can be patented and how.....Dec. 70
Boyack, Gerald, G. E. Moore and D. F. Clausen. Localization of brain tumors with radiodyes.....Part 1 Oct. 62
Bradford, W. R., H. O. Wyckoff and R. J. Kennedy. Broad and narrow beam attenuation of 500–1400 kv X-rays in lead and concentrate.....Nov. 62
Brown, Sanborn C. Theory and operation of Geiger-Müller counters Part 2 Aug. 50, Part 3 Oct. 46
Buys, W. L. Analysis of scale units. Nov. 49
Clausen, Donald F., Gerald Boyack and G. E. Moore. Localization of brain tumors with radiodyes....Part 1 Oct. 62
Cohn, Waldo E. Toxicity of inhaled or ingested radioactive products.....July 21
Cohn, Waldo E., G. W. Parker and E. R. Tompkins. Ion-exchangers to separate, concentrate and purify small amounts of ions.....Nov. 22
Comar, C. L. Radioisotopes in nutritional trace element studies....Part 1 Sept. 32
Part 2 Oct. 30
Part 3 Nov. 34
Cowing, R. F., F. H. Rudenberg, and C. K. Spalding. Measurement of P^{32} and I^{131} radiations with dental film Dec. 52
DeCew, Walter M. Chemical process industries and nuclear energy (*Edit.*) Oct. 69
The future of nuclear power (*Edit.*). Sept. 76
New legislation to replace the McMahon Act (*Edit.*).....July 2
The transition period (*Edit.*).....Aug. 2
Falkenheim, Marlene and John Schulman Jr. Review of conventions in radiotracer studies.....Oct. 13
Fluharty, Rex G. Interaction of isotopic radiation with matter....Part 2 July 46
Gemant, Andrew and H. M. Archer. Study on the radioactive-electric converter.....July 40
Goldblith, Samuel A. and B. E. Proctor. Effect of high-voltage X-rays and cathode rays on vitamins (niacin)....Aug. 32
Hine, Gerald J. Beta and gamma-ray spectroscopy.....Part 1 Dec. 32
Irvine, John W., Jr. Production of radionuclides.....Aug. 5
Kennedy, R. J., H. O. Wyckoff and W. R. Bradford. Broad and narrow beam attenuation of 500–1400 kv X-rays in lead and concrete.....Nov. 62
Kummer, Joseph T. Counter design for gaseous weak beta emitters.....July 27
Lapp, R. E. and H. L. Andrews. Health physics.....Sept. 60
Mandeville, C. E. and M. V. Scherb. Nuclear disintegration schemes and the coincidence method.....Oct. 2
Marvin, James F. and G. E. Moore. Localization of brain tumors with radiodyes.....Part 2 Oct. 63
Moore, George E., Gerald Boyack and D. F. Clausen. Localization of brain tumors with radiodyes....Part 1 Oct. 62
Moore, George E. and J. F. Marvin. Localization of brain tumors with radiodyes.....Part 2 Oct. 63
Morrison, Adair. Stray-radiation measurement with X-ray film.....Sept. 46
Pachner, Jaroslav. Design of an improved-yield discharge tube.....Dec. 43
Parker, George W., W. E. Cohn and E. R. Tompkins. Ion-exchangers to separate, concentrate and purify small amounts of ions.....Nov. 22
Present, R. D. The liquid-drop model for nuclear fission.....Sept. 25
Proctor, Bernard E. and S. A. Goldblith. Effect of high-voltage X-rays and cathode rays on vitamins (niacin)....Aug. 32
Pryce, M. H. L. Atomic energy work in Britain (*N.E.*).....Dec. 60
Purkayastha, B. C. Fission of atomic nuclei.....Part 1 Nov. 2, Part 2 Dec. 2
Rose, M. E. Nuclear physics and low temperatures.....Dec. 23
Nuclear physics of the deuteron and other two-particle phenomena..... Part 2 July 57
Rowlands, S. Methods of measuring very long and very short half-lives....Sept. 2
Rudenberg, F. H., R. F. Cowing, and C. K. Spalding. Measurement of P^{32} and I^{131} radiations with dental film Dec. 52
Scherb, M. V. and C. E. Mandeville. Nuclear disintegration schemes and the coincidence method.....Oct. 2
Schulman, John Jr. and Marlene Falkenheim. Review of conventions in radiotracer studies.....Oct. 13
Shull, C. G. and E. O. Wollan. Neutron diffraction and associated studies Part 1 July 8, Part 2 Aug. 17
Spalding, C. K., F. H. Rudenberg, and R. F. Cowing. Measurement of P^{32} and I^{131} radiations with dental film Dec. 52
Thode, H. G. Mass spectrometry and nuclear chemistry.....Sept. 14
Tompkins, Edward R., W. E. Cohn and G. W. Parker. Ion-exchangers to separate, concentrate and purify small amounts of ions.....Nov. 22
Western, Forrest. Problems of radioactive waste disposal.....Aug. 43
Wolf, Bernard S. Medical aspects of radiation safety.....Oct. 25
Wollan, E. O. and C. G. Shull. Neutron diffraction and associated studies Part 1 July 8, Part 2 Aug. 17
Wyckoff, H. O., R. J. Kennedy and W. R. Bradford. Broad and narrow beam attenuation of 500–1400 kv X-rays in lead and concrete.....Nov. 62
Yaffe, L. The fission products and their uses.....Sept. 68

(*Abstracts*)—*Cont'd. from page 84*

curve taken with a ten-channel pulse-height analyzer for the reaction $D(d,n)He^3$ is given. The He^3 particles are clearly resolved from the deuterons scattered by deuterium at 45°.

Coincidence device of 10^{-8}–10^{-9} second resolving power, Z. Bay, G. Papp (Univ. of Technical and Economic Sciences, Budapest, Hungary), *Rev. Sci. Instr.* **19,** 565–567 (1948). Two electron emission multiplier tubes of high resolving power were connected to a variation of the Rossi-type coincidence circuit. The resolving power, measured by changing the lead lengths (and thus the time-lag) and noting the corresponding change in coincidence rate, was 5×10^{-9} sec.

Focusing field for a 180° type spectrograph, F. M. Beiduk, E. J. Konopinski (Indiana Univ., Bloomington), *Rev. Sci. Instr.* **19,** 594–598 (1948). A radially varying field which perfectly focuses electrons emitted from a point source and moving in the median plane is derived. The effect of a finite source and of the orbits not confined to the median plane on defocusing is discussed. The transmission and resolution of an instrument using this field are obtained by plotting the fraction of electrons from a line source which fall outside an opening of given length (constituting a detector) for baffles of different sizes in a uniform field, and comparing the results with those of a shaped field.

A mass spectrograph for radioactive isotopes, L. G. Lewis, R. J. Hayden (Univ. of Chicago, Ill.), *Rev. Sci. Instr.* **19,** 599–604 (1948). A mass spectrometer is described which allows the separation of small quantities of radioactive isotopes, by allowing the ions to strike either a photographic plate or a collecting electrode. The activities in the detectors were measured either by a counter or a photographic plate. Thus mass numbers of various radiosotopes and radiation characteristics of various radioisotopes of the same element may be determined.

. . . HAROLD BROWN

Announcing

A NUCLEAR INSTRUMENT EXHIBIT

at the 1949 Radio Engineering Show of the IRE National Convention, March 7-10, 1948 at Grand Central Palace, New York City.

VISIT—The Nuclear Center, third floor! Attend the Nuclear Studies Session, and the Nuclear Symposium.

For full details, write:

William C. Copp, The Institute of Radio Engineers,
303 West 42nd Street New York 18, N. Y.

UNIVERSITY OF MICHIGAN LIBRARIES

THE new Tracerlab selfquenching Geiger tubes assure convenience, economy, and accurate results. A long flat plateau in excess of three hundred volts in length with a maximum slope of less than 5% assures consistent and reproducible results. Tracerlab Type TGC tubes possess an extremely low degree of photosensitivity seldom, if ever, achieved by other commercially available Geiger tubes. Low initial cost plus a long life in excess of 10^8 counts spells economy for the customer. Type TGC-1 is a general purpose thin mica window tube for beta-gamma counting while the TGC-2 tube is particularly suited for accurate and sensitive counting of low energy beta radiation from carbon-14 and sulfur-35. Closely regulated quality control permits us to make a 90-day guarantee of all Type TGC Geiger tubes.

Type TGC-1 (3-4 mg/cm² mica window)	$50.00
Type TGC-2 (less than 2 mg/cm² mica window)	$75.00
Write for bulletin 11C	F.O.B. Boston

Tracerlab

Commercial Radioactivity Center

instruments • isotope processing • tracer analyses
industrial applications • research

TRACERLAB INC., 55 OLIVER STREET, BOSTON 10, MASS.

er

cs

Eng. Lib
Direct

Engineering
Library
QC
173
A1
N96

NUCLEONICS VOL. 3, NO. 1, JULY, 1948

An International Journal for Techniques and Applications of Nuclear Science

EDITORIAL BOARD

L. B. Borst
John R. Dunning
H. H. Goldsmith
Clark Goodman
F. C. Henriques, Jr.
W. F. Libby
L. D. Marinelli
I. Perlman
Edith H. Quimby
Winfield W. Salisbury
T. I. Taylor

With the cooperation of . . .

ITALY — E. AMALDI
GREAT BRITAIN — J. D. COCKCROFT
FRANCE — F. JOLIOT-CURIE
SWITZERLAND — P. SCHERRER
THE NETHERLANDS — C. J. BAKKER
DENMARK and SWEDEN — GEORGE HEVESY
GERMANY — HANS KOPFERMANN

CONTENTS

Neutron Diffraction and Associated Studies—I 8
E. O. WOLLAN and C. G. SHULL

Toxicity of Inhaled or Ingested Radioactive Products 21
WALDO E. COHN

Counter Design for Gaseous Weak Beta Emitters 27
JOSEPH T. KUMMER

Atomic Energy Commission Documents 28

Particle Detection with Multiplier Tubes 34
JAMES S. ALLEN

Study on the Radioactive-Electric Converter 40
ANDREW GEMANT and HUGH M. ARCHER

Interaction of Isotopic Radiation with Matter—II 46
REX G. FLUHARTY

Nuclear Physics of the Deuteron and other Two-particle Phenomena—II 57
M. E. ROSE

EDITORIAL .....2 NUCLEONIC EVENTS ..65 ABSTRACTS 69

Walter M. DeCew ..... Technical Editor
Jerome D. Luntz ..... Assistant Editor
Ethel Pelzer ..... Assistant Editor
Robert Colborn ..... Washington Editor
Gladys Montgomery . Washington Editor
Keith Henney ..... Consulting Editor
E. J. Tangerman ..... General Manager

NUCLEONICS (with which is consolidated "Atomic Power" and "Atomic Engineering") July, 1948, Vol. 3, No. 1 Publication Office: 212 East York St., York, Pa. Editorial and Circulation Offices: 330 W. 42nd St., New York 18, N. Y. Published monthly by McGraw-Hill Publishing Company, Inc. Entered as second class matter December 17, 1947, in the Post Office at York, Pa., under the act of March 3, 1879. Copyright 1948 by McGraw-Hill Publishing Company, Inc. All rights reserved. James H. McGraw, Jr., President; J. A. Gerardi, Secretary; Curtis W. McGraw, Treasurer. Price per copy $2.00. Allow at least ten days for change of address. All communications about subscriptions should be addressed to J. E. Blackburn, Jr., Director of Circulation, 330 W. 42nd St., New York 18, N. Y. Subscription rates: United States and U. S. Possessions $15.00 a year. Canada and Latin America $20.00 a year. All other countries $25.00 a year. Return postage guaranteed. Member A.B.C.

New Legislation to Replace the McMahon Act

On August 1, 1946, less than one year after the first military use of the atomic bomb, the McMahon Atomic Energy Act was signed by President Truman.

The preamble of the McMahon Act explicitly states that this law is not intended to be permanent legislation. Section (a), *Findings and Declaration*, declares: "The effect of the use of atomic energy for civilian purposes upon the social, economic, and political structure of today cannot now be determined. It is a field where unknown factors are involved. Therefore, any legislation will be subject to revision from time to time."

The McMahon Act set up machinery for the exclusive ownership and management of nuclear energy by the United States federal government. Although many reasons were advanced to support this policy, the principal argument which determined the consent of Congress and the American people was the expectation that international accord on the control of atomic energy would enable the United States to transfer this national monopoly to an international atomic energy authority, which would be vested with world-wide monopoly of atomic energy. This expectation was embodied in the Acheson-Lilienthal report of March 28, 1946, and became official United States policy with the Baruch proposals of June 14, 1946.

In May, 1948, after two years and more than 200 meetings, the United Nations Atomic Energy Commission admitted that Soviet Russia's agreement to these proposals for international ownership and management of atomic energy could no longer be hoped for. The majority delegates formally agreed to suspend the U. N. Atomic Energy Commission, with the declaration that "No useful purpose can be served by carrying on negotiation." This is a blunt statement that none of the members of the United Nations can count on integrating its domestic atomic energy organization into an international pattern.

It is imperative that we should now reconsider the commitments of the McMahon Act. It is logical that we should now introduce legislation specifically designed to integrate the atomic energy industry into our national economy.

Although the necessity for such legislation has been realized in many quarters for some time, so far there has been made no public presentation of specific alternate legislation. To meet this need, we are advancing for consideration by the readers of this journal, as a basis for discussion, tentative proposals for new domestic atomic energy legislation. This does not necessarily represent the final policy of Nucleonics, but it is our hope that the ensuing discussion will result in the enactment of a workable, legal framework which will be acceptable to the Congress, the scientists, the military, industry, and the public at large.

Organization Chart

The organization chart on page 4 is provided to show an over-all picture of the structure of this proposed legislation. Its exposition will be aided by reference to this diagram.

Functions of the Coordinating Board

There will first be established a coordinating board with the duty of regulating the distribution of fissionable material production. It will be composed of a coordinator, appointed by the President, who will act as chairman of a board of delegates representing the Secretary of Defense, Secretary of State, Secretary of Commerce, and the chairman of the AEC, and four citizens representing fundamental science and industrial engineering. Two of the four people representing science and industry might well be the coordinator of the Research and Development Board, and the chairman of the National Science Foundation, if the latter should be set up. This Coordinating Board will coordinate the activities of the three independent groups of fissionable material users indicated in the accompanying organization chart.

The AEC and Production Corporation will submit annual budgets through the Coordinating Board for inclusion in the President's annual budget message to Congress. This will give both the President and Congress the opportunity to make an annual review of the programs and plans of the two agencies. All income from sale of atomic production and facilities will be deposited in the general fund of the U. S. treasury and will not be available for spending by the AEC or Production Corporation without specific authorization by Congress.

Philosophy of the Coordinating Board

The Coordinating Board simplifies the administrative functions by separating the responsibilities for research, production and military development into three separate administrative organs. At the same time, the all-important policy-making decisions become the function of a board with no administrative responsibilities. As befitting the importance of its decisions this board has cabinet rank. This is in accordance with the fundamental principle of our Constitution, which makes such decisions the province of members of the cabinet who are responsible politically to the executive and removable if the policies are not publicly acceptable. Continuity of the work is assured by having an administration that is thus insulated from changes in policy or in party politics. Inasmuch as the Coordinating Board will not sit permanently, the services of the best men in the country can be obtained.

Functions of the Production Corporation

The Production Corporation will be a government corporation for the manufacture of fissionable material. It will have the responsibility for operating the present producing plants of the government at Oak Ridge and Hanford. This corporation will have the power to lease or give contracts for operation of its facilities and also the right, with the approval of the Coordinating Board, to dispose of these plants by sale. It can do development work to improve its plants, or it can let contracts for this purpose.

The Production Corporation will supply fissionable material, with the approval of the Coordinating Board, to the military establishments, to the

Since its inception, NUCLEONICS has confined its editorial content to matters of technical interest. It will continue to do so. In this issue, an apparent exception to this policy has been made on a subject the editors believe to be of vital concern to every reader of this journal—the legislation governing the development of nucleonics in the United States. The proposals made in this editorial are offered in the public interest. *—The Publisher*

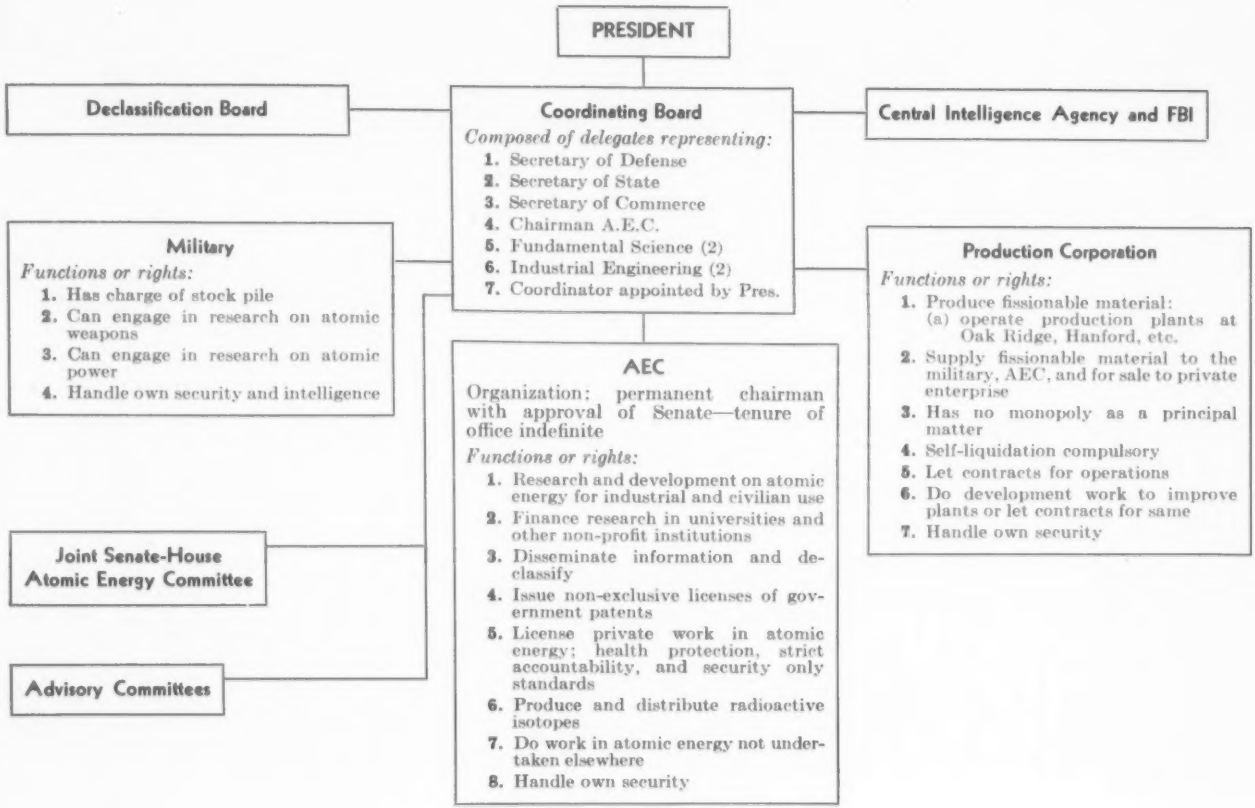
PRESIDENT
Declassification Board
Coordinating Board
Composed of delegates representing:
1. Secretary of Defense
2. Secretary of State
3. Secretary of Commerce
4. Chairman A.E.C.
5. Fundamental Science (2)
6. Industrial Engineering (2)
7. Coordinator appointed by Pres.
Central Intelligence Agency and FBI
Military
Functions or rights:
1. Has charge of stock pile
2. Can engage in research on atomic weapons
3. Can engage in research on atomic power
4. Handle own security and intelligence
Production Corporation
Functions or rights:
1. Produce fissionable material:
(a) operate production plants at Oak Ridge, Hanford, etc.
2. Supply fissionable material to the military, AEC, and for sale to private enterprise
3. Has no monopoly as a principal matter
4. Self-liquidation compulsory
5. Let contracts for operations
6. Do development work to improve plants or let contracts for same
7. Handle own security
Joint Senate-House Atomic Energy Committee
Advisory Committees
AEC
Organization: permanent chairman with approval of Senate—tenure of office indefinite
Functions or rights:
1. Research and development on atomic energy for industrial and civilian use
2. Finance research in universities and other non-profit institutions
3. Disseminate information and declassify
4. Issue non-exclusive licenses of government patents
5. License private work in atomic energy; health protection, strict accountability, and security only standards
6. Produce and distribute radioactive isotopes
7. Do work in atomic energy not undertaken elsewhere
8. Handle own security

AEC, and to private enterprise. The production of fissionable material by private firms during their operation of nuclear reactors does not come under the province of this corporation. The Production Corporation will be responsible for its own information and physical security, although it will be coordinated with other security systems as explained later.

Functions of the Military

As indicated by the organization chart and the functions of the Production Corporation, the Army, Navy and Air Force are given explicit rights to engage in research on atomic weapons and atomic power using fissionable material produced by the Production Corporation. The military is also given explicit rights to accumulate stock piles of atomic weapons according to its needs, as approved by the Coordinating Board. The military will be responsible for its own information and physical security, although it will be coordinated with others as explained later.

Because the military applications of atomic energy are for the time being of paramount importance to the defense of the American people, and because pre-eminence in this field is vital to our national existence, we have sought to include in the legislation provision for the widest participation of all qualified groups. Development of atomic weapons and atomic engines may well be decisive in another war; therefore this is a responsibility of the military as well as of the scientists. While we agree that science cannot flourish under military domination, we do not feel that the military arts should be subordinated to the leadership of the natural scientists.

Functions of the AEC

The function of the Atomic Energy Commission will be explicitly to carry on research and development of nuclear energy for its application to civilian and industrial uses, to produce and distribute radioisotopes, to finance research on basic science in universities and other non-profit organizations, and to conduct research on all phases of atomic energy, including production of fissionable material and nuclear weapons. It will have charge of its own security, and will cooperate with security organizations independently responsible for the information security of the military, the Production Corporation, and private firms, for the purpose of formulating uniform secrecy policies. The commission will have charge of the public dissemination of technical information consistent with security.

The Atomic Energy Commission will have the right to give non-exclusive licenses of government patents in atomic energy, and to authorize work in atomic energy by private individuals or corporations. The only standards governing the licensing of work in atomic energy will be standards of health protection, accountability, and security. The duties of the commission will include ensuring that strict account is taken of fissionable materials used by private parties and that work done on atomic energy is consistent with public health and national security. The commission has the primary responsibility for seeing that work in atomic energy is consistent with national security, and for administering security, clearance procedures, export regulations, and other general regulations.

The commission would continue its present function of producing radioisotopes and financing the early development of nuclear reactors.

In the absence of a national science foundation, it should continue to support fundamental research in physics, chemistry, and the life sciences, although logically, of course, this should not be its province.

Since the performance of the functions here outlined for the AEC makes possible a great reduction in the powers delegated to the commission by Congress, there seems no objection to having permanent commissioners. All the commissioners would, therefore, be appointed in the same manner as the department heads of the Bureau of Standards, with the approval of the Senate and with tenure indefinite.

Assisting Committees

The Joint Senate-House Committee on Atomic Energy would be continued. The Coordinating Board may also want to appoint such advisory committees as it deems necessary.

Security and Intelligence

The three main operating elements, the military, the Production Corporation and the AEC, will operate under substantially the same security regulations as are now enforced. The Federal Bureau of Investigation will continue to be responsible for the investigation of individuals presented for clearance. Obviously, the military is capable of handling its own security and intelligence. (It might be expedient for the AEC and Production Corporation to have a single security unit, instead of separate units as indicated. This is a question of convenience of administration.) Security for private industrial organizations will be the responsibility of the AEC security unit.

At the present time, private contractors are performing the most important functions of the Atomic Energy Commission, and there is no reason to believe that under a different legal setup, the same organizations will be less scrupulous about following security regulations. Everybody realizes that the main security of the United States rests not on keeping secrets, necessary and important as this is, but even more on outstripping all other nations in the development of atomic energy on all levels, scientific, industrial and military. This is the main advantage to security which this proposed legislation offers.

Provision for special security problems which are peculiar to atomic energy and not common to the other military developments, such as export regulations for uranium and other fissionable materials, and the dissemination of information, should be explicitly made in this bill.

Patent Provisions

Although many proposals and counter-proposals for the weakening or strengthening of the United States patent system have been advocated, we do not feel that a revision of the present patent laws should be attempted in atomic energy legislation. If it can be demonstrated that the present patent laws do not give sufficient protection to the interests of the American people, or sufficient stimulation to the development of inventions, new patent laws should be enacted by Congress. All the McMahon Act patent provisions will, therefore, simply be eliminated in this legislation.

Similarly, the anti-trust laws entered in the statute books effectively prevent monopoly in any field, and if in future circumstances they do not, the place to alter them is in a special anti-trust law, and not in atomic energy legislation. Therefore, the AEC is not given any special discretionary powers for giving or withholding patent licenses on interpretation of possible monopoly formations.

Keeping patent applications secret is a problem which atomic energy shares with many other military developments such as biological warfare and guided missiles, and a uniform procedure should be followed.

Because this is a new field, fears have been expressed that patents of such broad generalities can be obtained as

to stifle effectively further development. If this fear can be justified, and we do not believe that it can be, the remedy would be to provide that holders of patents of broad application should be required to grant non-exclusive licenses on a royalty basis. Patents of narrow applicability should remain valid as usual and as in any other field.

Compensation to the government for the use of its fissionable material should be in the form of a reasonable rental. In research and development under government contracts, the use of fissionable material should accordingly be treated as a government contribution and this should be taken into consideration in determining patent rights in government-sponsored research. These patent rights should depend on the various contributions, depending upon the kind of "know-how" contributed by industry, and the share of the cost borne by the government.

Summary of General Principles

All subjects which are not covered by explicit clauses in the preceding provisions are understood to function normally. For example: Mining and purchase of land containing source materials should proceed as for all other raw materials. This, and all other non-government contributions to the development of nuclear energy, should be allowed freely, provided provisions for strict accountability to AEC and AEC rights of inspection for purposes of security are met. In all these instances, the government rights stem from the need of strict accountability for materials, and not from any intrinsic rights of the government to monopolize production. Government expenditures for a certain development should be attuned to and justified in terms of the non-existence of private investment in the same development. The government should not engage in research and development work which is being widely pursued by the universities or private enterprise, but the government should engage in such fields where effort is lacking.

It is by no means the purpose of this bill to reduce the present extent of government support for nucleonics. Such support can, in fact, be augmented by this legislation. What is actually aimed at is to channel it in such a way that it will not displace other substantial sources of support. The sum effect of this proposed legislation will be to provide conditions under which competition between brains and enterprise will exist and assure accelerated advance in all fronts.

—*Walter M. DeCew*

The establishment of a supernational world government is an old idea of pacifists. Such a world government is not needed for the maintenance of peace, however, if democracy and an unhampered market economy prevail everywhere. Under free capitalism and free trade no special provisions or international institutions are required to safeguard peace. Where there is no discrimination against foreigners, when everyone is free to live and to work where he likes, there are no longer causes for war. —*Ludwig von Mises, "Omnipotent Government," (Yale University Press, New Haven, 1944)*

Neutron Diffraction and Associated Studies—I*

Neutron diffraction techniques are reviewed and compared with similar X-ray diffraction techniques. The experimental and theoretical description of the interaction of neutrons with crystals, molecules, and nuclei is presented and related to present and potential applications to metallurgy, crystal structure, and certain fundamental nuclear studies

By E. O. WOLLAN and C. G. SHULL

Oak Ridge National Laboratory, Oak Ridge, Tennessee

THE NEUTRON was discovered by Chadwick (*1*) in 1932. It entered the arena of known fundamental particles after the discovery of the quantum theory and after the experimental verification that material particles possess wave properties and hence exhibit interference effects similar to those observed with electromagnetic radiation. The early theoretical treatment of the interaction of neutrons with nuclei, as developed by Fermi (*2*) and extended by Wick (*3*), pointed to some of the interference effects which might be expected in the scattering of neutrons by crystalline media. The theory of the interaction of slow neutrons with crystals and molecules was subsequently extended by a number of investigators (*20–27*) and much of this theoretical work had to anticipate experimental verification at a later date when stronger neutron sources became available.

Early experiments designed to demonstrate the coherent scattering of neutrons by crystals were performed with Ra-Be sources which were embedded in paraffin for the purpose of slowing down the fast neutrons from the source. With such sources, Von Halban (*4*) and Preiswerk (*5*), and Mitchell and Powers (*6*) carried out experiments that showed small effects due to the diffraction of neutrons by crystals. The intensities available were, however, only sufficient to demonstrate the existence of interference effects, but did not permit any direct check of the theories to be made.

One application in which the Ra-Be source technique was found to give results of a more or less quantitative nature was in connection with the scattering cross-section measurements of ortho- and parahydrogen, in which interference effects in the scattering by hydrogen molecules is involved. The theory of this was worked out by Schwinger and Teller (*7*), and experimental verification has been obtained by several investigators (*8, 9*).

The interference effects between neutrons and electrons is evidenced in the experiments of Whitaker and Beyer (*10*) on the scattering of neutrons in paramagnetic substances and in the polarization experiments of Alvarez and Bloch (*11*) involving the scattering by magnetized iron. More recently, further observations involving neutron diffraction effects have been obtained by Anderson, Fermi and Marshall (*12*) who observed the lowering of the average temperature of neutrons transmitted through large thicknesses of graphite and in the experiments by Rainwater

* Part II, the second half of this paper, will be published next month.

and Havens (*13*) in which the transmission of neutrons through graphite was measured as a function of the energy. These latter experiments showed the transmission cross section to possess an energy-dependent structure corresponding to the successive diffraction of neutrons from various planes within the crystal.

The development of chain reactors has given us sources of slow neutrons of very much greater intensity than those previously available and it is now possible to make quantitative measurements of neutron diffraction effects comparable to similar measurements in the field of X-rays. The first measurements of the diffraction by single crystals using neutrons from a chain reactor were made by Zinn (*14*) with the Argonne reactor and by Borst (*15*) with the Oak Ridge reactor.

Neutrons from a Chain Reactor

A large fraction of the neutrons from a slow neutron chain reactor are in approximate thermal equilibrium with the atoms of the moderator material and hence these neutrons have an energy distribution which is approximately Maxwellian. The usual kinetic theory relationship, energy $= kT$, where k is the Boltzmann constant and T is the absolute temperature, applies as well to the neutrons that have been completely slowed down in a moderating material as to the molecules that make up that material. For a room temperature neutron ($T = 300°$ K), the energy equals 0.026 electron volts and the velocity is about 2200 meters per second.

The wavelength associated with a neutron can be obtained from the de Broglie relation $\lambda = h/mv = h/\sqrt{2mE}$ where h is Planck's constant, m is the neutron mass, v is the velocity and E is the energy of the neutron. For a 300° K neutron the wavelength is 1.8 A.U. and for the thermal neutrons from the Oak Ridge reactor the maximum of the Maxwellian distribution corresponds to a wavelength of about 1 A.U. and an energy of about 0.07 ev. There is sufficient intensity in the available beams of thermal neutrons so that some diffraction experiments can be performed over a large range of neutron wavelengths from about 5 A.U. to 0.02 A.U. which corresponds to the range of wavelengths commonly used in X-ray work.

Diffraction of Neutrons by a Single Crystal

Since slow neutrons have wavelengths comparable to those encountered with X-rays, it is to be expected that the diffraction effects observed when a sufficiently intense beam of neutrons falls on a crystal will be similar to the X-ray case. Although the neutron beams, obtainable from the present chain reactors, are not yet of as high an intensity as corresponding beams from a good X-ray tube, most of the X-ray techniques can now be used with neutrons. One disadvantage for some problems is the fact that no monochromatic emission lines exist in the neutron spectrum. One can, however, obtain a monochromatic beam by reflection from a single crystal which then picks out a narrow wavelength band from the continuous spectrum.

The apparatus used in neutron diffraction studies is essentially of the same form as that used in corresponding X-ray studies. As a typical single crystal spectrometer, there is shown in Fig. 1 the instrument used by Zinn (*14*). Other types of spectrometers will be discussed later in connection with other applications. A beam of neutrons from the pile is collimated by slits of Cd, boron, or some other good neutron absorber and this beam is passed over the center of the spectrometer table on which the crystal is located. The diffracted radiation is

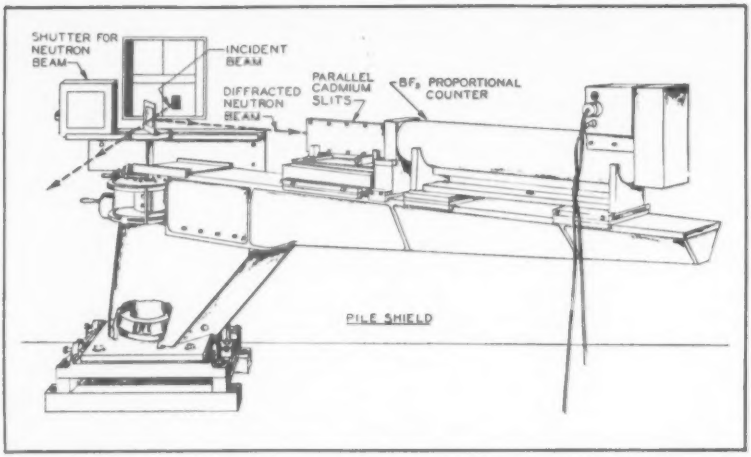

FIG. 1. A single crystal neutron spectrometer. (Zinn)

usually measured by having it pass along the axis of a long proportional counter filled with BF_3 in which the boron is enriched in B^{10} for greater neutron absorption.

A typical counter which has been used is 18 inches long and 2 inches in diameter and contains the enriched BF_3 at 30 cm Hg pressure. Such a counter will absorb about 80% of the neutrons of thermal energy ($E = 0.025$ ev) which traverse its entire length. The percent absorption can be calculated in the usual way from the relation $I = I_0 e^{-Nl\sigma}$ where N is the total number of boron atoms per cm^3 of the gas, l is the length of the counter, and σ is the absorption cross section which for B^{10} at $E = 0.025$ ev equals 3,500 barns (1 barn = 10^{-24} cm^2). The cross section of boron decreases as $1/v$, where v is the velocity of the neutrons; hence the efficiency of the detector decreases as the neutron energy increases.

In using such counters near a pile it is necessary to shield them against stray radiation. Shields containing ½ inch of powdered B_4C around the counter, with several inches of paraffin around this for the purpose of slowing down the stray fast neutrons, have been found satisfactory for most of the work. This heavily shielded detector makes it necessary to construct neutron spectrometers more sturdily than the usual X-ray instruments.

As an example of the reflection of neutrons by a single crystal, a rocking curve for a crystal of NaCl is shown in Fig. 2. The crystal was, in this case, the second in a double crystal arrangement of the type shown in Fig. 9.* The first crystal was used to pick out a monochromatic beam from the neutron spectrum and the curve of Fig. 2 gives the intensity as a function of the angle of setting of the second crystal. The width of this curve is not a measure of the energy spread since there is a focusing effect in the parallel position (1, −1) in which it was taken.

The narrowness of the energy band reflected from a crystal will be determined by the perfection of the crystal

* Fig. 9 is contained in Part II of this paper.

and by the degree of collimation of the neutron beam. The resolving power attainable at present is dictated primarily by the available neutron intensities. In the thermal region from about 0.01 ev up to about 0.3 ev, there is sufficient intensity from the present reactors so that accurate measurements of resonance line widths (~ 0.1 ev) can be made without difficulty. At the lower end of the thermal region (below ~ 0.03 ev), difficulties arise from the effects of higher orders.

This difficulty can be understood from Fig. 3 which shows the thermal neutron radiation from a pile as studied with a single crystal of NaCl. At any given setting of the crystal, neutrons of one wavelength or energy, λ_1 or E_1,

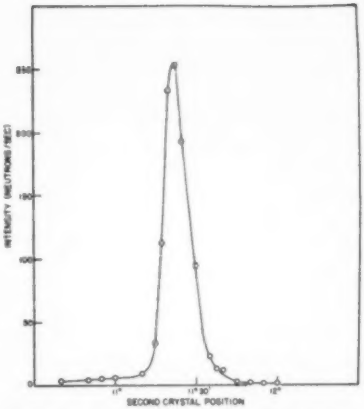

FIG. 2. Rocking curve for Bragg reflection from second NaCl crystal in (1, −1) position of a double crystal arrangement

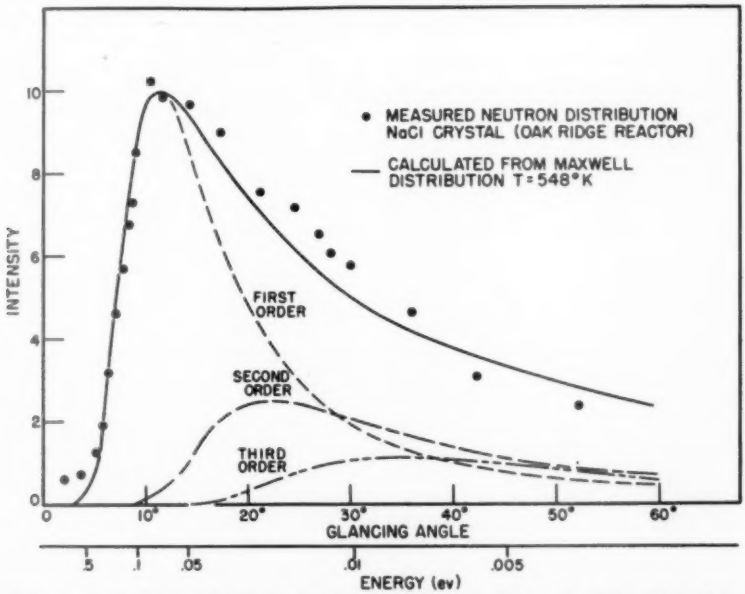

FIG. 3. Comparison of the calculated and the measured intensity distribution of the neutrons from the Oak Ridge reactor as obtained by reflection from a NaCl crystal. The curves were calculated by Seitz and Goldberger for a Maxwell distribution of neutron velocities with the temperature adjusted to fit the data. The fit of the measured and calculated curves shows that the intensity vs. energy curve for the reactor neutrons can be represented by the Maxwell distribution given by the first-order curve. The effect of higher orders is seen to distort the measurements for neutron energies to the right of the maximum

will be reflected in the first order, while neutrons of $\lambda_2 = \frac{1}{2}\lambda_1$ or $E_2 = 4E_1$ will be reflected in the second order. The relative amounts of first and higher orders for an NaCl crystal are shown.

The difficulty due to higher orders can to some extent be overcome by the proper choice of crystal. With a crystal of LiF, cut so that the reflections from the (111) planes are used, there will be zero intensity from the second order. In the region above thermal, where the neutron intensity from a reactor will in some cases drop off approximately as dE/E, higher orders will be suppressed by the reduced neutron intensity at higher energies. In the very-low-energy region, the best studies have been made with mechanical velocity selectors and by the modulated cyclotron method.

Measurements of Resonance Absorption

Before the development of chain reactors, the modulated cyclotron constituted the main tool for studying neutron resonance and other energy-dependent phenomena in the thermal and near-thermal region. With the neutron intensities now available from reactors, neutron diffraction gives us a second method for studying such phenomena. Each of these methods has advantages and disadvantages. The diffraction process allows a monoenergetic beam to be isolated in space and this admits of certain applications such as the activation of resonance detectors with neutrons of a given energy. The cyclotron time-of-flight method, which has been brought to a high stage of development during the past few years, can be used over a greater energy range than the crystal diffraction method. The diffraction method has, however, not yet been exploited to its full capabilities, especially since higher-flux reactors are being contemplated. It would seem also that the time-of-flight method may have the prospect of a greater potential range as new developments in high-speed detectors progress. In any case, both these techniques will find useful applications.

In attempting to obtain neutron beams of high intensity and with good resolution, three different crystal spectrometer arrangements have been used. Borst, Ulrich, Osborn and Hasbrouck (*15*) have used a modification of the Johansson-type reflection bent-crystal spectrometer. This type of spectrometer gives a large crystal aperture at large angles, but the aperture and the available intensity become small at higher neutron energies. This arrangement offers a distinct advantage, however, when transmission measurements are to be made on a strongly radioactive sample of which only a limited amount of material is available. Such a sample can be placed at the source slit, which in this instrument is located within the pile shield far from the detector so that the detector cannot be materially influenced by the strong gamma radiation from the source.

A bent crystal spectrometer of the transmission type, similar to that developed by Cauchois for X-ray work, has been adapted for neutron diffraction studies by Sawyer, Wollan, Bernstein and Peterson (*16*). This type of instrument has the advantage over the reflection type in that the focusing properties improve as the Bragg angle becomes smaller. It also has the advantage of allowing a large neutron beam to be used at small angles where the intensity difficulties are greatest.

The transmission spectrometer is probably the best type of crystal arrangement for obtaining a high-intensity beam with good resolution for work at small angles, i.e., at higher energies. Greater precision can be built into such an instrument than was done by Sawyer, *et al.* Recently DuMond (*17*) constructed such a spectrometer for

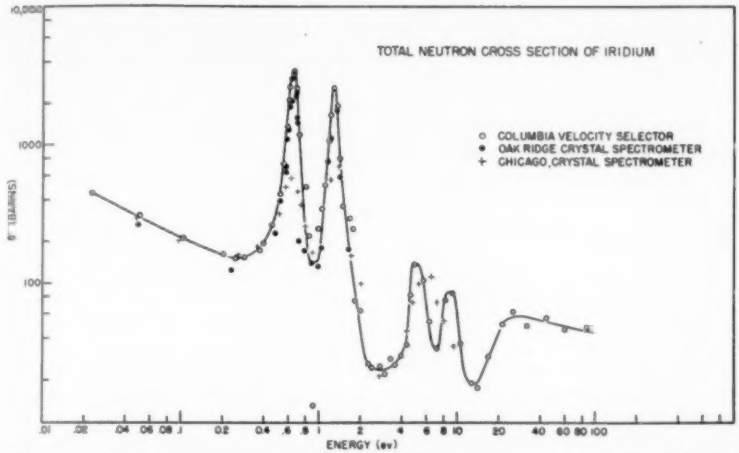

FIG. 4. The total neutron cross section of iridium as measured with the Columbia cyclotron time-of-flight method and with crystal spectrometers using neutrons from the Argonne and Oak Ridge reactors

the study of hard X-rays and gamma rays. With this instrument he has obtained a resolving power of about 100 with gamma rays of 1.75 Mev. If this were translated to the neutron case, a resolving power of 100 would be attainable with neutrons having energies of about 100 ev. Whether this can actually be attained or not depends to a great extent on the available neutron intensity. Sufficient intensity may be available from new reactors now being considered.

The most extensive work on the study of resonance absorption lines with a neutron crystal spectrometer has been carried on by Sturm (*18*) using a flat crystal arrangement. To increase the intensity, a number of flat crystals of LiF were lined up on the spectrometer table to give a large crystal area. With this instrument, resonance lines have been observed out to neutron energies of about 20 ev.

It is not the purpose of this paper to discuss the subject of resonance absorption except in so far as it illustrates the application of neutron diffraction to studies of this type. Such measurements can be carried out with high precision in the near thermal region. The Breit-Wigner constants for a number of low-energy resonance levels have been well determined by both the crystal spectrometer and the cyclotron time-of-flight methods (*19*). As the neutron energy becomes greater than about 1 ev, the resolution of the instruments becomes progressively poorer in relation to line widths to be measured.

A comparison of results obtained with crystal spectrometers and with the time-of-flight method by Rainwater and Havens (*19*) is shown in Fig. 4. The results of Sturm were carried out with reduced resolving power to permit measurements to be made to about 10 ev.

The Study of Crystal, Molecular and Nuclear Properties

Although neutron diffraction will constitute a useful tool for obtaining monoenergetic neutron beams for the study of resonance absorption and other energy-dependent phenomena, its great-

est application will probably be as partner to the X-ray and electron diffraction techniques for studying crystal and molecular structure. In at least one important respect, that of locating hydrogen positions, neutrons have a decided advantage over X-rays and electrons. The study of the interaction of neutrons with nuclei is an application of the diffraction technique which also promises to be of considerable significance. The remainder of this paper will deal primarily with these subjects.

The field is still very young and hence the work which has been done to date can be considered as only laying the ground work for studies in this field. The experimental work done so far has shown to some extent the potentialities of the method and it has shown that the underlying theory of the interaction of neutrons with crystals, molecules and with nuclei is in general well understood.

Theoretical Considerations

Although the scattering of slow neutrons and the scattering of X-rays are in many respects very similar problems, there are some distinct differences which make the scattering of slow neutrons a field in itself.

With X-rays, the atomic electrons are the scattering entities and the cross section for scattering by a single electron can be accurately calculated. On the basis of classical theory, one obtains the well-known Thomson formula which is valid for bound electrons. A free electron, however, takes up momentum from the incident photon and in this case one must apply quantum theory which leads to the Klein-Nishina Compton scattering formula. The scattering by an atom is obtained by summing up the scattering amplitudes of all the electrons with respect to their relative positions in the atom. This gives the atomic scattering factor which is defined in terms of the relative scattering by the whole atom to that of a single bound electron. With X-rays these atomic scattering factors can be determined experimentally; they can also be determined theoretically by the method of self-consistent fields.

With neutrons the scattering is almost entirely nuclear and since so little is known about nuclear structure, it is not expected that scattering cross sections can in general be determined theoretically. Aside from this fundamentally different mechanism of scattering, there exists a number of other basic differences between neutron and X-ray diffraction which will be of interest in connection with the experimental data. A general review of these is given in the following sections. Details on these discussion points can be found in earlier papers (*2*, *3*, *7*, *20–27*).

Scattering Theory. The theory of the scattering of neutrons by nuclei gives a relation between the scattering amplitude and the nuclear potential. For the case of slow neutrons, the theory is simplified by the fact that there is only *s* scattering which is spherically symmetric.

The wave equation representing the interaction of a neutron with a nucleus is

$$\nabla^2\Psi + k'^2\Psi = 0 \qquad (1)$$

where $k' = \sqrt{2m(E - V)/\hbar^2}$ is the wave number inside the nucleus whose potential function is $V(r)$. Correspondingly, the incident wave is represented by the same equation with $V = 0$ and then $k = \sqrt{2mE/\hbar^2} = 2\pi/\lambda$ where λ is the wavelength of the incident neutrons.

The solution of the wave equation (*28*) at large distances r from the nucleus (neglecting absorption) can be represented as the sum of an incident plane wave (along z) and a radially scattered wave

$$\Psi = e^{ikz} + f\frac{e^{ikr}}{r} \qquad (2)$$

where f is the amplitude of the scattered wave.

It can be readily shown that f depends on the phase shift of the total wave with respect to the incident wave and this phase shift depends on the nuclear potential $V(r)$. For slow neutrons there is only s scattering and, in this case, only the spherically symmetric part of the solution need be considered. The spherically symmetric part of the incident plane wave can be represented as the sum of an incoming and an outgoing wave

$$\frac{\sin kr}{kr} = \frac{e^{ikr} - e^{-ikr}}{2ikr} \qquad (3)$$

The corresponding spherically symmetric part of the total wave with the nuclear potential turned on will be given by the same function with different phase,

$$\frac{A \sin (kr + \eta_0)}{kr} = \frac{Ae^{i(kr+\eta_0)} - Ae^{-i(kr+\eta_0)}}{2ikr} \qquad (4)$$

The difference between Eqs. 3 and 4 will then represent the scattered wave

$$f\frac{e^{ikr}}{r} = \frac{(Ae^{i\eta_0} - 1)e^{ikr} - (Ae^{-i\eta_0} - 1)e^{-ikr}}{2ikr} \qquad (5)$$

In the scattered wave, however, there must be no incoming wave and for this condition to be satisfied, $A = e^{i\eta_0}$. Substituting this value for A back into Eq. 5 gives

$$f = \frac{(e^{2i\eta_0} - 1)}{2ik} \qquad (6)$$

and the cross section for scattering will be

$$\sigma_{scat} = 4\pi|f|^2 = \frac{4\pi \sin^2 \eta_0}{k^2} \qquad (7)$$

The phase shift η_0 is very small except in the near vicinity of a resonance level. Hence in most cases, only the first power of η_0 in the expansion of Eq. 7 need be considered so that

$$f = \frac{\eta_0}{k} \qquad (8)$$

and

$$\sigma = 4\pi\frac{\eta_0^2}{k^2} \qquad (9)$$

The phase shift η_0 can be given a simple geometrical interpretation in terms of a square potential well interaction between the neutron and the nucleus. The wave inside of the nuclear potential will have a very short wavelength and must be joined smoothly to the outside wave with equal value and slope at the edge of the well. This can in general be done only if the amplitude inside is small compared to its value outside of the nucleus. This is shown schematically in Fig. 5 in which the dotted curves show the unperturbed wave and the broken-line curves show the total wave fitted at the edge of the well. Curve A represents the case of a negative and curve B a positive phase shift. A negative phase shift has been taken by Fermi and Marshall (*29*) to correspond to a positive scattering amplitude which corresponds in the figure to the linear displacement of the two waves. Likewise, a positive phase shift has been taken as a negative scattering amplitude. This convention corresponds to taking the sign before the second term in Eq. 2 as negative. At a resonance level, the phase shift becomes $\pi/2$ and the amplitude of the wave inside the nucleus becomes equal to that of the outside wave, as shown in curve C of Fig. 5.

Small positive and negative phase shifts between total wave and unperturbed wave correspond to negative and positive scattering amplitudes (F and M convention) and hence the corresponding scattered waves will be 180 deg out of phase with each other. These phase differences in scattered waves can be determined in a variety of scattering experiments which will be

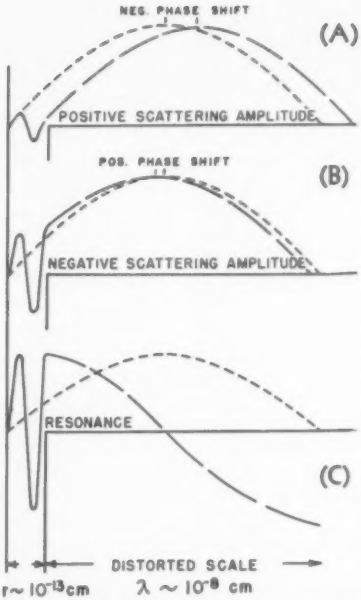

FIG. 5. Illustration of the phase shift in nuclear scattering and the corresponding positive and negative scattering amplitudes. The dotted curve represents the unperturbed incident wave and the broken line the total neutron wave which is made to fit the inside neutron wave in magnitude and slope at the nuclear radius. The amplitude of the inside wave is very small except in the very near vicinity of a resonance, but because of the very distorted linear scale the smallness of the inside wave is not properly represented

described in later sections. It is evident from a consideration of curves A and B in Fig. 5 that positive scattering amplitudes will be much more probable than negative scattering amplitudes since the latter will be observed only in the near vicinity of a resonance level. Negative scattering amplitudes will be most probable with nuclei of low atomic number since resonance level widths are greater for low Z.

It can be shown that the phase shift depends on the volume integral of the nuclear potential

$$\eta_0 = -C \int_0^\infty V(r) r^2 dr \qquad (10)$$

so that a knowledge of either the nuclear potential or the range of nuclear forces will give information on the other if the scattering amplitude has been measured.

For hydrogen the scattering cross section can be evaluated in terms of the binding energy and the range of forces in the triplet and singlet state of the deuteron. With heavy elements for which the nucleus behaves in most cases as an impenetrable sphere, rough estimates of the cross section can be made by taking $\sigma = 4\pi a^2$, where the radius a is approximately equal to the nuclear radius as obtained from other sources of information.

Binding, Isotope, and Spin Effects. The scattering cross section for a given nucleus depends on whether the nucleus is in a free or a bound state. The cross section for scattering by a rigidly bound nucleus will be greater than for the same nucleus in a free state by the square of the ratio of the neutron mass to the reduced mass for the neutron and scattering nucleus, i.e., $[(A + 1)/A]^2$, where A is the mass number of the scattering nucleus. Between the regions of completely free scattering centers and completely bound centers, there may be a more or less continuous gradation of partial binding for which the reduced mass effect will lie in the range from $[(A + 1)/A]^2$ to 1. The coherent scattering by crystals will always correspond to rigidly bound scattering centers.

When scattering measurements are made on an element containing more than one isotope the results will correspond to an average of the scattering by these isotopes. If the measurements are made with free nuclei, the total scattering cross section averaged over the isotopes will be

$$\sigma_f = 4\pi(p_1 a_1^2 + p_2 a_2^2 + \cdots) \qquad (11)$$

where the p's are the isotopic abundances and the a's are the free nuclear scattering amplitudes for the respective isotopes. If the atoms are bound but still act independently as far as interference effects are concerned, the corresponding cross section will be

$$\sigma_b = \sigma_f[(A+1)/A]^2$$
$$= 4\pi(p_1 f_1^2 + p_2 f_2^2 + \cdots) \quad (12)$$

where the f's are the scattering amplitudes for bound scattering centers.

The coherent scattering by the various isotopes of an element randomly distributed in a crystal will be

$$\sigma_{coh} = 4\pi(p_1 f_1 + p_2 f_2 + \cdots)^2 \quad (13)$$

since here the isotopic amplitudes must be combined algebraically into a total amplitude before squaring to obtain the intensity.

A situation similar to that of the isotope effect arises from the fact that neutron scattering may depend on the relative orientations of the spins of the neutron and the scattering nucleus. There will then be two amplitudes associated with each nucleus, one for parallel and one for antiparallel spins. The measured scattering cross section for a given nuclear species will then correspond to an average, weighted with respect to the probability for the two spin states. For scattering by free nuclei then

$$\sigma_f = 4\pi\left[\frac{i+1}{2i+1}\,a^2_{i+\frac{1}{2}} + \frac{i}{2i+1}\,a^2_{i-\frac{1}{2}}\right] \quad (14)$$

where i is the spin of the scattering nucleus and the a's are the free scattering amplitudes for parallel and antiparallel spin. For the coherent scattering by bound nuclei

$$\sigma_{coh} = 4\pi\left[\frac{i+1}{2i+1}\,f_{i+\frac{1}{2}} + \frac{i}{2i+1}\,f_{i-\frac{1}{2}}\right]^2. \quad (15)$$

These equations apply to the case where the nuclear spins are randomly oriented. In the case of ortho- and parahydrogen the situation is different since the spins of the two nuclei in the molecule have a definite orientation.

Scattering by Crystals. The theory of the diffraction of neutrons by crystals is too involved to take up in this article. The subject has been treated in its several phases by a number of investigators and it has been found that as far as coherent nuclear scattering is concerned the equations obtained for neutron diffraction are identical to the corresponding ones in X-ray diffraction theory with the polarization factor omitted. The differences which one observes in the Bragg scattering of neutrons and X-rays then results from the differences in the cross sections for the nuclear scattering of neutrons and the electronic scattering of X-rays.

The inelastic scattering effects observed with neutrons and X-rays may be quite different. This will be true whether the scattering takes place from a crystal or from a free atom or molecule. With X-rays the diffuse scattering consists of the Compton inelastic scattering and the temperature diffuse scattering, some of which may be inelastic. According to the Debye theory, the temperature diffuse scattering is given for a single crystal by $(1 - e^{-2W})f_0^2$ where f_0 is the atomic structure factor and W is given by Eq. 23.* This theory has been extended by Zachariasen (*30*) to include the quantized interaction of the radiation with the Debye waves of the crystal. For the neutron case, the corresponding theory has been developed by Weinstock (*24*) and extended by Seitz and Goldberger (*26*) and Finkelstein (*27*).

In the case of neutrons there will also be diffuse scattering arising from the spin and isotope effects. The over-all scattering by a crystal will be made up of the coherent Bragg scattering plus the diffuse scattering arising from

* Eq. 23 is contained in Part II of this paper.

various sources. The total scattering cross section for a crystal as measured, for example, by a transmission experiment with correction for the effects of absorption, can be written as

$$\sigma_{crystal} = \sigma_{Bragg} + \sigma_{DS} + \sigma_{DI} + \sigma_{DT}$$

where σ_{Bragg} is the total scattering in the Bragg peaks and σ_{DS}, σ_{DI} and σ_{DT} are the diffuse scattering cross sections for the spin, isotope and temperature effects, respectively.

As an example of the diffuse scattering arising from the spin effect, consider a crystal containing an element of one isotope ($\sigma_{DI} = 0$) and having a high characteristic temperature ($\sigma_{DT} \sim 0$) and if in addition A is large, then $[(A + 1)/A]^2 \sim 1$ and we obtain

$$\begin{aligned}\sigma_{DS} &= \sigma_{crystal} - \sigma_{Bragg} \\ &= 4\pi\left[\frac{i+1}{2i+1} f^2_{i+\frac{1}{2}} + \frac{i}{2i+1} f^2_{i-\frac{1}{2}}\right] \\ &\quad - 4\pi\left[\frac{i+1}{2i+1} f_{i+\frac{1}{2}} + \frac{i}{2i+1} f_{i-\frac{1}{2}}\right]^2 \\ &= 4\pi \frac{i(i+1)}{(2i+1)^2}[f_{i+\frac{1}{2}} - f_{i-\frac{1}{2}}]^2 \qquad (17)\end{aligned}$$

It will be seen from this equation that the diffuse scattering due to the spin dependence will be zero when the scattering amplitudes for parallel and antiparallel spins are equal. This will be the case for a nucleus with zero spin. The other extreme is reached when the two spin amplitudes are equal in magnitude but opposite in sign, in which case there will be no Bragg peaks from a crystal, all scattering being diffuse.

A situation similar to the one we have discussed here for the spin dependence will also exist with respect to the scattering by an element containing more than one isotope.

Transmission Measurements with Crystalline Powders

One of the new techniques which has been developed for the study of neutron diffraction effects is that of the transmission of slow neutrons through powder samples. This technique is referred to as new since an equivalent technique with X-rays or electrons is not at all feasible, as will be understood from later discussion.

Early experiments on the scattering cross section of iron by Whitaker and Beyer (*10*), as determined with thermal neutron radiation, showed pronounced differences depending upon the structural state of the sample, i.e., whether the sample was a single crystal or a powdered agglomerate. In explaining these differences theoretically, Halpern, Hamermesh and Johnson (*20*) derived an expression for the transmission cross section of a powdered crystal as a function of the neutron energy or wavelength λ as follows

$$\sigma_{trans} = \frac{\lambda^2 N}{8} \sum_{hkl} j_{hkl}\, d_{hkl}\, e^{-2W}\, R_{hkl}\, \sigma_b \qquad (18)$$

with the summation carried over all Bragg peaks (hkl) permitted for the wavelength λ by the Bragg relationship and where

$$R_{hkl} = \sum_{\substack{\text{unit} \\ \text{cell}}} \exp\,[2\pi i(hx + ky + lz)], \qquad (19)$$

summed over all atomic positions (x, y, z) in the unit cell.* In this, N is the number of unit cells per cm^3, j_{hkl} is the multiplicity value for the particular reflection, d_{hkl} is the interplanar spacing, e^{-2W} is the temperature correction factor necessary to correct for thermal oscillations of the atoms about their mean position, and σ_b is the scattering cross section of an individual bound nucleus. The Bragg relation $\lambda = 2d \sin\theta$ restricts the reflections to those planes for which $d_{hkl} \geqq \lambda/2$, so that for large λ only a few planes may be contributing to the transmission cross section. As λ is changed, the trans-

* The unit cell is defined as the smallest volume element which describes the geometrical configuration of the crystal structure. The complete crystal can be be made up of a series of unit cells which are displaced translationally from a unit cell at the origin.

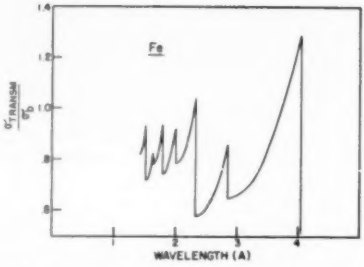

FIG. 6. Calculated transmission curve for Fe showing the abrupt changes in transmission at $\lambda = 2d_{hkl}$. (Halpern, Hamermesh and Johnson)

mission cross section varies drastically and even shows discontinuous changes or jumps at wavelengths corresponding to the appearance of the individual Bragg reflections. Halpern, Hamermesh and Johnson have calculated σ_{trans} for the case of iron powder as shown in Fig. 6. For wavelengths sufficiently large so that $d_{hkl} \geq \lambda/2$ is not satisfied, the cross section calculated from Eq. 18 becomes zero because there can be no coherent scattering. In practice, however, this may not be the case because of the presence of either crystal imperfections or spin or isotopic effects, as will be discussed later.

Fermi, Sturm and Sachs (*31*) have published experimental data on Be and BeO which agree well with the formula given by Eq. 18. By using either a mechanical velocity selector or a crystal monochromator with the thermal radiation from a pile, they were able to study the transmission cross section for finely powdered samples of these materials in the wavelength range from 0.40 to 4.5 A.U. Their curve for BeO is reproduced in Fig. 7. For a compound containing two different scattering centers, Eq. 18 must be modified slightly. The resultant calculated curve depends strongly on the relative phase of scattering for the two nuclei as well as on the spin dependence of the

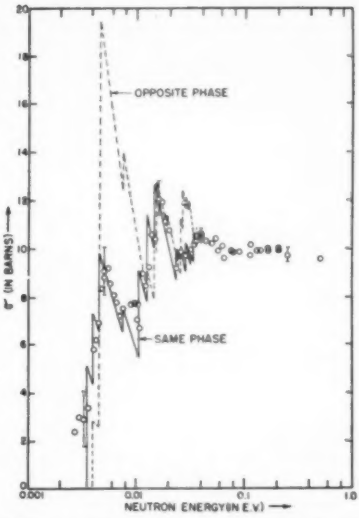

FIG. 7. Experimental and calculated total cross section as a function of neutron energy for BeO, showing the effects of the Bragg reflections from various planes in the crystal. The dashed and solid curves calculated for the same and opposite phase of scattering for the two centers show agreement with the data for the same phase. (Fermi, Sachs and Sturm)

scattering by Be and O. Curves calculated for the cases of the same and opposite phases of scattering for Be and O with the assumption of no spin dependence are shown in Fig. 7 for comparison with the experimental data. This comparison shows without doubt that the phases are the same and indicates that, if there is any spin dependence, it has a small effect on the observed transmission.

As has been previously pointed out (see Eq. 17), a monoisotopic element, for which the scattering amplitudes for parallel and antiparallel spin (of nucleus and neutron) are equal, will have no spin or isotope diffuse scattering and practically all of the scattering will be located in the Bragg peaks. In such a case, a curve of the type shown in

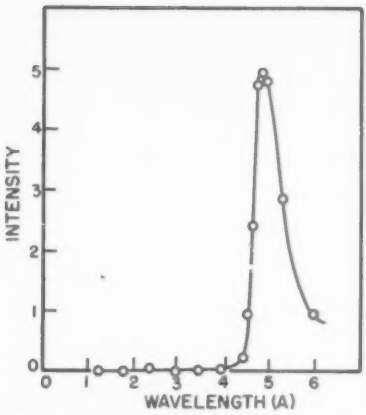

FIG. 8. Neutron spectrum resulting from transmission of pile neutrons through a long column of BeO. (Fermi and Marshall)

Fig. 7 will drop to a very low intensity (give a high transmission) for neutron energies below the first permissible Bragg peak. A measurement of the transmission of neutrons of energy below that corresponding to the first Bragg peak will then give information regarding the spin dependence of scattering by monoisotopic elements. Fermi and Marshall (*32*) have used this technique to show that the scattering by Be, Al and Bi has, if any, only a small spin dependence.

The small spin dependence of scattering by these elements has been used to obtain beams of long wavelength by filtering the neutrons through thick layers of BeO. The Bragg scattering cuts out the neutrons of wavelength greater than the first permissible peak and allows neutrons of larger wavelength to be transmitted with little loss. A spectrum of the neutrons transmitted by a long column of BeO is shown in Fig. 8. These low energy neutron beams are useful in other applications.

Powdered crystal transmission experiments have also been performed by the Columbia University group with the modulated cyclotron time-of-flight method for obtaining monoenergetic neutrons. For instance Wu, Rainwater and Havens (*33*) report pronounced crystal interference effects in the transmission cross section for columbium and germanium. This instrument has been used primarily in studying resonance levels of many nuclei at energies above those where crystal effects are prominent and no quantitative interpretation of the interference effects has been made.

Since a transmission measurement of the total cross section includes both the capture (or absorption) cross section and the scattering cross section, it is obvious that crystal interference effects are best studied for materials showing small capture. In fact, if the capture cross section becomes much larger than the scattering cross section it becomes almost impossible to use this technique. For this reason, experiments such as these cannot in general be performed with an X-ray or electron beam since, for these cases, the scattering efficiency is reduced to a very small value. Compton scattering, photoelectric absorption and other forms of inelastic scattering processes predominate so that the coherent scattering, interference effects, are washed out.

BIBLIOGRAPHY

1. J. Chadwick, *Proc. Roy. Soc.* **A136,** 692 (1932)
2. E. Fermi, *Ricerca sci.* **7,** part 2, 13 (1936)
3. G. C. Wick, *Physik. Z.* **38,** 403 (1937)
4. H. Von Halban, P. Preiswerk, *Compt. rend.* **203,** 73 (1936)
5. P. Preiswerk, *Helv. Phys. Acta.* **10,** 400 (1937)
6. D. P. Mitchell, P. N. Powers, *Phys. Rev.* **55,** 1101 (1939)
7. J. Schwinger, E. Teller, *Phys. Rev.* **52,** 286 (1937)
8. J. Halpern, I. Esterman, O. C. Simpson, O. Stern, *Phys. Rev.* **52,** 142 (1937)
9. F. G. Brickwedde, J. R. Dunning, H. J. Hoge, J. H. Manley, *Phys. Rev.* **54,** 266 (1938)
10. M. D. Whitaker, H. G. Beyer, *Phys. Rev.* **55,** 1101 (1939); with J. R. Dunning, *Phys. Rev.* **54,** 771 (1938)

11. L. W. Alvarez, F. Bloch, *Phys. Rev.* **57,** 111 (1940)
12. H. Anderson, E. Fermi, L. Marshall, *Phys. Rev.* **70,** 815 (1946)
13. L. J. Rainwater, *et al.* See review paper in reference *19*
14. W. H. Zinn, *Phys. Rev.* **70,** 102A (1946); *Phys. Rev.* **71,** 752 (1947)
15. L. B. Borst, A. J. Ulrich, C. L. Osborne, B. Hasbrouck, *Phys. Rev.* **70,** 108A (1946), *Phys. Rev.* **70,** 557 (1946)
16. R. B. Sawyer, E. O. Wollan, S. Bernstein, K. C. Peterson, *Phys. Rev.* **72,** 109 (1947)
17. J. W. M. DuMond, *Rev. Sci. Instr.* **18,** 626 (1947)
18. W. J. Sturm, *Phys. Rev.* **71,** 757 (1947)
19. L. J. Rainwater, W. W. Havens, C. S. Wu, J. R. Dunning, *Phys. Rev.* **71,** 65 (1947); see also H. H. Goldsmith, H W. Ibser, B. T. Feld, *Revs. Mod. Phys.* **19,** 259 (1947) in which resonance cross section measurements from several sources are brought together.
20. O. Halpern, M. Hamermesh, M. H. Johnson, *Phys. Rev.* **59,** 981 (1941)
21. H. A. Bethe, *Revs. Mod. Phys.* **9,** 69 (1937); also "Elementary Nuclear Theory," (John Wiley & Sons, Inc., New York, N. Y., 1947)
22. I. Pomerantshuk, *Physik. Z. Sowjetunion* **13,** 65 (1938)
23. R. J. Seeger, E. Teller, *Phys. Rev.* **62,** 37 (1942)
24. R. Weinstock, *Phys. Rev.* **65,** 1 (1944)
25. H. Feshbach, D. C. Peaslee, V. F. Weisskopf, *Phys. Rev.* **71,** 145 (1947)
26. M. L. Goldberger, F. Seitz, *Phys. Rev.* **71,** 294 (1947)
27. R. J. Finkelstein, *Phys. Rev.* **72,** 907 (1947)
28. See for example N. F. Mott, H. S. W. Massey, "The Theory of Atomic Collisions," (Oxford University Press, London, 1933)
29. E. Fermi, L. Marshall, *Phys. Rev.* **71,** 666 (1947)
30. W. H. Zachariasen, "Theory of X-ray Diffraction in Crystals," (John Wiley & Sons, Inc., New York, N. Y., 1945)
31. E. Fermi, W. J. Sturm, R. G. Sachs, *Phys. Rev.* **71,** 589 (1947)
32. E. Fermi, L. Marshall, *Phys. Rev.* **72,** 408 (1947)
33. C. S. Wu, L. J. Rainwater, W. W. Havens, *Phys. Rev.* **71,** 174 (1947)

Toxicity of Inhaled or Ingested Radioactive Products*

A general formulation is given and demonstrated which permits calculation of radiation dosage consequent upon inhalation or ingestion of radioactive material in terms of physiological behavior of the materials, nature of source and emitter

By WALDO E. COHN
Oak Ridge National Laboratory
Oak Ridge, Tennessee

THE PROBLEM of disposing of radioactive wastes, posed most severely in the case of the fission and other radioactive products of the chain-reacting pile (*1, 2*), centers primarily about keeping the degree of contamination of the water, food and air supplies of populated areas below those concentrations which can cause biological damage. Since any production of a radioactive material anywhere at any time results in some degree of contamination of this kind, the first problems to be solved in setting the "tolerance" concentrations of radioactive isotopes in such media are: (*a*) the relationship between external concentration and internal deposition, and (*b*) the relation between site of internal deposition, or passage, and biological effect.

The bodily deposition of an inhaled or ingested radioactive substance is governed by the metabolic behavior of the substance in question, particularly

* This work was done at Clinton Laboratories, a part of the Plutonium Project, during 1944, under Contract No. W-7405-eng-39 for the Manhattan District.

its degree of absorption from gut or lung, and the degree of concentration in and retention by one or another tissue. The relative hazard created by such deposition depends upon the physical properties of half-life, radiation type (α, β or γ radiation) and radiation energy, and upon the radiosensitivity and biological importance of each tissue involved.

In order to translate the information obtained from tracer experiments (to determine degree of absorption and pattern of tissue localization) and from radiotoxicological experiments (to relate biological damage to tissue concentration) into tolerance concentrations in water, food or air, we require a general formulation which takes into account the variabilities in type of exposure (*e.g.*, single or continuous intake, single or continuous pollution) and the variations in the metabolic behavior and biological effectiveness of each radioisotope and its compounds.* The importance of the latter consideration—the biochemical individuality of each radiosubstance—is pointed up by the results of tracer studies with the fission products (*3*), which show that only iodine, barium and strontium are moderately well absorbed from the intestinal tract and, subsequently, firmly deposited in certain tissues, each with its own peculiar type of radiosensitivity. Because of these two factors, there arises the hazard of day-by-day accumulation of these radioelements up to a maximum set by the rates of decay and of excretion. When the latter are low (*i.e.*, long half-life, low excretion rate), the possibility of building up toxic tissue concentrations from the continued intake of otherwise innocuous amounts of a radiosubstance arises.

This paper presents a general formulation† which relates the concentration of a radiosubstance in air, water or food to the total dose or daily intensity of radiation received by a given tissue as a result of the type and extent of intake of a polluted source. This relationship is expressed in terms of the biological constants (degree of absorption, pattern of deposition, rate of excretion), and physical constants (half-life, radiation energy) of the contaminating substance. Only β-radiation is considered since γ-radiation, because of its low specific ionization, is much less dependent upon localization for biological effectiveness. However, the formulation presented is easily modified to take both α- and γ-radiation into account.

* Most radioisotopes are encountered, and are effective, as their inorganic ions. Such is not the case for C^{14}, which exists in an infinity of compounds, each of which has its own metabolic pattern. Each compound must therefore be treated as a separate entity.

† K. Z. Morgan (*4*) has published a series of specific formulations on this subject.

Symbols and General Formulas

The symbols used in the formulation have the following meanings and involve the following assumptions:

Q = curies present in a given organ, all the radiation from this amount being absorbed uniformly in the mass, W, of this tissue (gamma radiation is usually ignored because of the large volume through which it is dispersed compared to beta radiation)

Q_{t_1} = value of Q at time t_1 after continuous intake has begun

q = curies taken into the body per day (inhalation or ingestion)

q_0 = value of q at $t_1 = 0$, the time when intake from the source is commenced

a = fraction of ingested (or inhaled) activity absorbed into blood
d = fraction of absorbed material being deposited in mass W of the given tissue
W = weight of organ, in grams, absorbing all β-radiation from Q curies
D = total dose, in r, received by organ during and after exposure of time t_1
I = dose rate, in r per day, as a result of Q
I_{t_1} = intensity of irradiation, or dose rate, in r per 24 hours, being received by mass W at time t_1 after start of exposure to source
I_m = maximum value of I_t that can be achieved in the organ during an infinitely long exposure of the subject to an intake of q curies per day (q_0 curies per day at $t_1 = 0$). This dose rate is achieved at time t_m
t_1 = duration of intake from the source, in days, the intake being continuous
t_2 = time after end of intake period (t_1) during which Q_{t_1} undergoes decay (λ) and excretion (β)
t_m = time after start of exposure when I_m is reached, in days
E = average energy of β-particles, in electron volts
λ = decay constant of emitter, in days^{-1}
β = excretion constant of emitter from organ, in days^{-1}
γ = dilution constant of source of supply, in days^{-1}

The following basic formulas are used:

$$q_{t_1} = q_0 e^{-(\lambda+\gamma)t_1}; \qquad I_{t_2} = I_{t_1} e^{-(\lambda+\beta)t_2} \qquad \text{(decay law)}$$

$$I_{t_1} = Q_{t_1} \times 3.7 \times 10^{10} \times 0.864 \times 10^5 \times E \times 1.6 \times 10^{-12} \times 0.012 \times 1/W = 60EQ_{t_1}/W \qquad (1)^*$$

$$D_0^t = \int_0^t I\,dt \qquad \text{(dose from time = 0 to any time } t\text{)} \qquad (2)$$

Whence:

$$D_{t_1}^{t_2} = \frac{I_{t_1}[1 - e^{-(\lambda+\beta)t_2}]}{(\lambda + \beta)} \qquad \text{(dose from end of exposure, } t_1\text{, to } t_2\text{)} \qquad (3)$$

Derivation of Formulas

The basic formula, which states that the rate at which activity is accumulated in an organ is the difference between the rates of deposition and of loss due to excretion and decay, is given by

$$\frac{dQ}{dt} = qad - \lambda Q - \beta Q = q_0 ade^{-(\lambda+\gamma)t_1} - (\lambda + \beta)Q$$

whence, by integration,

$$Q_{t_1} = q_0 ad\,\frac{e^{-(\lambda+\gamma)t_1} - e^{-(\lambda+\beta)t_1}}{\beta - \gamma}$$

and therefore, from (1),

$$I_{t_1} = 60\,\frac{E}{W}\,q_0 ad\,\frac{e^{-(\lambda+\gamma)t_1} - e^{-(\lambda+\beta)t_1}}{\beta - \gamma} \qquad (4)$$

This is the general formula giving the intensity of radiation in any organ at any time during the continuous ingestion or inhalation of a radioactive medium.

---

* 3.7×10^{10} = disintegrations/second-curie; 0.864×10^5 = seconds/day; 1.6×10^{-12} = ergs/electron volt; $0.012 = \frac{1}{\text{ergs/gm-roentgen}}$.

There are a number of special cases which deserve consideration, since most practical problems involve special cases.

1. If $\gamma = -\lambda$ (*i.e.*, fresh material is supplied to the source as fast as the old material decays, so that $q_{t_1} = q_0$):

$$I_{t_1} = 60 \frac{E}{W} q_0 a d \frac{1 - e^{-(\lambda+\beta)t_1}}{\lambda + \beta} \tag{5}$$

2. If $\gamma = \beta$ (*i.e.*, dilution of the source occurs at the same rate as the elimination from the body):

$$I_{t_1} = 60 \frac{E}{W} q_0 a d t_1 e^{-(\lambda+\beta)t_1} \tag{6}$$

3. If t_1 is very small compared to the reciprocals of the various time constants, λ, β and γ:

$$I_{t_1} = 60 \frac{E}{W} q_0 a d t_1 \tag{7}$$

In most situations, the activity in any organ will rise to a maximum and then decrease. The maximum value of I that can be achieved occurs at t_m, where $dI/dt = 0$. Hence, from (4),

$$(\lambda + \gamma)e^{-(\lambda+\gamma)t_m} = (\lambda + \beta)e^{-(\lambda+\beta)t_m}$$

and

$$t_m = \ln \left(\frac{\lambda + \gamma}{\lambda + \beta}\right)^{\frac{1}{\gamma - \beta}} \tag{8}$$

Therefore, from (4),

$$I_m = 60 \frac{E}{W} q_0 a d \frac{1}{\lambda + \beta} \left(\frac{\lambda + \gamma}{\lambda + \beta}\right)^{\frac{\lambda + \gamma}{\beta - \gamma}} \tag{9}$$

Again, two special cases will be considered.

1. If $\gamma = -\lambda$ (source solution is replenished at exactly the rate of decay):

$$I_m = 60 \frac{E}{W} q_0 a d \left(\frac{1}{\lambda + \beta}\right) \tag{10}$$

2. If $\gamma = \beta$ (source solution is diluted at exactly the rate of elimination from the tissue):

$$I_m = 60 \frac{E}{W} q_0 a d \left(\frac{1}{(\lambda + \beta)e}\right) \tag{11}$$

The total dose, D_0^∞, is the sum of the dose received during the exposure period itself (t_1) and the dose received from then on due to the internally deposited material.

$$D_0^\infty = D_0^{t_1} + D_{t_1}^\infty$$

Whence, from (3), $t_2 = \infty$,

$$\begin{aligned} D_0^\infty &= \int_0^{t_1} I dt + \frac{I_{t_1}}{(\lambda + \beta)} \\ &= 60 \frac{E}{W} \frac{q_0 a d}{\beta - \gamma} \left[\frac{e^{-(\lambda+\beta)t_1} - 1}{\lambda + \beta} - \frac{e^{-(\lambda+\gamma)t_1} - 1}{\lambda + \gamma} + \frac{e^{-(\lambda+\gamma)t_1} - e^{-(\lambda+\beta)t_1}}{\lambda + \beta}\right] \\ &= 60 \frac{E}{W} q_0 a d \frac{1 - e^{-(\lambda+\gamma)t_1}}{(\lambda + \beta)(\lambda + \gamma)} \end{aligned} \tag{12}$$

Special cases of D_0^m:

1. If $\lambda = -\gamma$: $D_0^m = 60 \frac{E}{W} q_0 ad \frac{t_1}{(\lambda + \beta)}$ (13)

2. If t_1 is very small: $D_0^m = 60 \frac{E}{W} q_0 ad \frac{t_1}{(\lambda + \beta)}$ (14)

If t_1 is greater than t_m, the dose up to t_m [from (2); *cf.* (12)] is

$$D_0^m = 60 \frac{E}{W} q_0 ad \frac{1}{(\lambda + \beta)(\lambda + \gamma)} \left[1 - \left(\frac{\lambda + \beta}{\gamma + \lambda} \right)^{\frac{\lambda + \beta}{\beta - \gamma}} - \left(\frac{\lambda + \gamma}{\lambda + \beta} \right)^{\frac{\lambda + \gamma}{\beta - \gamma}} \right] \quad (15)$$

Special cases of D_0^m:

1. If $\gamma = -\lambda$ (constant source), there is no maximum short of ∞ and hence no finite value for D_0^m [see (5)].
2. If $\gamma = \beta$:

$$D_0^m = 60 \frac{E}{W} q_0 ad \frac{1}{(\lambda + \beta)(\lambda + \gamma)} \left(1 - \frac{2}{e} \right) \quad (16)$$

The above formulas also apply to the special cases of (*a*) the dose to the lung (for inhaled material), and (*b*) to the gut (for ingested material) with the following modifications:

1. LUNG: For *ad*, substitute $(1 - a)$; for β, use the rate of absorption from the lung.
2. GUT: Since this organ does not accumulate the material put into it, the formula

$$I_{t_1} = (60E/W) q_0 (1 - a) e^{-(\lambda + \gamma) t_1} \quad (17)$$

is sufficient to describe the dose rate, and the cumulative dose after t_1 days continuous intake is:

$$D_{t_1} = \frac{60E}{W} q_0 (1 - a) \frac{1 - e^{-(\lambda + \gamma) t_1}}{\lambda + \gamma} \quad (18)$$

Use of the Formulas

These formulas can be applied to cover a variety of situations. For the purposes of demonstration, the following cases are chosen:

A. How much of a given product, *inhaled or ingested in a single dose*, will give rise to
   1. A (possibly lethal) dose of 500 r in 10 days? (3, 17)
   2. A (sub-acute toxic) dose of 3600 r in 1 year? (3, 17)
   3. 0.1 r per day at maximum (initial) rate? (1)

B. How much of a given product, *if inhaled or ingested daily from a source which is held at constant activity* (example: a reservoir poisoned daily, in which case $\lambda = -\gamma$), will give
   1. A possibly lethal dose rate of 50 r per day after 10 days intake? (5)
   2. A toxic dose rate of 10 r/day after 1 year intake? (5)
   3. A maximum dose rate of 0.1 r/day after infinite exposure? (10)

C. How much of a given product, if *inhaled or ingested daily from a source which is decaying but not being diluted* (example: a reservoir poisoned once, in which case $\gamma = 0$), will give
   1. 50 r/day after 10 days exposure? (4)
   2. A maximum of 0.1 r/day? (And at what time will this maximum be achieved)? (9, 8)
   3. A dose rate 0.1 r/day after 1 year exposure? (4)

The following values for certain biological constants are assumed for an average man:

ad = 0.20 (for Sr, Ba, I, P)

β = 0.0015 (for Sr, Ba and I, once internally deposited, and for the rate of absorption from the lung of an insoluble material)

W = 1,800 grams (marrow), 25 grams (thyroid), 1,200 grams (lung), 1,000 grams (gut)

E (in Mev) = 0.6 (P^{32}), 0.7 ($Ba^{140} + La^{140}$), 0.4 (Sr^{89}), 0.6 ($Sr^{90} + Y^{90}$), 0.15 (I^{131}), 0.4 (insoluble elements)

Results of Calculations

	Dose delivered in						
	Bone (Marrow)				*Thyroid*	*Gut*	*Lung*
	P^{32}	*Ba*	Sr^{89}	Sr^{90}	*I*	*Insoluble material/day*	
A. Single dose, to give							
1. 500 r in 10 days (mc)	15	14	20	12	1.0	2	2.6
2. 3600 r in 1 year (mc) (*cf.* 1)	45	43	19	3.2	4.4	0.4	2.2
3. 0.1 r/day initial rate (μc)	25	22	38	25	1.4	4	5
B. Daily dose from constant source, to give							
1. 50 r/day after 10th day (mc)	1.6	1.4	2.0	1.2	0.1	—	0.26
2. 10 r/day after 1 year (μc)	125	120	50	9	12	—	7
3. 0.1 r/day at maximum (∞) (μc)	1.25	1.2	0.5	0.04	0.12	—	0.07
C. Daily dose (as of t_0) from decaying source, to give							
1. 50 r/day after 10th day (mc)	2.1	1.9	2.1	1.2	0.17	—	0.28
2. 0.1 r/day at maximum (μc)	3.6	3.2	1.4	0.04	2.0	—	0.18
3. 0.1 r/day after 1 year (μc)	—	—	—	0.16	—	—	—
Time of maximum days	20	18	76	2200	11.3	—	76

BIBLIOGRAPHY

1. Plutonium Project, *J. Am. Chem. Soc.* **68**, 2411 (1946); *cf.* E. Tompkins, J. Khym, W. E. Cohn, *ibid.* **69**, 2769 (1947),Table 1
2. Manhattan Project, *Science* **103**, 697 (1946); Isotopes Branch, U. S. Atomic Energy Commission, "Radioisotopes: Catalog and Price List No. 2," (1947) [published in NUCLEONICS **1**, No. 1, 64 (1947)]
3. J. G. Hamilton, *et al.*, MDDC 1002 and 1275 (1947)
4. K. Z. Morgan, *J. Phys. and Colloid Chem.* **51**, 984 (1947)

Instrumentation

Counter Design for Gaseous Weak Beta Emitters

By JOSEPH T. KUMMER

Multiple Fellowship, Gulf Research and Development Company
Mellon Institute, Pittsburgh, Pennsylvania

In the use of C^{14} as a tracer, it has been found desirable to construct a thin-window Geiger tube for counting gaseous samples with less effort than is reqsuired by the usual procedure of using solid $BaCO_3$.

For this purpose, a pressure-seal, mica-window counter kit* was altered as shown in the figure by replacing the ring seal by a cylindrical, brass chamber into which had been soldered two ⅛ in. Kovar tubes. These Kovar tubes were sealed directly into the glass vacuum system containing the gas that was to be analyzed.

* Mark 7, Radiation Counter Laboratories, 1451 E. 57 St., Chicago 37, Ill.

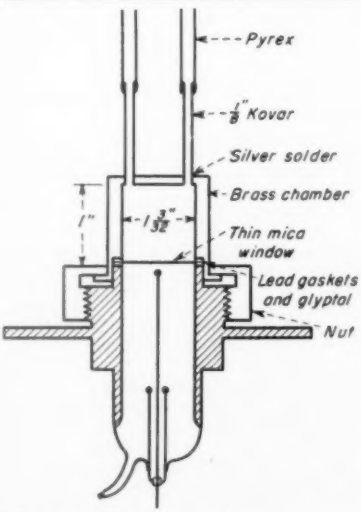

Typical Operating Data

Pressure, mm	*Temperature, °C*	*Counts per min†*	*Counts per min per mm*
533.2	29	13,060	24.5
255.8	29	6,470	25.3
199.2	29	5,010	25.0
145.5	29	3,640	25.0
106.0	29	2,650	25.0
66.0	29	1,660	25.1
32.5	29	805	24.8

† Corrected for background and deadtime

With this modified Geiger tube, it was found possible to measure continuously the activity of any gas circulated through the chamber or to measure the activity of a stationary gas sample introduced at a known pressure into the evacuated chamber.

In practice, this modified tube worked very satisfactorily. No difficulty was encountered in making the brass chamber vacuum tight and no "memory effect" was encountered while counting carbon dioxide, carbon monoxide, or hydrocarbon gases. The tube was painted with picein to exclude light and was filled, in most of the work, with 6 mm of ethyl alcohol vapor and 94 mm of helium. Care was taken to operate the tube in a vertical position. Otherwise the central wire would bend toward the wall of the tube, thereby decreasing the size of the observed voltage plateau.

A typical set of operating data for a sample of carbon monoxide containing

$C^{14}O$ is shown in the table. The constancy of the number of counts per minute per unit pressure shows that self-absorption can be neglected over the pressure range used.

It is interesting to note that the same gas, counted as an "infinitely thick" sample of $BaCO_3$ (sample area of 2.5 cm^2), gave a value of 306 counts per minute in a standard, thin-window counting assembly. It follows from the counts given in column 3 of the table that counting the radioactive material as a gas in this apparatus is not only more convenient but also more sensitive than counting it as $BaCO_3$.

ATOMIC ENERGY COMMISSION DOCUMENTS

ADDITIONAL TITLES of Manhattan District Declassified Documents recently made available to NUCLEONICS appear below and supplement the nine lists previously published therein.

Listed with the name of the paper are its author(s) and MDDC (Manhattan District Declassification Code) or AECD (Atomic Energy Commission Document) number, as the case may be.

Requests for further information concerning the documents may be directed to the Atomic Energy Commission, Technical Information Division, Oak Ridge Directed Operations, Oak Ridge, Tenn. The Technical Information Division will advise requestors where the information in the document has been published or otherwise made available, or will provide copies of documents for purchase if the information in them cannot be obtained otherwise.

Slow Neutron Velocity Spectrometer Studies of Cu, Ni, Bi, Fe, Sn and Calcite. W. W. Havens, Jr., L. J. Rainwater, C. S. Wu, J. R. Dunning. MDDC 1645

Tungsten Wire Straighteners. A. A. Jarrett. MDDC 1646

The Effect of Lethal Dose of Total Body X-Ray on Uric Acid and Allantoin Excretion in Dogs. H. Krizek, I. Silverbach, S. Schwartz. MDDC 1647

The Preparation and Properties of High Polymers of Trifluorochloroethylene. W. T. Miller. MDDC 1648

Uranium Hydride. II. Radiochemical and Chemical Properties. A. S. Newton, *et al.* MDDC 1649

Thermal Neutron Absorption Cross Sections for Separated Isotopes. H. S. Pomerance, J. I. Hoover. MDDC 1650

Rochester Ion Meter Construction and Operation Details. W. F. Bale. MDDC 1651

Low Pressure Alpha Counters. W. B. Bennet. MDDC 1652

The Effect of Plutonium on Tissue Metabolism of Rats. E. S. G. Barron. R. Abrams, R. D. Finkle, R. P. Rhoades. MDDC 1653

Methods of Analysis in Preparation of Sulfide Materials. L. Brewer, *et al.* MDDC 1654

Radiation Chemistry and Nuclear Energy. M. Burton. MDDC 1655

Radiotoxicity of Inhaled or Ingested Radioactive Products. W. E. Cohn. MDDC 1656

The Electrodeposition of Plutonium. O. Cook. MDDC 1657

A Prophylactic Approach to the Anaphylactic Factors in Irradiation Disease. J. B. Field, P. E. Rekers. MDDC 1658

The Ignition of U_3O_8 in Oxygen at High Pressures and the Crystallization of UO_2. S. Fried, N. H. Davidson. MDDC 1659

Search for Elements 94 and 93 in Nature—Presence of 94^{239} in Carnotite. C. S. Gardner, N. A. Bonner, G. T. Seaborg. MDDC 1660

Columbia Scaling Circuits. H. A. Glassford, J. R. Dunning. MDDC 1661

Optical Properties of UF_4. W. W. Harris, R. A. Wolters. MDDC 1662

Aberrant Tissue Developments of Rats Exposed to Beta Rays. The Late Effects of P^{32} Beta Rays. P. S. Henshaw, R. S. Snider. MDDC 1663

The Clinton Pile Oscillator. J. I. Hoover, *et al.* MDDC 1664

A Study of the Reaction between Beryllium and Aurin Tricarboxylic Acid. G. E. Kosel, W. F. Neuman. MDDC 1665

Fluorescence Studies of Plutonium, Neptunium, and Americium. G. R. Price. MDDC 1666

The Beta Spectrum of W^{185}. D. Saxon. MDDC 1667

The Beta Spectrum of Au^{198}. D. Saxon. MDDC 1668

Laue Photography of Neutron Diffraction. C. G. Shull, M. C. Marney, E. O. Wollan. MDDC 1669

Mass Spectrometer for Leak Detection. F. S. Stein, J. E. Binns. MDDC 1670

Portable Battery Operated Two Stage Radiation Meter. C. S. Wu, J. Rainwater. MDDC 1671

Ionizing Irradiation Disease and a Study of the Protective Nature of Flavonones. J. B. Field, P. E. Rekers. MDDC 1672

Production of Rarer Metals. G. Meister. MDDC 1673

The Crystal Structure of α-UF_5 and β-UF_5. W. H. Zachariasen. MDDC 1674

The Crystal Structure of U_2F_9 and $NaTh_2F_9$. W. H. Zachariasen. MDDC 1675

Stars in Photographic Emulsions Initiated by Deuterons. Part I. Experimental. E. Gardner, V. Peterson. MDDC 1676

Stars in Photographic Emulsions Initiated by Deuterons. Part II. Theoretical. W. Horning, L. Baumhoff. MDDC 1677

A Constant Current Regulator. Los Alamos Laboratory. MDDC 1678

Fission Excitation Functions. J. Jungerman, S. C. Wright. MDDC 1679

Utilization of Nicotinic Acid and Its Amide by the Human Erythrocyte in Vitro. E. Leifer, J. R. Hogness, L. J. Roth, W. Langham. MDDC 1680

Additivity of Lethal Effects of External Beta and Gamma Irradiation (Supplement to MDDC-498). J. R. Raper, K. K. Barnes. MDDC 1681

The Effect of Crystal Orientation on the Scattering of Slow Neutrons. R. G. Sachs, V. W. Myers. MDDC 1682

A New Photographic Material for Gamma-Ray Dosimetry. H. O. Whipple, C. S. Hornberger, J. C. Hoffman, J. F. Nolan. MDDC 1683

Magnetic Moment of He^3. H. L. Anderson, A. Novich. MDDC 1684

Cross Section and Crystal Orientation in Extruded Graphite and Alumnium. C. Arnold, R. Sternheimer, A. Weber. MDDC 1685

The Beta and Gamma Spectra of Ga^{72}. S. K. Haynes. MDDC 1686

The Isotopic Constitution of Europium, Cadolinium, and Terbium. D. C. Hess, Jr. MDDC 1687

Improved Ion Exchange Method for Separating Rare Earths in Macro Quantities. F. H. Spedding, *et al.* MDDC 1688

The Effects of Roentgen Rays on the Embryos and Larvae of the Chinook Salmon. A. D. Welander, *et al.* MDDC 1689

Radioactive Isotopes as Sources in Industrial Radiography. G. H. Tenney. MDDC 1690

The Concentration of Isotopes of Chlorine by the Counter-Current Electro-Migration Method. S. L. Madorsky, S. Straus. MDDC 1691

Radiation Meter Model "A." R. Watts. MDDC 1692

Potassium Plutonium (III) Sulfates. H. H. Anderson. MDDC 1693

Plutonium Project Record, Vol 9B, Chapter 7. M. Sugarman. MDDC 1694

Zinc and Gallium Activities in Uranium Fission. J. M. Siegel, L. E. Glendenin. MDDC 1694-A

The 33m Br^{84}. S. Katcoff, B. Finkle, N. Sugarman. MDDC 1694-B

Search for Se^{79} and the Absence of Long-lived Se Activities in Fission. L. E. Glendenin. MDDC 1694-C

Preliminary Study of the 17-h $Zr^{(97)}$ Chain. C. D. Coryell. MDDC 1694-D

Characteristics of 67-h Mo and Absence of Long-lived Mo^+. S. Katcoff. MDDC 1694-E

Absence of Long-lived Mo in Fission. J. A. Swartout. MDDC 1694-F

Discovery of the $\sim 10^6$y $43^{(99)}$ Isotope, II. R. P. Schuman. MDDC 1694-G

Note on a Long-lived Element-43 Activity in Fission. L. F. Glendenin. MDDC 1694-H

Discovery of Long-lived Ru Activities in U Fission. B. L. Goldschmidt, I. Perlman. MDDC 1694-I

Identification of a 4h Ru $\rightarrow$ 34h Rh Chain in Slow Neutron Fission. N. R. Sleight. MDDC 1694-J

Characterization of the 4.5h Ru Produced in Fission. W. H. Sullivan, N. R. Sleight, E. M. Gladrow. MDDC 1694-K

Characterization of the 36.5h Rh Daughter of 4.5h Fission Ru. W. H. Sullivan, N. R. Sleight, E. M. Gladrow. MDDC 1694-L

Identification and Mass Assignment of a 4.5h Ru $\rightarrow$ 36.5h Rh Decay Chain in Neutron and Deuteron-Irradiated Ru. W. H. Sullivan, N. R. Sleight, E. M. Gladrow. MDDC 1694-M

Characterization of the 4.5h Ru Produced in Neutron and Deuteron-Irradiated Ru. W. H. Sullivan, N. R. Sleight, E. M. Gladrow. MDDC 1694-N

Characterization of the 36.5h Rh Daughter of 4.5h Ru Produced in Neutron- and Deuteron-Bombarded Ru. W. H. Sullivan, N. R. Sleight, E. M. Gladrow. MDDC 1694-O

Identity of the 4.5h Ru → 36.5h Rh Decay Chain Produced in Fission and in Neutron- and Deuteron-Bombarded Ru. W. H. Sullivan, N. T. Sleight, E. M. Gladrow. MDDC 1694-P

Identification, Characterization and Mass Assignment of a 42d Ru Activity in Neutron- and Deuteron-Irradiated Ru. W. H. Sullivan, N. R. Sleight, E. M. Gladrow. MDDC 1694-Q

Identity of the ~30d Ru Found in Fission with the 42d Ru^{103} Produced in Neutron- and Deuteron-Bombarded Ru. W. H. Sullivan, N. R. Sleight, E. M. Gladrow. MDDC 1694-R

The 57m Rh Activity and Its Ru Parent. W. H. Sullivan, N. R. Sleight, E. M. Gladrow. MDDC 1694-S

Short-lived Ru-Rh Decay Chains. L. E. Glendenin. MDDC 1694-T

A Note on the 9h Rh Activity in Fission. N. E. Ballou. MDDC 1694-U

Absence of Long-lived Ru in Fission, II. Upper Limit to the Fission Yield of 210d Rh^{102}. J. A. Swartout, W. H. Sullivan. MDDC 1694-V

Search for Pd^{107} and Absence of Long-lived Pd Activities in Fission, II. L. E. Glendenin. MDDC 1694-W

The 43d $_{48}Cd^{115}$. L. Seren, *et al.* MDDC 1694-X

Long-lived Sn in Fission. G. R. Leader. MDDC 1694-Y

The 93h Sb^{127} Activity. N. R. Sleight, W. H. Sullivan. MDDC 1694-Z

The Long-lived Sb in U Fission, II. C. W. Stanley. MDDC 1694-AA

Radiations from the 32d–72m Te^{129} Fission Chain. T. B. Novey. MDDC 1694-BB

Characteristics of the 8d I^{131}. J. H. Goldstein. MDDC 1694-CC

Search for Long-lived Iodine. G. R. Leader, W. Sullivan. MDDC 1694-DD

The Characteristics of the 9.2h Xe^{135}. E. J. Hoagland, N. Sugarman. MDDC 1694-EE

The Half-life and Radiations of 13m Xe^{135}. T. B. Novey, J. D. Knight. MDDC 1694-FF

A Note on the Mass Assignment of 33y Cs^{137}. L. E. Glendenin, J. D. Knight. MDDC 1694-GG

Further Study of the 13d Cs Activity. L. E. Glendenin. MDDC 1694-HH

A Note on the 18m Ba. A Goldstein. MDDC 1694-II

Water Absorption Curve of the γ Radiation from 40h La^{140}. L. S. Goldring. MDDC 1694-JJ

Radiations from 3.7h La^{141}. S. Katcoff. MDDC 1694-KK

The Discovery of 14d Pr as a U Fission Product. N. Ballou. MDDC 1694-LL

Characteristics of the 13.8d Pr^{143}. J. H. Goldstein. MDDC 1694-MM

Characteristics of the 28d Ce^{141}. J. H. Goldstein. MDDC 1694-NN

The Characteristics of the 275d Ce^{144}. J. H. Goldstein. MDDC 1694-OO

Further Work on the Long-lived Ce-17.5m Pr Chain. V. Nedzel. MDDC 1694-PP

Absence of the Long-lived Daughters of Long-lived Ce. N. E. Ballou. MDDC 1694-QQ

Discovery of a Long-Lived Rare-Earth Activity. N. Ballou. MDDC 1694-RR

Study of the 25m $Sm^{(155)}$ in Fission. L. Winsberg. MDDC 1694-SS

Preliminary Study of the Fission Products of Th. N. E. Ballou, *et al.* MDDC 1694-TT

High Frequency Vacuum Breakdown Tests for Copper and Copper Plated Ceramic Surfaces. P. C. Bettler. MDDC 1695

Some Observations on the Chemistry of Element-43 (Technetium). G. E. Boyd, Q. V. Larson, E. E. Motta. MDDC 1696

Design Study for a 10-Bev Magnetic Accelerator. M. W. Brobeck. MDDC 1697

The Effect of Roentgen Irradiation on Antibody Formation in Rabbits. C. G. Craddock, J. S. Lawrence. MDDC 1698

Angular Correlation of Fission Neutrons. S. DeBenedetti, J. E. Francis, W. M. Preston, T. W. Bonner. MDDC 1699

The Absorption Spectra of Transuranium Salts at Low Temperatures. S. Freed, F. Leitz. MDDC 1700

Preparation of 1-C^{14}-Propene-1 and the Mechanism of Permanganate Oxidation of Propene. B. A. Fries, M. Calvin. MDDC 1701

The Magnetic Susceptibilities of Some Uranium and Neptunium Compounds. C. A. Hutchison, Jr., N. S. Elliot. MDDC 1702

The Potential of the U(V), U(VI) Couple and the Kinetics of U(V) Disproportionation in Perchlorate Media. D. M. H. Kern, E. F. Orlemann. MDDC 1703

Summary Report on Neutron Counter Work. S. A. Korff, W. B. Sparks, J. A. Simpson. MDDC 1704

The Hydrolytic Behavior of Uranium and the Transuranic Elements. K. A. Kraus, F. Nelson. MDDC 1705

The Chemical Identification of Isotopes

Formed in the Bombardment of Uranium with High Energy Particles. P. R. O'Connor. MDDC 1706

The Determination of Silica in Beryllium Metal Powder. J. F. O'Leary. MDDC 1707

Electrolytic and Polarographic Determination of Zinc in Thorium. J. H. Patterson, C. V. Banks. MDDC 1708

Preparation of Carrier-Free Ac^{228} ($MsTh_2$) Tracer. S. Peterson. MDDC 1709

The Higher Chlorides of Uranium. C. H. Prescott, Jr. MDDC 1710

Comparison of Methods of Obtaining Surface Area of Crystalline Solids from Vapor Absorption Isotherms. S. Ross. MDDC 1711

Equilibrium in the Vapor Phase Hydrolysis of $PuBr_3$. I. Sheft, N. R. Davidson. MDDC 1712

Equilibrium in the Vapor Phase Hydrolysis of $PuCl_3$. I. Sheft, N. R. Davidson. MDDC 1713

Determination of p-Toluenesulfonamide. J. Sirota. MDDC 1714

The Toxicity of Hexachlorpropylene and Trichloracrylyl Chloride. C. J. Spiegl, R. E. Howe, L. LaFrance. MDDC 1715

Introductory Remarks. J. A. Swartout. MDDC 1716

Design of Radiochemistry Laboratories for Research with Low Levels of Radioactivity. J. Swartout. MDDC 1717

The Tracer Chemistry of Americium and Curium. S. G. Tompson, R. A. James, L. O. Morgan. MDDC 1718

Influence of Radioactivity on Chemical Laboratory Technique and Design. P. C. Tompkins, H. A. Levy. MDDC 1719

Pile Neutron Physics. A. M. Weinberg. MDDC 1720

Fluorescence Spectra of Uranyl Compounds. J. Bigeleisen, M. G. Mayer. MDDC 1721

The Thermodynamics of the Actinides. L. Brewer. MDDC 1722

The Formation of Be^{10}. C. Eggler, D. J. Hughes, C. Huddleston. MDDC 1723

Physical Properties of Chlorotrifluoroethylene Polymers as a Function of Molecular Weight. II.—Molecular Fractionation, Density, Viscosity, Molecular Weight and the Correlation of These Properties of Chlorotrifluoroethylene Polymers. J. L. Gabbard, *et al.* MDDC 1724

The β-Spectrum of Be^{10}. D. J. Hughes, C. Eggler. MDDC 1725

Oscillatory Method for Measuring Neutron Cross-Sections by the Effect on the Reactivity of a Chain Reacting Pile. A. Langsdorf, Jr. MDDC 1726

Absorption Spectra of Some Uranyl Salts. M. G. Mayer, J. Bigeleisen. MDDC 1727

Management and Treatment of Exposed Personnel. J. E. Wirth. MDDC 1728

Vapor Phase Chlorination of Uranium Oxides. H. G. Reiber, H. A. Young. MDDC 1729

Exchange Reactions of Uranium Ions in Solution. E. Rona. MDDC 1730

Control Exposure Chamber Studies. G. F. Sprague, Jr. MDDC 1731

Effect of Electron Beams on Aqueous Dichromate Solutions. L. H. Treiman. MDDC 1732

The Fluorescence of Uranium Trioxide Hydrates. D. T. Vier, M. L. Schultz, J. Bigeleisen. MDDC 1733

Metabolic Studies on a Solution of Purified Human Albumin Given Intravenously to Man. C. Waterhouse, K. Cusson, S. H. Bassett. MDDC 1734

Total Neutron Cross-Sections of Compounds with Different Crystalline Structures. L. Winsberg, D. Meneghetti, S. S. Sidhu. MDDC 1735

Studies on the Mechanism of the Propionic Acid Fermentation. S. F. Carson, *et al.* MDDC 1736

Oxides of Transuranium Elements. D. M. Gruen, J. J. Katz, MDDC 1737

The Isolation of Actinium and Preparation of Some of Its Compounds. F. Hageman. MDDC 1738

The Relation of Backscattering to Self-absorption. P. E. Yankwich, J. Weigl. MDDC 1739

The Isotopic Constitution of Praseodymium and Neodymium. M. G. Inghram, D. C. Hess, Jr., R. J. Hayden. MDDC 1740

Chemical and Physical Properties of Uranium Peroxide. C. E. Larson. MDDC 1741

Preparation of Radiactivdy Pure Ac^{228} ($MsTh_2$). C. K. McLane, S. Peterson. MDDC 1742

Alpha Branching of Actinium-227. S. Peterson, A. Ghiorso. MDDC 1743

The Radiocolloidal Properties of Some Fission Products. J. Schubert. MDDC 1744

Plutonium Project Record, Volume IX-B, Chapters 9 and 12. N. Sugarman. MDDC 1745

Van de Graaff Generator Drawings: 2N 3835A, 2n 1485, 3A 5764A, 3A 5544, 2N 2594B, 2N 4344A, 2N 9254A, 2N, 9534B, 3A 2745, 3A 8845, 3A 7045. C. M. Turner. MDDC 1746

The Thermal Conductivity of Uranium Hexafluoride. P. A. Agron, A. H. Taylor. MDDC 1747

Correlation of Theories of Ion-Exchange

Column Separations. G. E. Boyd, L. A. Matheson. MDDC 1748

Equations of the Neher-Harper Circuit. R. W. Cole. MDDC 1749

Experiments with the Neher-Harper Circuit. R. W. Cole. MDDC 1750

Observations on the Preparation of the Tribromide and Triiodide of Uranium. E. D. Eastma[illegible] J. Fontana, R. A. Webster. M[illegible]

The Direct S[illegible] Solutions Usin[illegible] [illegible]ation and the Porous Cup [illegible] C. Feldman. MDDC 1752

The Chemistry of Americium Compounds. S. Fried. MDDC 1753

Nuclear Isomers Produced by Slow Neutron Capture. M. Goldhaber, C. O. Muehlhause. MDDC 1754

Preparation and Properties of the Uranium Halides. N. W. Gregory. MDDC 1755

Neutron Scattering Resonances in Elements from Calcium to Bromine. S. P. Harris, A. S. Langsdorf, Jr. MDDC 1756

Ionic Species of Plutonium Present in Aqueous Solutions of Different Acids. J. C. Hindman. MDDC 1757

Hemin Synthesis with Glycine Containing C^{14} in Its Alpha-Carbon Atom. K. I. Altman, *et al.* MDDC 1758

Neutron Deficient Isotopes of Tellurium and Antimony. M. Lindner, I. Perlman. MDDC 1759

The Oxidation States of Neptunium in Aqueous Solutions. L. B. Magnusson, J. C. Hindman, T. J. LaChapelle. MDDC 1760

Ultramicrochemical Investigations of the Solubilities of Some Plutonium Compounds. D. F. Mastick, A. C. Wahl. MDDC 1761

Equilibrium and Rate Measurements on the Exchange Absorption of Several of the Trivalent Rare Earths. L. S. Myers, Jr., G. E. Boyd. MDDC 1762

The Cultivation of the Hematopoietic Tissues by Tissue Culture Methods. P. E. Rekers. MDDC 1763

Homotransplantation of the Mammalian Adult Kidney. P. E. Rekers. MDDC 1764

Comparison of Methods of Obtaining Surface Area Crystalline Solids from Vapor Adsorption Isotherms. S. Ross. MDDC 1765

Operation and Service Notes on a Batteryless Type-A Counting System Using Parallel Plate or Concentric Cylinder Chambers, Mark 6 Model 30 and Mark 10 Model 32. J. A. Schoke. MDDC 1766

The System Uranyl Sulfate—Water, I. Temperature—Concentration Relationships below 300° C. C. H. Secoy. MDDC 1767

Equations for the Pulse from a G-M Counter. R. W. Cole. MDDC 1768

Plutonium Project Record, Vol. IX-B, Papers from Chapter 6, Introduction to F[illegible]on. N. Sugarman. MDDC 1769

[illegible]mparison of Individual Fission Activities with Gross Activity (Summation Study), II. W. Robinson, *et al.* MDDC 1769-A

Calculation of γ Wattage Escaping from the Slug in the Calorimetric Experiments. K. Way. MDDC 1769-B

Ranges of Fission Recoil Fragments of Known Mass Numbers, I. M. S. Freedman, R. P. Metcalf, N. Sugarman. MDDC 1769-C

Ranges of Fission Recoil Fragments of Known Mass Numbers, II. B. Finkle, E. Hoagland, S. Katcoff, N. Sugarman. MDDC 1769-D

Ranges of Fission Recoil Fragments of Known Mass Numbers, III. B. Finkle, E. Hoagland, S. Katcoff, N. Sugarman. MDDC 1769-E

Triple Fission, I, Sulfur. R. P. Metcalf. MDDC 1769-F

Triple Fission, II. Chlorine. J. A. Seiler. MDDC 1769-G

Triple Fission, III. Calcium. E. P. Steinberg. MDDC 1769-H

Triple Fission, IV. Scandium. L. Winsberg. MDDC 1769-I

Triple Fission, V. Iron. R. P. Metcalf. MDDC 1769-J

The Isolation of Protactinium from Uranium Ore Residues and Some Observations on Its Chemical Behavior. R. C. Thompson. MDDC 1770

Problems Encountered in the Design of Radioisotope Building. P. C. Tompkins. MDDC 1771

The Isolation and Properties of Curium. L. B. Werner, I. Perlman. MDDC 1772

Thermochemical Measurements on the Transuranium Elements. E. F. Westrum, Jr. MDDC 1773

Plutonium Project Record, Volume IX-B, Radiochemistry and the Fission Products Papers from Chapter 7, Data on the Fission Products. N. Sugarman. MDDC 1774

Absence of Long-lived As in Fission, II. G. R. Leader. MDDC 1774-A

Chemical Isolation of the 56s Br and the 23s I Delayed Neutron Activities. J. S. Levinger, *et al.* MDDC 1774-B

The Characteristics of 57d Y^{91}. R. R. Edwards. MDDC 1774-C

The Characteristics of 53d Sr^{89}. R. R. Edwards, A. F. Voigt. MDDC 1774-D

The Identification of Sr^{89} and Y^{90} in U Fission. R. W. Nottorf. MDDC 1774-E

Further Studies on Sr^{89} and Y^{90}. L. E. Glendenin, C. D. Coryell. MDDC 1774-F

Discovery and Characterization of the 10h Y Fission Product. N. E. Ballou. MDDC 1774-G

Half-life and Radiations of 5.9h 43^{99}. L. E. Glendenin. MDDC 1774-H

Discovery of the 10s Isotope $43^{(99)}$. D. C. Lincoln, W. H. Sullivan. MDDC 1774-I

The Characteristics of 7.6d Ag^{111}. J. H. Goldstein. MDDC 1774-J

Characteristics of the 54m I. J. H. Goldstein. MDDC 1774-K

The Characteristics of the 5.3d Xe^{133}, I. N. Elliott. MDDC 1774-L

Mass Assignment of 33y Cs. A. Turkevich, E. P. Steinberg, B. Finkle, N. Sugarman. MDDC 1774-M

Search for Cs^{135} from Xe^{135}. D. W. Engelkemeir. MDDC 1774-N

The Decay Characteristics of 32m Cs^{138}. J. H. Goldstein. MDDC 1774-O

Half-life of Ba^{139}. C. R. Dillard, H. Finston, R. M. Adams. MDDC 1774-P

Spectrometer Measurements of the 12.8d Ba^{140} Radiations. R. Wilkinson, W. Hall. MDDC 1774-Q

Discovery of the Chain 1.8h–4.7h Pr in U Fission. N. E. Ballou. MDDC 1774-R

The Radiations of the 4.7h $Pr^{(143)}$. S. Katcoff. MDDC 1774-S

Characteristics of the 33h Ce^{143}. J. H. Goldstein. MDDC 1774-T

The Fission Yield of the 33h Ce^{143}. S. Katcoff, B. Finkle, N. Sugarman. MDDC 1774-U

The Ce and Pr Activities of Masses 141 *and* 143. N. E. Ballou, W. H. Burgus. MDDC 1774-V

The Identification and Characterization of 4.5y Element 61^{147}. J. A. Marinsky, L. E. Glendenin. MDDC 1774-W

The Discovery, Identification and Characterization of 47h Element-$61^{(149)}$. J. A. Marinsky, L. E. Glendenin. MDDC 1774-X

Study of the 60m $Eu^{(156)}$ and 15.4h $Eu^{(157)}$. Activities in Fission. L. Winsberg. MDDC 1774-Y

Study of the Chain 10h $Sm^{(156)}$–15.4d Eu^{156} in Fission. L. Winsberg. MDDC 1774-Z

Study of the 2y Eu^{155} in Fission. L. Winsberg. MDDC 1774-AA

Plutonium Project Record, Vol. IX-B, Papers from Chapters 9, 11, *and* 12. N. Sugarman. MDDC 1775

The Theory of Removal of Noble Gases from Solutions with Carrier Gases. R. Livingston, E. Shapiro, N. Elliot. MDDC 1775-A

*Separation Order of Elution of Rare Earths from Amberlite IR-*1 *with* 5% *Ammonium Citrate.* J. A. Marinsky. MDDC 1775-B

Absorption Study of the Radiation Characteristics of 6.8d U^{237}. E. L. Brady, W. Rubinson. MDDC 1775-C

Chemical Identification of the 8s *Activity Found in Pile-irradiated Oxygen Compounds.* T. B. Novey, J. D. Knight, D. S. Schover, N. Elliot[illegible] MDDC 1775-D

The Half-life and [illegible] of Se^{75}. H. [illegible] MDDC 1775-E

[illegible] *of Cs^{134}.* L. E. Glendenin. [illegible]75-F

Discovery of a 5.[illegible] *Activity in Deuteron-Bombarded Ru.* W. H. Sullivan, N. R. Sleight, E. M. Gladrow. MDDC 1775-G

Discovery and Characterization of a 21h Rh Activity in Deuteron-Bombarded Ru, W. H. Sullivan, N. R. Sleight. MDDC 1775-H

Discovery, Characterization and Mass Assignment of a 2.8d Ru Activity. W. H. Sullivan, N. R. Sleight, E. M. Gladrow. MDDC 1775-I

A Study of Sm and Eu Activities Induced by Deuteron and Neutron Irradiation of Sm. J. A. Marinsky, L. E. Glendenin. MDDC 1775-J

Packing Fraction Measurements of the Heavy Elements. A. J. Dempster. MDDC 1776

The Quantitative Spectrographic Analysis of the Rare Earths Elements, III. Determination of Major Constituents in Complex Mixtures. V. A. Fassel, H. A. Wilhelm. MDDC 1777

The Metabolism of Carrier-Free Radioactive Silver in the Rat. K. G. Scott MDDC 1778

Plutonium Project Record, Vol. IX-B, Papers from Chapter 7. N. Sugarman. MDDC 1779

Uranium Tetrachloride—Two One-Year Inhalation Toxicity Studies of Animals at 0.2 *and* 0.05 *mg U/m³.* N. J. Ashenburg. AECD 1780

Activation Cross Sections by Boron Absorption. S. M. Dancoff, *et al.* AECD 1781

Methods for the Complete Decomposition of Rock and Ore Samples to be Analyzed for Very Small Amounts of Uranium and Thorium. M. D. Foster, *et al.* AECD 1782

Characteristics of Bismuth Fission with High Energy Particles. R. H. Goeckermann, I. Perlman. AECD 1783

Properties of 86s $I^{(132)}$. S. Katcoff, C. W. Stanley. AECD 1784

Metabolism of Americium in the Rat. K. G. Scott, D. H. Copp, D. Axelrod, J. G. Hamilton. AECD 1785

Hyperfine Structure in the Spectrum of Np^{237}. F. S. Tompkins. AECD 1786

Column Separations. G. E. Boyd, L. A. Matheson. MDDC 1748

Equations of the Neher-Harper Circuit. R. W. Cole. MDDC 1749

Experiments with the Neher-Harper Circuit. R. W. Cole. MDDC 1750

Observations on the Preparation of the Tribromide and Triiodide of Uranium. E. D. Eastm[illegible] J. Fontana, R. A. Webster. M[illegible]

The
Solu
Poro
MD

The
S. F.

Nucl
Capt
haus

Prep
Hali

Neut
from
A. S.

Ioni
Aque
J. C.

Hem
C^{14}
Altm

Neut
and
MD

The
Aque
J. C.
1760

Ultra
Solul
D. F.

Equi
Exch
Triva
G. E

The
by Ti
MDI

Hom
Adul
1764

Comp
face Areas Crystalline Solids from Vapor Adsorption Isotherms. S. Ross. MDDC 1765

Operation and Service Notes on a Batteryless Type-A Counting System Using Parallel Plate or Concentric Cylinder Chambers, Mark 6 Model 30 and Mark 10 Model 32. J. A. Schoke. MDDC 1766

The System Uranyl Sulfate—Water, I. Temperature—Concentration Relationships below 300° C. C. H. Secoy. MDDC 1767

Equations for the Pulse from a G-M Counter. R. W. Cole. MDDC 1768

Plutonium Project Record, Vol. IX-B, Papers from Chapter 6, Introduction to F[illegible]on. N. Sugarman. MDDC 1769

A[illegible]mparison of Individual Fission Activities with Gross Activity (Summation Study), II. W. Robinson, *et al.* MDDC 1769-A

Calculation of γ Wattage Escaping from the Slug in the Calorimetric Experiments. K. Wa[illegible] MDDC 1769-B

TYP
CUT-O

Chemical Isolation of the 56s Br and the 23s I Delayed Neutron Activities. J. S. Levinger, *et al.* MDDC 1774-B

The Characteristics of 57d Y^{91}. R. R. Edwards. MDDC 1774-C

The Characteristics of 53d Sr^{89}. R. R. Edwards, A. F. Voigt. MDDC 1774-D

The Identification of Sr^{90} and Y^{90} in U Fission. R. W. Nottorf. MDDC 1774-E

Further Studies on Sr^{90} and Y^{90}. L. E. Glendenin, C. D. Coryell. MDDC 1774-F

Discovery and Characterization of the 10h Y Fission Product. N. E. Ballou. MDDC 1774-G

Half-life and Radiations of 5.9h 43^{99}. L. E. Glendenin. MDDC 1774-H

Discovery of the $10^{6}y$ $43^{(99)}$ *Isotope.* D. C. Lincoln, W. H. Sullivan. MDDC 1774-I

The Characteristics of 7.6d Ag^{111}. J. H. Goldstein. MDDC 1774-J

from Amberlite IR-1 with 5% Ammonium Citrate. J. A. Marinsky. MDDC 1775-B

Absorption Study of the Radiation Characteristics of 6.8d U^{237}. E. L. Brady, W. Rubinson. MDDC 1775-C

Chemical Identification of the 8s Activity Found in Pile-irradiated Oxygen Compounds. T. B. Novey, J. D. Knight, D. S. Schover, N. Elliot. MDDC 1775-D

The Half-life and [illegible] *of* Se^{75}. H. [illegible] DDC 1775-E

[illegible] ^{134}. L.

[illegible]euteron- [illegible] N. R. 1775-G

[illegible] *21h Rh* [illegible] *Ru*, W. [illegible] MDDC

[illegible] *Mass* [illegible] W. H. [illegible]adrow.

[illegible] *Induced* [illegible]*ation of* [illegible]ndenin.

[illegible]*he Heavy* [illegible]DC 1776

[illegible] *Analysis* [illegible]*I. De-* [illegible]*in Com-* [illegible] H. A.

[illegible] *Radio-* [illegible]. Scott

[illegible] *IX-B,* [illegible]garman.

[illegible]*One-Year* [illegible]*imals at* [illegible]enburg.

[illegible]*ron Ab-* [illegible] AECD

[illegible]*osition of* [illegible]*lyzed for* [illegible]*ium and* [illegible] AECD

1774-Z

Study of the 2y Eu^{155} *in Fission.* L. Winsberg. MDDC 1774-AA

Plutonium Project Record, Vol. IX-B, Papers from Chapters 9, 11, and 12. N. Sugarman. MDDC 1775

The Theory of Removal of Noble Gases from Solutions with Carrier Gases. R. Livingston, E. Shapiro, N. Elliot. MDDC 1775-A

Separation Order of Elution of Rare Earths

1782

Characteristics of Bismuth Fission with High Energy Particles. R. H. Goeckermann, I. Perlman. AECD 1783

Properties of 86s $I^{(131)}$. S. Katcoff, C. W. Stanley. AECD 1784

Metabolism of Americium in the Rat. K. G. Scott, D. H. Copp, D. Axelrod, J. G. Hamilton. AECD 1785

Hyperfine Structure in the Spectrum of Np^{237}. F. S. Tompkins. AECD 1786

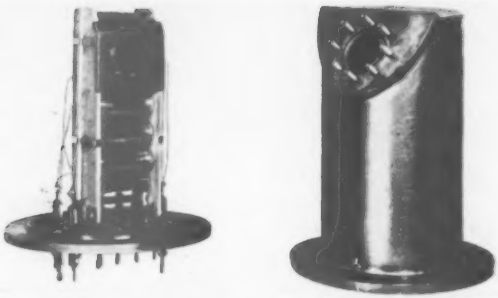

Electrode system and metal tube shell of a 13-stage tube

PARTICLE DETECTION WITH MULTIPLIER TUBES

Electron multiplier tubes have been used in two ways for fast counting—by direct detection of particles, and by use of a target screen to emit light for detection purposes. Design of tubes, nature of screens, and specific circuits are described

By JAMES S. ALLEN

Institute for Nuclear Studies, University of Chicago
Chicago, Illinois

PARTICLE DETECTORS have played an important role in nuclear physics from the time when alpha particles were first observed by the scintillations produced in a fluorescent screen. Recent experiments conducted with the synchro-cyclotron at Berkeley, California, have shown the need for detectors capable of recording nuclear particles separated by intervals of time less than 10^{-7} seconds. Not only must the instrument be capable of resolving two particles separated by this short time, but also be able to operate at counting rates of the order of 10^6 per second without serious losses.

The speed of conventional detectors such as the Geiger-Müller counter, the proportional counter or the ionization chamber is limited by the drift velocity of the electrons moving through the gas in the counters or chambers. These electrons are produced as a result of the ionization of the gas due to the passage of the primary particle through the counter. In practice, the lower limit for the resolving time of a gas-filled counter is about 10^{-7} seconds, although somewhat lower values have been reported.

At present, the electron multiplier tube is one of the few detectors whose operation does not depend upon the motion of electrons or ions through a gas. Although the response of a multiplier tube is not infinitely rapid, the

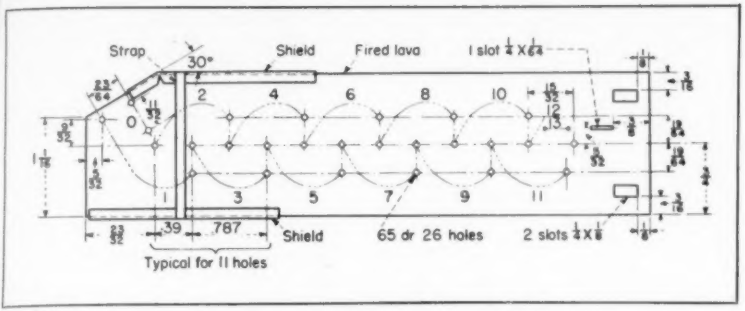

Electrode structure of a typical electron multiplier tube

resolving time should be less than one-tenth that of a gas-filled counter. In practice, the resolving time is limited by the electronic recording equipment and not by the multiplier tube.

In general, multiplier tubes have been used either directly or indirectly as detectors of charged particles such as electrons, positive ions, or gamma radiation. For the direct mode of operation, the primary particles enter the tube and eject secondary electrons from the first electrode. The secondaries are multiplied at the remaining electrodes and finally sufficient charge is produced at the output to permit further amplification by conventional methods. The indirect mode of operation consists in using a photomultiplier tube to record the flashes of light produced by the passage of the primary particles through a fluorescent screen or some other substance which will emit light along the path of the incident particle.

Multiplier Tubes

Two types of multiplier tubes have been used as particle counters. The first is an all-metal tube (*1*) intended to be connected to the vacuum system in which the primary particles are produced. The beam of particles is focussed upon the first electrode of the tube and produces secondary electrons which are in turn multiplied at the following electrodes. The second type (*2*) is the photomultiplier tube developed by RCA, Farnsworth Television, Bell Telephone Laboratories, and numerous other companies. This tube has been used to count the flashes of light produced when single photons, alpha particles, and beta rays strike suitable substances. Fluorescent screens have been used for this purpose with considerable success. The most recent discovery is that naphthalene crystals transform a large fraction of the energy of an incident beta ray or gamma ray into light. A single, high-speed electron will produce sufficient light to produce a voltage pulse at the output of a photocell multiplier placed near the naphthalene.

Design and Operation of Metal Multiplier Tube

The most important factors governing the choice of a suitable metal for the electrodes of a multiplier tube are the secondary-primary electron ratio, and the thermionic emission. G. Gille (*3*) and I. Matthes (*4*) have shown that the secondary-primary electron ratio of BeCu alloy may be increased to a value of about ten by suitable heat treatment. Figure 1 shows data ob-

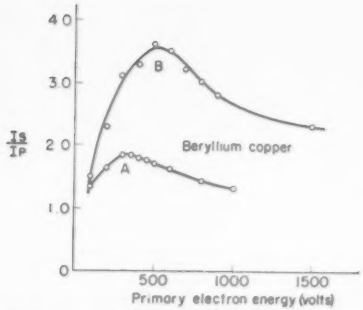

FIG. 2. Multiplication of a BeCu alloy surface: (A) in the unactivated state, (B) after activation by heat treatment

tained by the author for a sample of this alloy. Curve A represents the multiplication of a freshly polished strip of the alloy before heat treatment, and curve B the increase in the multiplication as a result of r-f heating for 15 minutes at a temperature of about 700° C in a vacuum of 10^{-6} mm of Hg. An electrode activated by this method may be exposed to air without a serious decrease in the multiplication. The thermionic emission at room temperature is of the order of 5 electrons per minute per sq cm of electrode area.

An alloy consisting of silver plus a few percent of magnesium has secondary electron properties similar to those of BeCu. Zworykin and Pike (*5*) have investigated this alloy and obtained a maximum multiplication of about ten and a more stable value of four.

The design of the electrode system of a typical metal tube is shown on page 35. The electrodes are formed from 5 mil thick BeCu alloy and are supported between two lava strips. The particles enter the tube through a port opposite electrode No. 1 and eject secondary electrons from the curved inner surface of this electrode. The multiplied burst of electrons is collected at electrode No. 13 which is in the form of a grid. The completed electrode system and metal envelope are shown on page 34. The shield at the top of the electrode structure prevents ions produced near the output electrode

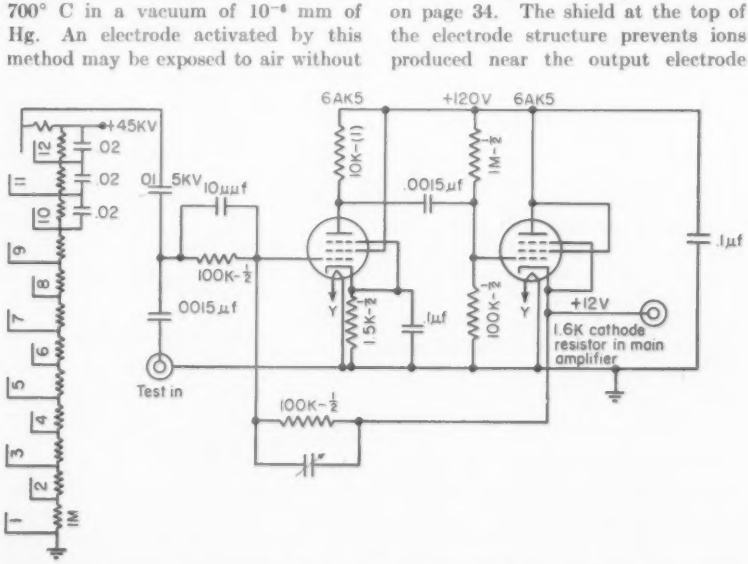

FIG. 3. Schematic diagram of a method of coupling the multiplier tube to the preamplifier

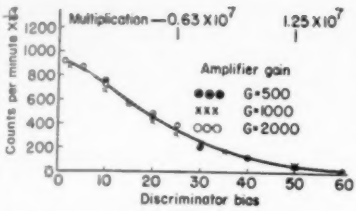

FIG. 3. Counting rate as a function of the average voltage per stage of a 13-electrode multiplier tube. Energy of the electrons entering the tube is 900 volts

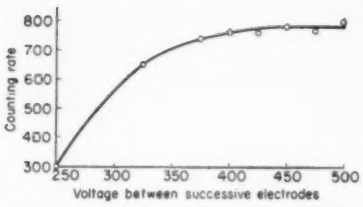

FIG. 4. Discriminator bias curve for 500-volt electrons. A counting rate of 900 × 64 counts per minute represents 100% efficiency of detection

from reaching the input. The electrical leads to the electrodes are brought out through metal-to-glass seals in the base plate. For activation, the electrode structure is removed from the base plate and placed in a separate vacuum system for r-f heat treatment and then transferred back to the tube shell.

Figure 2 shows a schematic diagram of the method of coupling the tube to a preamplifier. This arrangement is suggested when low-energy electrons are to be counted. In practice 4 to 6 kv is applied across the multiplier tube voltage divider. The preamplifier has a gain of unity but inverts the pulse so that a positive pulse is supplied to the main amplifier. The remainder of the electronic equipment may consist of a pulse amplifier with a voltage gain of about 10^4 and a suitable scaling circuit and recorder.

Counting with Metal Tube

Figure 3 shows a typical curve obtained when the counting rate is recorded as a function of the voltage between successive electrodes. For this experiment, a beam of 900-volt electrons entered the tube. The fact that the counting rate becomes nearly constant above 450 volts per stage indicates that the multiplication per stage reaches an almost constant value at this voltage. Due to the wide spacing of the electrodes the tubes may be operated with 500 volts per stage.

Since previous observations had indicated that the pulses at the output of a multiplier tube had a very wide distribution in size, a detailed investigation was made of the shape of this distribution. Figure 4 shows a distribution curve obtained by recording the counting rate as a function of the discriminator bias. Apparently, if the bias is nearly zero, 100% of the electrons entering the tube will be recorded. The bias curve for alpha particles has the same general shape as that obtained with electrons. However, the electron curve drops more rapidly than does that for alpha particles. By a proper adjustment of the discriminator bias, alpha particles may be counted against a background of high-energy electrons. The efficiency of this type of multiplier tube as an electron counter is 100% for electrons of from 300 to 500 volts energy and decreases as the energy of the electrons increases, reaching a value of about 40% for 6 kv electrons and 10 to 20% for 150 kv electrons.

Scintillation Counters

As mentioned earlier in this paper, multiplier tubes have been used indirectly as particle counters. In this application, part or all of the energy of the incident particle is converted into light in a fluorescent screen placed in

front of the photo-cathode of the tube. For example, the burst of light caused by the passage of an alpha particle through the screen will produce a corresponding burst of photo-electrons in the tube. These electrons are multiplied in the tube by a factor of 10^4 to 10^6 and amplified further by a pulse amplifier. In addition to alpha particles, high-energy electrons and gamma rays can be recorded in this manner with high efficiency.

R. Sherr (*6*) has described a compact, portable, alpha-particle scintillation counter using a 931-A photomultiplier tube. In this case, the phosphor was hex. ZnS: Ag, a silver-activated zinc sulfide. The emission spectrum of this phosphor matches the sensitivity curve for the 931-A tube almost exactly. In order to place the phosphor as close to the photo-cathode as possible, a thin layer of the active material was deposited on the outside of the glass surface of the 931-A tube.

The circuit for the scintillation counter is shown in Fig. 5. Two methods of detection are provided: a set of headphones to register single alpha particles, and a microammeter for use with strong sources. Additional amplification (beyond that provided by the multiplier tube) is not necessary when headphones are used.

Measurements of the range of Po α-particles with the scintillation counter gave 3.65 ± 0.05 cm using headphones, and 3.70 ± 0.02 with an oscilloscope, in comparison with the known value of 3.80 cm. The energy of an alpha particle of 1 mm residual range is 100 kev. Apparently, this represented the lower limit to the energy of an alpha particle that could just be detected with this counter.

The efficiency for auditory detection

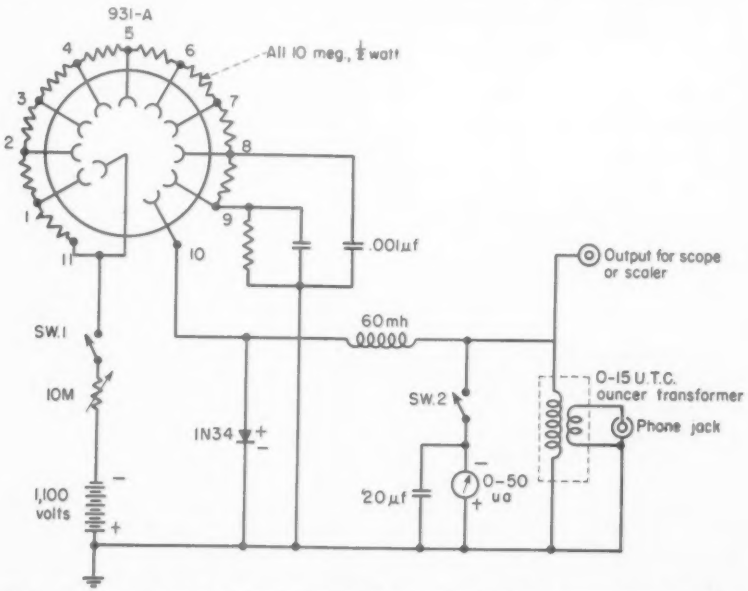

FIG. 5. Circuit for a portable multiplier tube scintillation counter from a design by R. Sherr

of alpha particles was found to be about 80%. The pulse size distribution was very broad, varying from pulses indistinguishable from the dark-current pulses to pulses fifty times the size of those due to the dark current.

J. W. Coltman (*7*) has described experiments with a multiplier tube scintillation counter using a small fluorescent screen (Patterson D X-ray screen) placed near the photo-cathode. In Fig. 6 are shown the curves obtained by Coltman for various types of radiations. These curves have been multiplied by different normalization constants and can be compared only in regard to shape.

H. Kallman (*8*) has described a scintillation counter using a naphthalene screen and a photomultiplier. Since this paper is not readily available at the present time, the only published information is the work of M. Deutsch (*9*). He has investigated this type of scintillation counter and has discovered that every electron is counted if it spends sufficient energy in the screen, namely, about 0.15 Mev at room temperature or 0.05 Mev at dry ice temperature. Screens several centimeters thick have been used giving an efficiency of 20% for counting 1.2 Mev gamma rays and even higher for softer gamma rays. Energies of beta and gamma rays can be determined from bias curves with accuracy comparable to ordinary absorption measurements. Since the response of this type of counter is extremely fast, resolving times at least as short as 10^{-7} seconds can be used without losses.

The author has carried out some preliminary investigations of this type of counter, using a 931-A photomultiplier tube and a naphthalene screen. In order to reduce the high background counting rate, the tube was cooled with dry ice and operated at 600 volts. When beta rays of maximum energy of 0.87 Mev were allowed to strike the naphthalene screen, a high counting rate was observed. Measurements with a Geiger counter indicated that the scintillation counter was recording approximately 100% of the electrons striking the naphthalene.

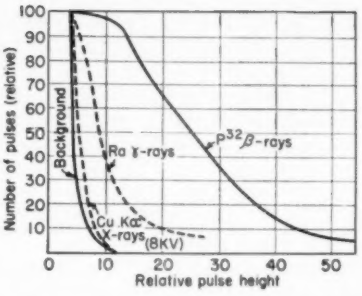

FIG. 6. Pulse height distributions for various types of radiations entering a scintillation counter (after J. W. Coltman)

BIBLIOGRAPHY

1. J. S. Allen, *Rev. Sci. Instr.* **18,** 739 (1947)
2. V. K. Zworykin, J. A. Rajchman, *Proc. I.R.E.* **27,** 558 (1939) and J. R. Pierce, *Bell Lab. Record* **16,** 305 (1938)
3. G. Gille, *Z. tech. Physik* **22,** 228 (1941)
4. I. Matthes, *Z. tech. Physik* **21,** 232 (1941)
5. V. K. Zworykin, J. E. Ruedy, E. W. Pike, *J. Applied Phys.* **12,** 696 (1941)
6. R. Sherr, *Rev. Sci. Instr.* **18,** 767 (1947)
7. J. W. Coltman, Brookhaven Conference Report, Aug. 14–15 (1947) p. 18; J. W. Coltman, Fitz-Hugh Marshall, NUCLEONICS **1,** No. 3, 58 (1947)
8. H. Kallman, *Natur u. Tech.* July, 1947
9. M. Deutsch, *Bull. Am. Phys. Soc.* **23,** 7 (1948); also NUCLEONICS **3,** No. 3, 58 (1948)

Study on the Radioactive-Electric Converter

A design, utilizing grids, for the direct conversion of radioactive energy into electric energy is discussed from both the electrical and nuclear viewpoint. The efficiency of a specific design containing one peripheral and four grid electrodes, for cylindrical geometry and spherical geometry, is calculated

By ANDREW GEMANT and HUGH M. ARCHER

Research Department, The Detroit Edison Company
Detroit, Michigan

IN CONNECTION with the utilization of atomic power for power production, the question of direct conversion of atomic energy into electric energy (*1*) is of special interest. If part of the fission fragments (*2*) should be released as high-velocity charged particles predominantly of one sign, then these particles could be directed against a suitably arranged electrode which would assume a high potential (*3*). The present paper is concerned with elaborating on a few pertinent details of a radioactive-electric converter.

Consider a radioactive source, which is located on a central electrode; another electrode is arranged peripherally. The capacitance between them is C and they are externally connected by a resistance R. The source, considered homogeneous for the moment, emits n particles per second of charge e and energy eV_0. (V_0 = characteristic voltage of particles.) The particles collect upon the outer electrode and charge it to a voltage V. The variation of the potential V with time t is given by

$$V = enR(1 - e^{-t/Rc}) \qquad (1)$$

Equation 1 is valid for $V \lesseqgtr V_0$, or $R \lesseqgtr V_0/en$ because, for larger voltages, the particles would not reach the electrode but would turn around and fall back into the source. For $R < V_0/en$, only part of the kinetic energy of the particles is utilized, the balance being transformed into heat when the particles hit the electrode. Hence, maximum current *and* voltage, *i.e.*, maximum power (namely $e^2n^2V_0$), are obtained for $R = V_0/en$.

Up to this point, it was assumed that all particles emitted by the radioactive source have the same energy, eV_0. However, particles usually have energies ranging from zero up to a certain maximum eV_0. Curve 1 in Fig. 1 shows the distribution curve (*4*) of electrons for the phosphorus isotope P^{32}; the abscissa shows energies, the ordinates show distribution frequencies in fractions of maximum values. With an inhomogeneous source of this kind only a certain fraction of the particles would reach the outer electrode. All other particles would be stopped in the high electric field, which decelerates them, and would return to the central electrode; hence, only a fraction of the total available power would be utilized electrically.

Let us now introduce a grid between the two electrodes, and an external grid resistance R_g. This grid assumes a potential V_g which is determined by the grid resistance R_g in the following manner: All particles between energies eV_0 and eV_g, the number n_g of which can be read from curve 1 of Fig. 1,

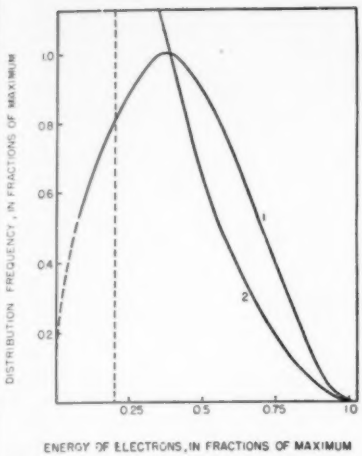

FIG. 1. Energy distribution of electrons emitted by source

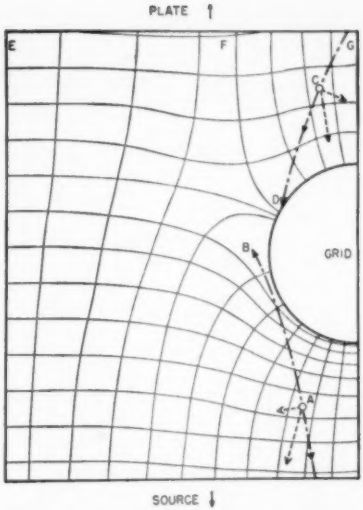

FIG. 2. Approximate field and potential pattern around a cylindrical grid between the source and the plate

are stopped in the space between outer electrode and grid; they then return and collect at the grid. Since n_g is a function of V_g, the latter is determined by the relation $V_g = R_g n_g e$, where n_g has to satisfy its relation to V_g according to Fig. 1. The n_g particles lose a certain fraction of their energy in the form of heat when they hit the grid; only the amount eV_g is utilized. Particles stopped between the grid and the source would again return to the source. Such a device would be an improvement over the original device without a grid; a further improvement might be attained by having several grids instead of one. In this manner, the total available potential eV_0 is subdivided into smaller fractions, the available current in the external circuit increasing as the central electrode is approached.

The efficiency of the mechanism of the grids as pictured above is by no means perfect. A fraction of electrons flying centrifugally is intercepted by the wires of the grids. Also a certain fraction of electrons flying centripetally will miss the first grid and collect perhaps on the next one or at the source. An estimate of the magnitude of this efficiency was obtained in two independent ways: by an analysis of the field pattern around grids, and by an experimental procedure on a pentode tube.

As far as the first method is concerned, Fig. 2 shows the approximate field and potential pattern for a two-dimensional grid structure. The source is assumed to be positive, the plate negative, and the grid has an intermediate potential. Consider an electron at point A, traveling centrifugally in a direction such that, without a field, the electron would be intercepted by the grid. The field at A and its components are shown diagrammatically. One component decelerates the electron, the other deflects its path toward B making it possible for the

TABLE 1

Power Output (Pentode vs. Diode)

Circuit	*Electrode pair*	*Resistance, ohms*	*Current, μamp*	*Voltage, volts*	*Power, μwatt*
Diode		2000	200	0.40	80
Pentode	Plate-suppressor	1800	34	0.061	2.1
"	Suppressor-screen	1400	77	0.108	8.3
"	Screen-control	1000	158	0.158	25
"	Control-filament	600	410	0.246	101
				Sum:	136.4

electron to avoid the grid. Consider, on the other hand, an electron at C, traveling centripetally. According to its direction, it would bypass the grid wire. In the field, as shown, the electron is accelerated and deflected toward D, thus obtaining a chance of collecting on the grid. Thus, the probability of collection of centripetal electrons is favorable only if the returning electron crosses the EFG plane between points F and G. The efficiency of collection may be roughly estimated as the ratio FG to EG, which is 35 to 40% for a structure of 75% opening.

Experimentally, the grid efficiency was estimated by tests carried out with a No. 77 pentode tube. In a pentode, the rather limited number of electrons that emerge from the space charge surrounding the filament represents the source. Table 1 gives the data for a particular 3-grid circuit as compared with the optimum power obtainable from the corresponding "diode" circuit (control grid plus filament as one electrode versus all other electrodes). The power in the first case is 136.4 μwatt, as compared with 80 μwatt for the diode, indicating that the mechanism as assumed above is operative.

An estimate of the grid efficiency can be made from another test, summarized in Fig. 3. Here, the potentials and currents, referred to the various electrodes for a particular set of resistances, are taken as an arbitrary zero level. In the subsequent measurements indicated by 1, 2, and 3, the resistances were changed, and the corresponding changes in potentials (dotted lines) and currents (solid lines) from our arbitrary zero level were plotted. It can be seen that raising the potential of an electrode lowers the corresponding current, as is to be expected. The solid lines show that any decrease in current is accompanied by increases from the other, centrally located grids, according to the mechanism assumed. The net change, however, is not zero, as a 100% efficiency would require, and is always negative. From these data, the efficiency may be estimated as 50 to 60%.

The construction of the electrodes may be spherical or cylindrical. Cylindrical electrodes and grids would be constructed according to more conventional designs than would spherical electrodes.

If, however, a cylindrical design is used, a complication arises because of

the directional effect of the emitted particles. The emitted particles have velocities in all possible directions. The electric field, however, which decelerates the particles, has a radial direction; thus only the radial component of the particle velocity can be utilized. The following equations are derived on a classical basis, although it is realized that, for fast velocity particles, relativistic equations ought to be used. It is perhaps right to say that, for energies up to 0.5 Mev, the results of the two calculations will not differ appreciably, but that for energies above 0.5 Mev (as in the case of P^{32}) the corrections, as computed classically and relativistically, will differ to a certain extent.

Let us consider a point source on the axis of a long cylinder, and assume for the moment that it is homogeneous, emitting n_0 particles of energy $E_0 = eV_0$. The angle between the particle velocity and the axis is φ. For a given φ $(0 < \varphi < \pi/2)$ the differential spatial angle is twice $2\pi \sin \varphi \, d\varphi$, and since there are n_0 particles over a spatial angle 4π,

$$dn = n_0 \sin \varphi \, d\varphi \qquad (2)$$

Since only the radial component of the velocity is utilized, the utilizable energy E is given by

$$E = E_0 \sin^2 \varphi \qquad (3)$$

Eliminating φ, one has for the number of particles with utilizable energy between E and $E + dE$:

$$dn = \frac{n_0 dE}{2E_0 \sqrt{1 - E/E_0}} \qquad (4)$$

The ratio of average utilizable to total energy according to equation 4 is $\frac{2}{3}$, whereas the extreme relativistic case would yield $\frac{1}{2}$.

Let us now apply equation 4 to the case of a nonhomogeneous point source with energies E_0 from zero to a maximum E_m, the number of particles between E_0 and $E_0 + dE_0$ being fdE_0. Each group fdE_0 contributes a certain

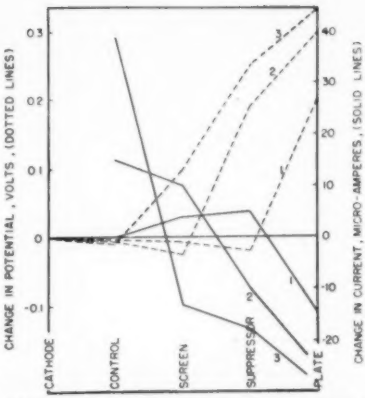

FIG. 3. Results of measurements on a pentode tube No. 77 using a 3-grid collecting circuit

number fdE to particles of energies between E and $E + dE$, whereby $E < E_0 < E_m$. In equation 4, we now have $n_0 = fdE_0$, and, by integration,

$$f = \int_E^{E_m} \frac{fdE_0}{2E_0 \sqrt{1 - E/E_0}} \qquad (5)$$

As an illustration, it shall be assumed that all particles are equally distributed among energies from zero to E_m; in this case, $F = 1$. By substituting $x = 1/E_0$ and $p = E/E_m$, one has

$$f = \frac{1}{2} \int_{1/E_m}^{1/E} \frac{dx}{x \sqrt{1 - Ex}}$$

$$= \frac{1}{2} \left| \log \frac{\sqrt{1 - Ex} - 1}{\sqrt{1 - Ex} + 1} \right|_{1/E_m}^{1/E}$$

$$= \frac{1}{2} \log \frac{1 + \sqrt{1 - p}}{1 - \sqrt{1 - p}} \qquad (6)$$

This same analysis will be applied to the actual distribution curve (curve 1, Fig. 1) later.

As far as the source is concerned, there is a great variety of possible materials; many new ones have been made available through the U. S. Atomic Energy Commission (*5*). As an example, let us select radioactive phosphorus, P^{32}, which is a beta emitter. With such a source, the central electrode is positive,

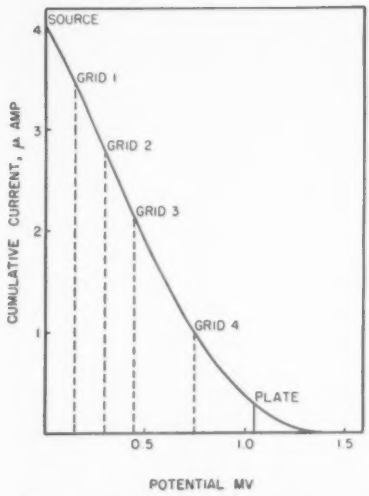

FIG. 4. A suggested arrangement of electrodes and grids shown on the voltage-current characteristic

and the outer electrode is negative. The half-life of P^{32} is 14.3 days which means that it would have to be renewed, say, every 2 weeks. The specific activity available at present is 0.1 c per gram of solids. Let us specify the total activity of a source at 10^3 curies. The total available current *ne* is then 5.9 microamperes.

There is a self-absorption of electrons in the source which can be estimated. One thousand c is contained in 10 kg of solids. For a cylindrical source, 10 m high and about 30 cm in diameter, the total area is about 10^5 cm^2, and the surface density is 0.1 gm/cm^2. The radioactive material might be applied by means of traces of a binder upon a suitable light fabric made conducting by graphitization, for instance. Such a source has no other solid material as backing support, and the only absorption takes place in the radioactive material itself. Since electrons are emitted both away from and toward the axis, the actual thickness traversed by the electron ranges from zero to twice the entire layer; hence the average thickness is 0.1 gm/cm^2.

By use of range versus energy relations valid for soft beta rays (*6*), it follows that energies up to 0.34 Mev are absorbed by such a layer. Electrons of higher energies lose part of their energy in transit through that layer. All these losses can be approximately accounted for by shifting the ordinate axis of Fig. 1 to the dotted line at 0.34 Mev, which now becomes the new zero point. The directional analysis on a cylindrical device is now applied to curve 1 of Fig. 1 with the shifted ordinate axis. We approximate that curve by two straight line sections, and, with the same substitutions as before, one has for $0.26 < p < 1.0$:

$$f = (0.68 - 0.34p) \log \frac{1 + \sqrt{1-p}}{1 - \sqrt{1-p}} - 0.68\sqrt{1-p} \quad (7)$$

The function is plotted as curve 2 of Fig. 1.

The next question is: Through what medium should the particles pass in traveling from the source to the outer electrode? A vacuum of at least 10^{-5} mm Hg is known to have excellent electrical insulation, so that the electrostatic field is maintained as long as no electrons are liberated by the high field from the electrodes. As far as the separation of the electrodes is

TABLE 2

Values for Spherical Design

Electrode pair	*Voltage, mv*	*Current, μamp*	*Resistance, 10^{12} ohms*	*Power, watts*
Source—Grid 1	0.15	3.47	0.043	0.52
Grid 1— " 2	0.15	2.82	0.053	0.42
" 2— " 3	0.15	2.16	0.070	0.33
" 3— " 4	0.30	1.01	0.30	0.30
" 4—Plate	0.30	0.29	1.0	0.09

TABLE 3
Efficiency of Design

	Spherical design		*Cylindrical design*	
	Watt	*Percent*	*Watt*	*Percent*
Total theoretical power	4.10	100	4.10	100
Theoretical power after correcting for absorption, directional effect and secondary emission	2.03	49	1.45	35
Diode circuit	0.97	24	0.61	15
4-grid circuit—theoretical	1.66	40	1.10	27
" " practical	1.30	32	0.86	21

concerned, data by Trump and Van de Graaff (7) have been considered. A reasonable estimate is a gap between neighboring grids of 50 mm per 100 kv. The total separation between source and outer electrode must then be 1 m.

As to the material of the electrodes, it has to be considered that the impinging electrons liberate a certain number of secondary electrons. This secondary electron emission is unwanted, and it is essential, therefore, to select a surface for the electrodes that exhibits this characteristic to a low degree. Secondary emission is measured by a coefficient giving the ratio of the number of secondary electrons to primary electrons. Trump and Van de Graaff (7) obtained data for energies from 0.04 to 0.34 Mev. Aluminum and graphite exhibit the lowest figures. An average value for graphite of, say, 0.15 may be estimated for the whole energy range. Thus, if graphitized electrodes are used, a loss of about 15 % has to be taken into account.

The following design serves as an illustration. If the source is 10^3 curies, as assumed, the total area below curve 1, Fig. 1, corresponds to 5.9 μamp. The analysis differs according as to whether spherical or cylindrical geometry is taken. Final results will be given for both. We start from curve 1, Fig. 1, for the spherical case, and from curve 2, for the cylindrical case. On this basis the cumulative currents, starting from the endpoint at 1.5 Mev, can be evaluated. The result for the spherical case is given in Fig. 4, which shows the cumulative current in μamp versus the potential in mv. The location of the electrodes in a specific design is indicated in this figure; their intercept with the abscissa gives their corresponding potentials. To make this arrangement possible, the external resistance between neighboring grids must be assigned the value, potential difference divided by the cumulative current. Table 2 shows, for the spherical design, the voltages, currents, and external resistances between neighboring electrodes as identified in Fig. 4.

Table 3 indicates the efficiency figures for both the spherical and cylindrical designs.

Since, according to our results, the efficiency of the grids is about 50%, the gain in power of the 4-grid circuit over that of the diode circuit was halved in order to obtain the figures for the last row in Table 3.

BIBLIOGRAPHY

1. John C. Parker, Statement from AEIC before the Senate Committee on Atomic Energy, Feb. 18, 1946
2. Plutonium Project Report, *Revs. Mod. Phys.* **18,** 513 (1946)
3. P. H. Miller, *Phys. Rev.* **69,** 666 (1946)
4. Kai Siegbahn, *Phys. Rev.* **70,** 127 (1946)
5. Radioisotopes Price List, U. S. AEC, NUCLEONICS **1,** No. 1, 64 (1947); also E. G. Linder, *Phys. Rev.* **71,** 129 (1947)
6. W. F. Libby, *Anal. Chemi.* **19,** 2 (1947)
7. J. G. Trump, R. J. Van de Graaff, *J. Applied Phys.* **18,** 327 (1947)

Interaction of Isotopic Radiation with Matter—II*

Photons interact with matter in three ways—photoelectric effect, Compton effect, and pair production. Means for calculating absorption coefficients for the different types of interactions are given in this second of two papers

By REX G. FLUHARTY

Department of Physics and Laboratory for Nuclear Science and Engineering
Massachusetts Institute of Technology, Cambridge, Massachusetts

WHEN A NUCLEUS undergoes a transition from one energy level to a lower one, electromagnetic radiations (photons) are emitted during that transition. Whereas in the first part of this paper,† the effect of alpha and beta particles was discussed, we will consider here the interaction of X- and gamma radiations with matter.

Gamma rays are those quanta (or photons) which originate in the nucleus. However, since the mode of interaction of a photon is quite independent of its source, the general discussion will not be restricted to gamma rays.

Although X-ray photons range in energy from 0.005 to 100 Mev, only the range from 0.1 to 5 Mev will be considered in this discussion. The different sources of X-rays are characterized by different energy distributions, *i.e.*, they have different numbers of photons for a given energy.

X-RAYS

The three types of interactions which are important for the photon energies under consideration are: photoelectric effect, Compton effect, and pair production. Each is pictorially represented in Fig. 1.

For a given material, each type of interaction is found to be predominant in a particular energy region. Thus, at low energies it is frequently found that only the photoelectric effect need be considered, whereas for very high energies, pair production is the most important. For gamma rays absorbed in materials (Z varying from 10 to 35), it is usually sufficient to consider only the Compton effect.

The usual designation of an X-ray photon is in terms of its wavelength λ, the common unit for which is the Angström (1 Angström = 10^{-8} cm). Another means of identification, generally used for gamma rays, is by its energy, usually expressed in Mev. The following equation‡ can be used to convert from one to the other:

$$\lambda = \frac{1238}{E_\gamma} \times 10^{-13} \text{ cm} = \frac{1238}{E_\gamma} \times 10^{-5} \text{ A.U.}$$

where E is the energy in Mev, and A.U. is the Angström unit.

When a beam of X-rays penetrates an object, the fraction of the energy lost in a small distance Δx is found to be

* This work was supported in part by the Office of Naval Research.

† NUCLEONICS **2**, No. 5, 29 (1948).

‡ This equation is derived from the equations, $E = h\nu$ and $\lambda\nu = c$, where E is the energy of the photon in ergs, h is Planck's constant, ν and λ are the frequency and wavelength of the photon, respectively, and c is the velocity of light in cm per sec. Also 1 Mev is equal to 1.6×10^{-6} ergs.

$$f = \Delta I/I = -\mu \Delta x$$

where ΔI is the rate of energy loss, I the rate at which energy is passing through, and μ a constant depending upon the beam energy and the material being penetrated. The constant μ is known as the linear absorption coefficient. In other words, the fraction lost or absorbed is equal to a constant times the thickness. In the discussion of photon interactions, equations will be given from which the absorption coefficients for the various types of interactions can be calculated.

Photoelectric Effect

In the photoelectric effect (Fig. 1*a*), the photon reacts with the whole atom and the ejection of one of the atomic electrons results. The emitted electron is found to have an energy equivalent to that of the initial photon minus the energy required to remove the electron from the atom. Since the photon is completely absorbed, pure photo-absorption will not change the energy distribution in the transmitted photon beam—merely the number of photons.

Since the electric and magnetic fields of the quanta are at right angles to the direction of motion of the photon, the electrons are emitted nearly normal to the initial photon direction, and interact with absorbing material the same as any other high-energy electron. The direction of electron emission will vary, but the energy will be discrete, the value depending upon the type of atom and the particular shell involved (*K* electron, *L* electron, *etc.*). With increasing photon energy, a more forward direction of emission of the electron will be observed.

Compared to the photon energy, the binding energy of the electron can usually be neglected and the assumption made that the electron carries away the total energy. Thus, the photon energy is distributed as ionization and excitation along an electron track starting at the point of encounter.

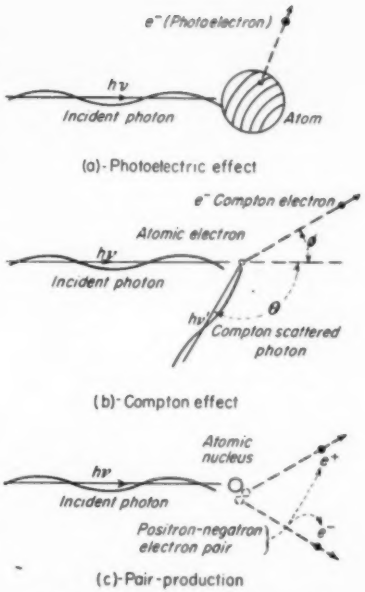

FIG. 1. Important interactions for photons having energies of gamma rays

The probability that the photoelectric effect will take place is proportional to the linear photo-absorption coefficient, which is given by the following empirical equation from Lea (*1*):

$$\tau = 0.0089\rho \left(\frac{Z^{4.1}}{A}\right) \lambda^n$$

where τ is in cm^{-1}, ρ is the density (τ/ρ is the mass absorption coefficient), λ the wavelength in A.U., Z the mean atomic number of the absorbing material, A the mean atomic weight, and n a number which has a value of 3.05 for N, C and O, and 2.85 for Na to Fe. τ is the fraction of the photons lost per centimeter by photo-interactions from the beam, and is related to the interaction probability.

When λ has values of the order of magnitude of the characteristic radia-

tion of the absorbing material, this equation will no longer hold and it is necessary to use handbook values. For ordinary materials ($Z = 6$ to 13), this means a value of λ or E_γ of the order of 1 to 10 A.U. or 0.001 to 0.01 Mev. For lead, it is about 0.15 A.U. or 0.085 Mev.

Compton Effect

In a Compton interaction (Fig. 1*b*), the photon collides with an atomic electron and is elastically scattered, *i.e.*, momentum and energy are conserved. On the assumption of a free electron, a reasonably straightforward derivation gives the energies of the struck electron and secondary quantum in terms of the deflection angles, mass, and energies. The assumption of the free electron is quite valid for most γ-ray energies in comparison to the electron binding energy. It is to be noted in the Compton interaction that the absolute number of photons is unchanged, even though they change direction and lose energy.

The energy of the secondary photon is found to be

$$E_\gamma = \frac{0.51}{1 + \frac{0.51}{E_0} - \cos\theta}$$

where E_γ is in Mev, E_0 is the energy of the incident photon in Mev, and θ is the angle the scattered photon makes with the initial direction. The 0.51 Mev term corresponds to the rest energy of the electron. If E_0 is large compared to 0.51 Mev, E_γ approaches 0.25 Mev at 180 deg and 0.51 Mev at 90 deg.

The energy given to the electron will be the difference between the energies of the primary and secondary photons, and hence will be given by

$$E = \frac{E_0}{1 + \frac{0.51}{E_0(1 - \cos\theta)}}$$

The maximum value will occur when $\theta = 180$ deg ($\phi = 0$) and the electron comes off in the forward direction. When E_0 is large compared to 0.51 Mev,

$$E_{max} \rightarrow (E_0 - 0.25) \text{ Mev}$$

With an initial beam of homogeneous X-rays, Compton electrons will be found with all energies. The relative number of higher energy, forward-scattered electrons will increase with increasing energy.

As the interaction is between a photon and an electron, the probability that a Compton encounter will occur depends upon the number of electrons per unit cross-sectional area. The absorption coefficient is generally divided into two parts, σ_a and σ_s. The sum of the two (σ) is related to the probability that an interaction will occur; σ_a is a measure of the fraction of the initial photon energy going into electron energy, and σ_s that part going into final photon energy. An apparent conflict is that σ is considered for a single photon, whereas σ_a and σ_s are taken from the averages of many. The total Compton absorption coefficient is given by

$$\sigma = \sigma_a + \sigma_s = NZ(f_a + f_s)$$

where N is the number of atoms per cubic centimeter, Z the number of electrons per atom, and f_s and f_a functions of the energy. The values of $f(f = f_a + f_s)$ and f_s can be derived from a theory given by Klein and Nishina (*2*) and hence f_a can be obtained by subtraction.

Pair Production

In the pair-production interaction (Fig. 1*c*), the electromagnetic energy of the photon is converted into two electrons, one positive and one negative, plus kinetic energy. Energy is converted into mass, with the photon requiring 1.02 Mev (the rest mass per electron is equivalent to 0.51 Mev) before this interaction can take place.

The effect, which is only important for high Z materials, takes place near the nucleus because of the high electric

field present. Equal sharing of the energy excess by the two electrons is the most probable but all energies are possible, as in the Compton encounter. Like the photo-effect, this encounter results in the complete removal of the photon.

The pair-production absorption coefficient is given approximately by

$$K = kNZ^2(E - 1.02)$$

where K is the linear absorption coefficient, k a proportionality constant, N the number of atoms per cubic centimeter, Z the atomic number, and E the photon energy in Mev.

Absorption of X-rays

In comparison with heavy charged particles and electrons, the absorption of X-rays is more truly exponential. Thus, no maximum range can be observed and the number of photons will approach zero in an exponential fashion (equations 1 and 2).

The intensity of a beam of X-rays is proportional to the energy per second passing through a unit cross section perpendicular to the beam. Thus, it is proportional to the sum of the energies of the photons which pass through the cross section per unit time. When each photon has the same energy, it is simply the product of the number and energy of the photons.

For a parallel beam of X-rays in which each photon has the same energy (monochromatic or homogeneous), the intensity at a thickness x of absorbing material perpendicular to the beam is usually given by

$$I = I_0 e^{-\mu x} \quad \text{or} \quad 2.303 \log_{10} \frac{I}{I_0} = -\mu x \tag{1}$$

where I is the intensity at the point x, I_0 the intensity at the surface, and μ the linear absorption coefficient, a constant which depends upon the material and energy of the photons. Where such theory is valid, a plot of I versus x made on semilog paper will be a straight line. For a beam of several energies, the following equation is applied:

$$\begin{aligned} I &= I_1 e^{-\mu_1 x} + I_2 e^{-\mu_2 x} \cdots I_i e^{-\mu_i x} \\ &= N_1 E_1 e^{-\mu_1 x} + N_2 E_2 e^{-\mu_2 x} \\ &\qquad \cdots N_i E_i e^{-\mu_i x} \end{aligned} \tag{2}$$

where I_i is the intensity associated with N_i photons of energy E_i and μ_i is the corresponding absorption coefficient.

For a given energy and absorbing material, the μ to be used is frequently taken as the sum of the fractional coefficients due to the various reaction mechanisms, *i.e.*:

$$\begin{aligned} \mu_0 &= (\tau + \sigma + K) \\ &= (\tau + \sigma_a + \sigma_s + K) \end{aligned} \tag{3}$$

where μ_0 is the total absorption coefficient; τ the photoelectric coefficient; σ the total Compton coefficient which is composed of σ_a, the Compton absorption, and σ_s, the Compton scattering coefficients; and K the pair-production coefficient. However, it is important to realize that *this absorption coefficient can only be properly used under the special condition that the energy* (E_i) *stays constant.**

Equations 1 and 2 are therefore valid if only the photo or pair-production coefficient is to be considered. (We are neglecting second-order effects such as secondary radiation from the electrons, and annihilation radiation from the positron created during pair production.)

At each photo encounter, a photon disappears so that the photons that are left still retain the same interaction probabilities, and hence exponential absorption actually amounts to an

---

* In its differential form, equation 1 becomes

$$N dE + E dN = \mu E N dx$$

We already know that μ is not a constant independent of E; thus, the case where N = constant is ruled out. The other case would imply that

$$\frac{dE}{E} + \frac{dN}{N} = -\mu dx$$

and that therefore dE/E and dN/N are dependent, which is not true.

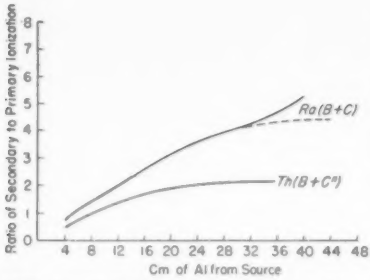

FIG. 2. Relative energy contributed by secondary photons to the energy contributed by primary photons from point sources of Ra and Th gamma rays in aluminum (*5*)

exponential decrease in the number of photons:

$$N = Ne^{-\mu x} + N_1 e^{-\mu_1 x} + N_2 e^{-\mu_2 x} \cdots \quad (4)$$

where each term is completely independent of any others. The intensity is obtained by weighting each number component with its proper energy as in equation 2.

In the Compton interaction, the absolute number of photons remains unaltered, so that theories similar to those shown in equations 1, 2, 3 and 4 do not describe the general situation. However, since the photons are scattered and deflected, the theory will apply in the case of "good geometry." In this special case, the beam is narrow (small diameter compared to its length, such that $1/\mu_0$ is much larger than the beam diameter). Virtually all scattered photons leave the beam and are not allowed to re-enter. In this case, the total μ_0 can be used and equations 1 and 2 are valid, since for each encounter, the photon is lost. Except for this special case, some scattered photons will re-enter the beam and must be taken into account. This more general case would be classified as "poor geometry" according to the above notation.

The Klein-Nishina theory for Compton interaction has been developed to cover the case of *first encounter only*, and does not consider the degraded photon radiation. Thus, experimental procedures for checking the theory will make use of "good geometry" wherein the photon beam consists only of photons which have not interacted with the material. A general method of theoretical approach to the multiple interaction case is given by Hull (*3*) for the case of very thick layers, where averages are valid. He outlines a general method of approach and solves the special cases of point and linear sources in extended media.

The limitation of thick layers implies that the distances considered in the absorber are greater than $1/\mu_0$ (see Figs. 3, 4, 6). Photons, after leaving the source, travel in a straight line, as though in free space, until an encounter occurs; the average distance can be shown to be $1/\mu_0$. For distances small compared to $1/\mu_0$, few encounters will take place, and first order degradation photons (quanta from first collisions) only need be considered where corrections are desired.

The usual practice is to approximate the actual variation from exponential absorption by assuming the exponential absorption in conjunction with an effective absorption coefficient μ (*4*, *5*, *6*, *7*). In general, it can be said that μ will certainly not exceed μ_0, and the intensity will not be smaller than that obtained using μ_0 for the absorption coefficient. Likewise μ will usually not be smaller than $\mu - \sigma_s$.*

Gray (*5*) measured the ionization in small air cavities at various distances from a radium gamma-ray source embedded in a large cylinder of aluminum. The ionization in the cavities is an excellent measure of the ionization

* Near the source, the photon intensity can exceed the value obtained using $\mu - \sigma_s$ since backscattering can actually increase the intensity.

created (energy lost) in the aluminum by the emerging photons, provided proper corrections are made for the relative stopping power of two media. Figure 2 is a plot of the ratio of the primary ionization to the secondary ionization created by scattered photons. Thus, at 5.3 cm, the secondary ionization is equal to the primary ionization calculated from $\mu_0 - \sigma_s$. In the distances out to 8 cm, an apparent absorption coefficient of less than $\mu_0 - \sigma_s$ is actually observed.

The effective μ approaches μ_0 at 40 cm (Fig. 2) and beyond, hence the degraded photons are losing energy at the rate at which they are being produced, and are said to be in equilibrium with the primary beam. The effective absorption cross section used by Gray is an incremental cross section describing the change of ionization compared to the total at a given point. The actual total ionization is in excess of that computed from exponential absorption theory using μ_0, since a smaller average cross section has been effective up to that point.

Curves of the absorption coefficients for Al and Pb are given in Figs. 3 and 4, respectively. The values of μ_0, the total absorption coefficient, were calculated and checked by C. M. Davison and previously reported by Evans (*4*). Where τ can be neglected, we see that μ_0 can be calculated from theories previously mentioned, and in this region the correlation is excellent.

To obtain absorption coefficients for other materials, either of these sets of curves can be used to obtain the proper partial coefficient for Pb and Al, and these in turn can be converted to the partial coefficients for the desired material by the following equations:

$$\tau = \tau_i(\rho/\rho_i)(W_i/W)(Z/Z_i)^{4.1}$$

$$K = K_i(\rho/\rho_i)(W_i/W)(Z/Z_i)^2$$

$$\sigma = \sigma_i(\rho/\rho_i)(W_i/W)(Z/Z_i)$$

where ρ, W, and Z are the density, atomic weight and atomic number for the absorbing material, and ρ_i, W_i, and

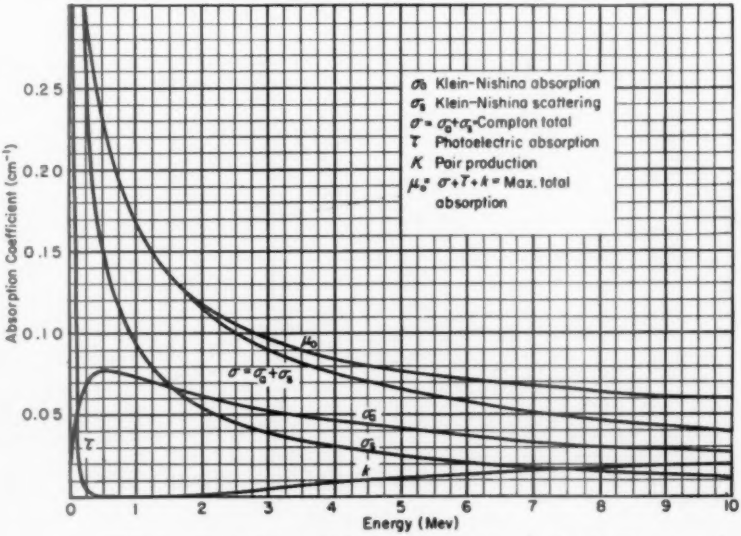

FIG. 3. Absorption coefficients of gamma rays in aluminum

Z_i are the corresponding values for the material for which the coefficients are known (Pb or Al). If the material is complex and contains more than one element, then each component must be weighted separately for τ and K, *i.e.*, weighted according to Z^4 and Z^2.

GAMMA RAYS

In comparison to α and β particles, γ-rays are characterized by relatively little absorption and ionization per unit volume. Their absorption is continuous in the sense that they have no finite range, and the number penetrating increasing thicknesses of material approaches zero in an exponential, or asymptotic fashion. Like α particles, they have discrete energy spectra, and, in this sense, are much easier to deal with from the applied standpoint than the ordinary continuous X-ray spectra emitted by the vacuum tube.

Because of their relatively high energy and small absorption, γ-rays are widely used for shadow photographs of thick, dense materials (steel plates, castings, *etc.*). They find useful application in deep X-ray therapy since large internal dosage can be given with less surface damage.* They will find increasing application as a means of measuring radioactive tracers as the efficiency of detection is increased.

Many of the observed γ-ray energies lie in the 0.1–2.0 Mev energy range, and the Compton interaction is the only important mode of interaction for ordinary materials (Z from 6 to 13). Thus, the attenuation will be proportional to the number of electrons per unit volume in the absorber, *i.e.*, the intensity will depend only upon the number of grams per square centimeter of material penetrated. In the case of

* This is due to the smaller fraction of energy absorbed in the material between the target area and the surface, and to less backscattering, since more of the photons are scattered forward at higher energies.

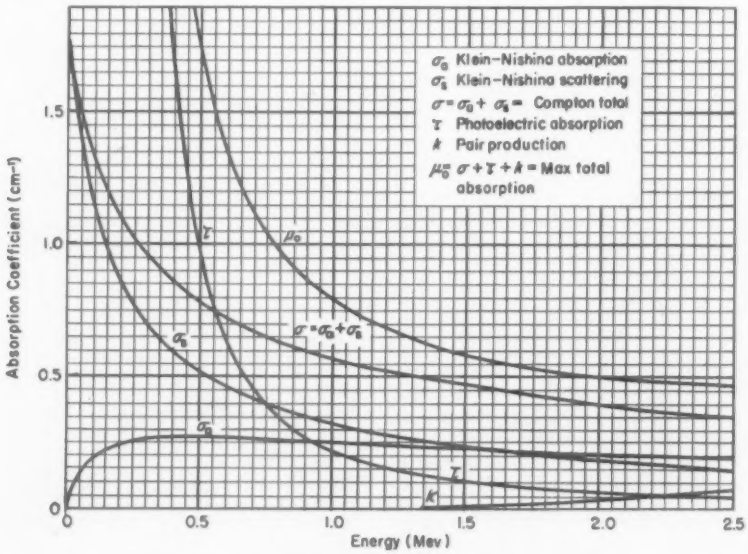

FIG. 4. Absorption coefficients of gamma rays in lead

"good geometry" for 1 Mev γ-rays, μ_0 is found to be (Fig. 3):

$$\mu_0 = \sigma = \sigma_s + \sigma_a = 0.095 + 0.073 = 0.168 \text{ cm}^{-1}$$

Thus, if we have 4.12 cm of Al, the fractional intensity for the "good geometry" is given as:

$$I/I_0 = e^{-0.168 \times 4.12} = e^{-0.693} = \tfrac{1}{2}$$

and 4.12 cm is the half-thickness of Al (the thickness of absorber required to reduce the γ-ray intensity to one half its initial value). Taking the density of Al as 2.7, we have 2.7×4.12 or 11.1 grams per square centimeter. Since the absorption in light materials depends only upon the number of grams per square centimeter, the same number will be the "good-geometry" half-thickness for air, tissue, copper, wood, brass, *etc.* To determine the half-thickness in centimeters, we merely divide by the density.

In most cases, the absorption will be "poor geometry," and the effective absorption coefficient μ is approximated better by σ_a. Thus, for 1 Mev γ-rays:

$$I/I_0 = \tfrac{1}{2} = e^{-0.073 X_{1/2}}$$

or

$$X_{1/2} = 0.693/0.073 = 9.49 \text{ cm } (25.6 \text{ gms/cm}^2)$$

Thus, the half-thickness from this calculation is twice the value obtained using the total absorption coefficient and is approximately 22 meters in air! In lead, the value is about 1.5 cm ($16\tfrac{3}{4}$ gm/cm^2); neglecting τ gives 2.77 cm. Thus Pb is not an ordinary material.

For thin absorbers and ordinary materials ($x \ll 1/\mu_0$), the limits upon the intensity are much narrower and to a good approximation are given by

$$I/I_0 = 1 - \sigma x \text{ (lower limit)}$$
$$I/I_0 = 1 - \sigma x + \sigma_s x \text{ (upper limit)}$$

Thus, for 1-Mev γ-rays and $\tfrac{1}{4}$ cm thickness of Al, $(I/I_0)_{min} = 0.96$ and $(I/I_0)_{max} = 0.98$, with the latter value being favored.

In an estimation of the gamma-ray intensity, geometrical factors must be considered as well as absorption. Thus, the fact that the intensity from a point source falls off inversely as the square of the distance is a geometrical factor which is of utmost practical importance. When the source size is comparable with the distance, other factors of the type encountered in measurement of light intensity must be considered. The problem of intensity calculation involves three factors—absorption, geometry and scattering—and many special cases. The simplest of these have already been considered (*3*, *5*, *6*, *7*, *9*) and will not be discussed here.

The consequence of secondary effects, such as Compton scattered photons, annihilation quanta, and photo- and Compton electrons from surfaces, can be of extreme importance. Thus, for high-energy γ-rays, where pair-production positrons are being formed, annihilation radiation, as well as Compton scattered photons, will always be present. In the shielding of a β-ray counter for minimizing background, the inner surface of the lead shield is a more efficient source of photo- and Compton electrons than a low-Z material, hence the sensitive part of the β-ray counter should be shielded with a low-Z material.

Intensity and dosage estimates can be made for special cases, but accurate results will require experimental measurements. Calculations, where possible, are laborious and very frequently are approximations. Aside from the complications introduced by the scattered quanta, geometrical factors can only be approximated, except in the simplest cases. Shielding design procedures are given by Failla (*8*) and dosage calculations by Marinelli, *et al.* (*9*). The procedures outlined will give reasonable estimates, but accurate values will require actual experimental

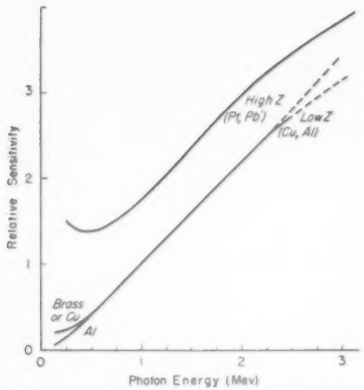

FIG. 5. Idealized relative efficiencies of Geiger-Müller counters of low and high Z materials (*10, 11, 12*)

measurements or phantom dosage chart measurements.

A knowledge of the sensitivity of the detector will be important. We will define the detector sensitivity at a given energy as the response (ion pairs or counts) of the detector per photon at that energy traversing the sensitive volume of the detector. In most detection equipment, the response depends upon ionization in a gas volume. However, *the ionization in the gas is due to secondary electrons created by γ-rays in the walls of the chamber*. The amount of material in the gas is negligible compared to the chamber wall; thus the γ-rays interact mainly with the walls. If the amount of material required to absorb the secondary electrons is small (2–400 mg/cm²) compared to the wall thickness, the *sensitivity will be a surface effect from the chamber walls.*

Figure 5 shows a curve of the relative sensitivity of Geiger counters of low and high Z (70–90) materials, as a function of energy. The work of Peacock (*10*), Maier-Liebnitz (*11*), and Bradt, *et al.* (*12*), seems to be in substantial agreement. The curves shown have been normalized to the same sensitivity at 1 Mev, and the subsequent experimental points from the various data plotted. The shape for low-Z materials is in good agreement (±5%) between 0.5 and 2 Mev, whereas for the curve of high-Z materials, the fit is more approximate (±20).

It shows that much higher sensitivity can be obtained by Pb or Pt cathodes, especially for energies below 0.5 Mev. The linearity of the counter response to γ-ray energy for low-Z material walls shows that the response is proportional to the intensity between 0.5 and 2 Mev.

Figure 6 is a plot of the absorption coefficients in air as a function of the photon energy, where $\mu_a - \sigma_s$ is given instead of μ_a. This coefficient gives the fraction of the energy converted from electromagnetic energy, and its use then assumes that the total beam energy distribution is known, *i.e.*, if scattered photons are present, their energy is known and they are considered primary radiation. Thus, theoretically, the energy lost in air can be calculated, but, practically, the scattered components can only be calculated in special cases.

Figure 7 is a plot of the average number of ion pairs per cm of path length in air per photon versus the photon energy in Mev. To have meaning, this has been taken for a large number of photons. Where the number and energy of the photons is known the roentgen dosage rate* can be calculated from this curve. Thus, if we have ten, 4-Mev photons and eighty, 0.5-Mev photons per second traversing a square cm cross section of air, the roentgen dosage would be:

* The roentgen is that amount of X- or γ-radiation in air which will cause the creation of 1 esu of charge in 1 cc of dry air at 760 mm Hg pressure and 0° C. Since each ion pair requires an average energy of 32.5 electron volts, it can readily be shown that:

$$1 \text{ Mev} = 3.08 \times 10^4 \text{ ion pairs}$$

and

$$1 \text{ r} = 1.61 \times 10^{13} \text{ ion pairs/gm air}$$
$$= 5.24 \times 10^7 \text{ Mev/gm air} = 83.3 \text{ ergs/gm air}$$

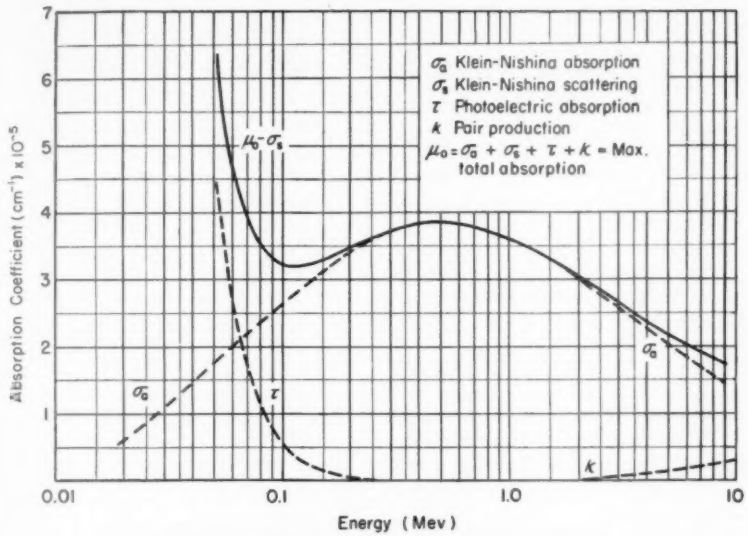

FIG. 6. Absorption coefficients of gamma rays in air

$$\frac{40 \times 1.90 + 40 \times 0.59}{1.6 \times 10^{12}} = 62 \times 10^{-12} \text{ r/sec}$$

For the same intensity ($4 \times 10 + 80 \times 0.5 = 80$ Mev/sec), or eighty, 1-Mev photons, r/sec $= 55 \times 10^{-12}$. Thus, the roentgen dosage is not exactly representative of the intensity. To the extent that the line is straight ($\pm 15\%$ between 0.1 and 4 Mev), the roentgen dosage will be proportional to the intensity. Since the number of counts from a Cu, Al or brass Geiger-Müller counter is proportional to the intensity ($\pm 5\%$ between 0.5 and 2 Mev), the counter will give roentgen dosage to $\pm 10\%$ between the limits specified.

Air-walled chambers can be constructed (4) which will read, directly, the roentgen dosage. Since the wall material will determine the ionization in the chamber, the response will be determined by the walls. These can be used externally or internally in phantoms, *etc.* Where accurate dosage estimations are needed, the experimental technique, if possible, is desired.

Ionization chambers and G-M counters have low detection efficiencies because of the small amount of material in the walls which is effective for interaction. Thus counters detect, at most, 2% of the photons passing through them. In addition, geometry

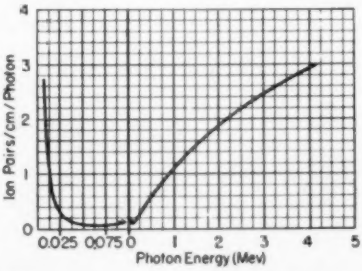

FIG. 7. Average number of ion pairs per centimeter of path length per photon, averaged over a large number of photons

will lower this value by factors of ½ to 0, as the effective detection solid angle decreases. Thus, by comparison with β-rays, detection and use with G-M tubes require much higher activities. Recent developments in solid counters point the way to high-sensitivity (10–50%) γ-ray detection; thus γ-ray measurements will become more and more important.

Since γ-rays do not have a maximum range and are not as highly scattered as β particles, use can be made of the inverse square law to obtain high accuracy (*i.e.*, small distance changes can be minimized). Thus, accuracies of 0.1% are quite feasible, whereas for β particles and α-rays, these accuracies would require very elaborate experimental procedure. To obtain such results, γ self-absorption corrections should be made (7).

K-CAPTURE AND X-RAYS

Since very soft X-rays (1–100 kev) can frequently be detected with a higher efficiency than γ-rays, they are of importance as tracer radiations. This is especially true where they are the only radiations present. The predominant interaction, in this case, will be photo-absorption so that detectors must have low absorption windows, but high absorption fillings. Self-absorption in the measurement of samples will be important as these rays are more strongly absorbed than most β-rays, particularly if high-Z elements are present. But a theory and practice of the type outlined for β particles should suffice to make corrections and determine coefficients.

Peacock, *et al.* (*13*) describe beryllium-window counters and high-pressure argon fillings with a detection of 3% of the disintegrations of Fe^{55}. This isotope disintegrates by K-capture only and in ~25% of the disintegrations the characteristic X-rays of Mn^{55} are given off. Thus the counters have an efficiency of about 9–10% of the photons traversing the counter. In this case, the main interaction is with the gas in the counter.

BIBLIOGRAPHY

1. D. E. Lea, "Actions of Radiations on Living Cells," (The Macmillan Co., New York, 1947)
2. O. Klein, Y. Nishina, *Z. Physik* **52**, 853 (1929)
3. M. H. Hull, MDDC 348 (1946)
4. R. D. Evans, "Advances in Medical Physics," Vol. 1 (Academic Press, Inc., New York, to be published)
5. L. H. Gray, *Proc. Roy. Soc.* (London) **159A**, 263 (1937)
6. C. B. Braestrup, *Radiology* **46**, 385 (1946)
7. R. D. Evans, R. O. Evans, *Revs. Mod. Phys.* **20**, 305 (1948)
8. G. Failla, *Am. J. Roentgenol. Radium Therapy* **54**, 553 (1945)
9. L. D. Marinelli, E. H. Quimby, G. J. Hine, NUCLEONICS **2**, No. 4, 56 (1948)
10. W. C. Peacock, Thesis, MIT (1944)
11. H. Maier-Liebnitz, *Z. Naturforsch.* **1**, 234 (1946)
12. H. Bradt, P. C. Gugelot, O. Huber, H. Medicus, P. Preiswerk, P. Scherrer, *Helv. Phys. Acta* **19**, 77 (1946)
13. W. C. Peacock, R. D. Evans, J. W. Irvine, Jr., W. W. Good, A. F. Kip, S. Weiss, J. G. Gibson, 2nd, *J. Clin. Invest.* **25**, 605 (1946)

Nuclear Physics of the Deuteron and Other Two-Particle Phenomena—II

In this concluding article, the author examines the experimental evidence for his theory for the direct deduction of nuclear forces from models of two-particle nuclear systems

By M. E. ROSE

Oak Ridge National Laboratory, Oak Ridge, Tennessee

V. Scattering of Neutrons by Ortho- and Parahydrogen

TO DECIDE whether the singlet state is real (positive binding) or virtual, it is necessary to have a process in which the singlet and triplet scattering interfere, or are coherent. This will be the case if scattering from two centers, as in a hydrogen molecule, is considered. Ordinary hydrogen is, under equilibrium conditions, a three-to-one mixture of orthohydrogen (parallel proton spin and molecular spin 1) and parahydrogen (antiparallel proton spin and molecular spin zero). Since the scattering is spin-dependent different interference effects and different cross sections must be expected if measurements are made with pure parahydrogen and with pure orthohydrogen (or ordinary hydrogen) as scatterers.

Since the internuclear distance in the hydrogen molecule is 0.75×10^{-8} cm, to obtain interference effects the neutrons must have very low energy so that the wavelength $\lambda = \hbar/p$ will be of this order of magnitude. The corresponding energy is a small fraction of an ev, and it will be possible to excite the low-lying rotational energy levels in H_2. Because of the identity of the protons the rotational states in the two kinds of H_2 are different; the identity of the protons requires that the wave function Ψ describing the molecule be antisymmetric; that is, it must change sign when the two protons are interchanged. Now the total Ψ of the molecule is a product of three Ψ functions corresponding to the degrees of freedom associated with the vibration, rotation, and spin.

$$\Psi = \Psi_{vib}\Psi_{rot}\Psi_{spin}$$

The Ψ_{vib} depends only on the absolute value of the internuclear distance. On interchange it is symmetric, that is, it does not change sign. Since Ψ_{spin} is symmetric for spin 1 and antisymmetric for spin 0, we may conclude that Ψ_{rot}

EDITOR'S NOTE: In the first half of this paper, published last month, the author discussed the two-body problem, the qualitative consideration of nuclear forces, data of the two-part phenomena, ground state of the deuteron, and scattering of neutrons by protons. The numbering of sections, equations, and bibliography references in the second half of the paper is a continuation from the first half.

is symmetric for parahydrogen and antisymmetric for orthohydrogen. The rotational energy levels in a diatomic molecule like H_2 are given by

$$E_J = \frac{\hbar^2}{2I} J(J+1), \qquad J = 0, 1, 2 \cdots$$

where I is the moment of inertia of the molecule. We also know that J odd makes Ψ_{rot} antisymmetric and that J even makes Ψ_{rot} symmetric. Therefore in parahydrogen, only levels with even J (0, 2, 4 . . .) are allowed and the missing levels $J = 1, 3, 5 \ldots$ are the only ones allowed in orthohydrogen.

In a collision with room-temperature neutrons ($E = kT = 0.026$ ev), the transition from the ground level of para- to orthohydrogen is energetically possible since the energy difference is $E_1 - E_0 = 0.0155$ ev and the threshold energy, allowing for the recoil energy of the molecule, is $\frac{3}{2}(E_1 - E_0) = 0.023$ ev. This transition involves a spin change of the molecule from $0 \rightarrow 1$ and is possible only because the nuclear forces are spin-dependent. Similarly, ortho $\rightarrow$ para conversion (molecular spin change $1 \rightarrow 0$) can take place at any energy with spin-dependent forces. Other inelastic collisions with and without spin change (including excitation of vibrations) are removed from consideration unless the neutron energy is higher. In addition elastic collisions $0 \rightarrow 0$ and $1 \rightarrow 1$ can take place in para- and orthohydrogen, respectively, at any energy with and without spin-dependence. Summarizing, for room-temperature neutrons, we have the following transitions possible with spin-dependent forces:

	in para
elastic	$0 \rightarrow 0$ threshold 0
inelastic	$0 \rightarrow 1$ threshold 0.023 ev
	in ortho
elastic	$1 \rightarrow 1$ threshold 0
inelastic	$1 \rightarrow 0$ threshold 0

With cold neutrons (*e.g.*, liquid air for which $T = 90°$ K), the $0 \rightarrow 1$ process is ruled out. Then, any difference observed in the scattering of cold neutrons in ortho- and parahydrogen must be attributed to the $1 \rightarrow 0$ transition and the contribution to the $1 \rightarrow 1$ transition due to molecular spin. The observation of a difference is, therefore, confirmatory evidence of the spin-dependence of the forces.

The use of cold neutrons also permits an unambiguous decision as to the virtual or real character of the ^1S state. In parahydrogen, the neutron spin will be parallel to the spin of one of the protons and antiparallel to the other. Thus, the scattering amplitudes of both singlet and triplet states enter as a sum with appropriate weight factors, as follows (7):

$$\sigma_{para} = C_1(3f_1 + f_0)^2 \qquad (20)$$

where the 3 is due to the greater statistical weight of the triplet state and C_1 is a constant depending on the neutron energy and on parameters pertaining to the molecular structure. For 20° K neutrons in parahydrogen at the same temperature $C_1 = 6.444$. For orthohydrogen the cross section is

$$\sigma_{ortho} = C_2(3f_1 + f_0)^2 + C_3(f_1 - f_0)^2 \qquad (21)$$

representing the contributions of the $0 \rightarrow 0$ and $1 \rightarrow 0$ transitions. At 20° K, $C_2 = 6.450$ and $C_3 = 14.653$. It turns out that $3f_1 \approx -f_0$ for a virtual ^1S state, and $3f_1 \approx f_0$ for a real ^1S state. Therefore, in the former case we would expect σ_{para} to be smaller than σ_{ortho} by at least an order of magnitude (that is, by a factor of 10 or more) while in the latter case they would be of the same order of magnitude.

The experimental results (*4*) at 20° K are

$\sigma_{para} = 3.97$ barns, $\sigma_{ortho} = 124$ barns so that one can conclude that the ^1S state is *virtual*.

We may now conclude that $\epsilon_0 = -0.069$ Mev and from this datum determine the depth of the ^1S well as a

function of range. The result for a range of 2.8×10^{-13} cm is $V_0 = 11.6$ Mev.

The value for the range cited immediately above is subject to considerable doubt. As described in the foregoing, the measurement of f_1, f_0, and ϵ_1 permits the determination of three parameters V_1, V_0 and r_0. Thus from the triplet cross section, see (17), we have a relation between f_1^2 and ϵ_1, r_0. From σ_{para} and σ_{ortho} we can solve for f_1 and f_0. Actually, since $(3f_1 + f_0)^2$ and $(f_1 - f_0)^2$ are involved in the cross sections, there are two ambiguous signs and therefore four possible sets of values for f_1 and f_0. Of these, two give $f_1 > 0$ in contradiction to the elementary deuteron theory according to which a bound state requires $f_1 < 0$. A third set of values leads to the highly improbable range value 9×10^{-13} cm. Using the fourth set, f_1 is determined and hence the range. With the quoted values for σ_{para} and σ_{ortho} the range is 1.5×10^{-13} cm. From the range one can deduce V_1 and V_0 from (6) and the known value of σ_{fp}. As a check, the value of σ_{fp} (free proton σ)* can be deduced from f_1 and f_0. The result, 21 barns, agrees very well with the directly measured result (6).

* The free proton σ (of 19) can also be written

$$\sigma_{fp} = 4\pi\left(\frac{3f_1^2 + f_0^2}{4}\right) = \frac{\pi}{4}[(3f_1 + f_0)^2 + 3(f_1 - f_0)^2]$$

VI. Proton-Proton Scattering

The theory of scattering of protons by protons differs from the treatment of the neutron-proton scattering problem in two important respects. First, there is a Coulomb repulsion, $V_c = e^2/r$ where e is the proton charge. Second, the protons are identical particles and cannot exist in ^3S states or any other symmetrical state.† Therefore, for slow protons only the scattering in the ^1S state need be considered. For protons well above 10 Mev, the effects of ^3P scattering would be expected unless the ^3P well is very shallow. In any case the requirement of antisymmetry in the wave function must be observed.

The Coulomb potential is of long range, and particles of essentially all values of angular momentum will be scattered by this electric interaction. Consequently this part of the problem is conveniently treated by a somewhat different method which does not break up the scattering into contributions from partial waves of different values of L. On the other hand, only those collisions which are head-on ($L = 0$) will contribute to the nuclear scattering. Since both types of scattering take place simultaneously and coherently, the cross section is given by the square of the total scattering amplitude

$$\sigma(\vartheta) = |f_c + f_N|^2$$

where f_c and f_N refer to Coulomb and nuclear scattering respectively. The existence of a cross term $\sim f_c f_N$ is advantageous since in the energy and angular range where $f_c^2 \gg f_N^2$ the effect of nuclear scattering is enhanced by being coupled, so to speak, with the larger Coulomb scattering. In addition, under any circumstances which make the cross term large enough to be evaluated from the measurements, the repulsive or attractive nature of the ^1S proton-proton force can be determined. This follows because the cross term changes sign when the phase shift (see *IV*) changes sign, whereas the

† An S state is symmetrical since it depends only on the distance r between particles which is unchanged when the particles change positions.

purely nuclear term f_N^2 is independent of the sign of the phase shift. Moreover, it follows from the discussion on Fig. 3 that the phase shift is positive (perturbed wave shoved outwards) for a repulsive potential, and negative for an attractive one.

For a square-well potential added to a Coulomb potential

$$V = -V_0 \qquad r < r_0 \qquad (22)$$
$$V = \frac{e^2}{r} \qquad r > r_0$$

the scattering per unit solid angle in the laboratory system is

$$\sigma(\theta) = \frac{e^4}{E_0^2}\left[\frac{1}{\sin^4\theta} + \frac{1}{\cos^4\theta} - \frac{1}{\sin^2\theta\cos^2\theta} - \frac{2\hbar v}{e^2}\frac{\sin\eta_0\cos\eta_0}{\sin^2\theta\cos^2\theta} + \left(\frac{2\hbar v}{e^2}\right)^2 \sin^2\eta_0\right]\cos\theta \qquad (23)$$

where η_0 is the phase shift of the S-wave due to nuclear scattering. The first three terms represent the Coulomb scattering, the $\cos^{-4}\theta$ term being due to the existence of a recoil proton at $(\pi/2) - \theta$ for every proton scattered through angle θ, and $\cos^{-2}\theta \sin^{-2}\theta$ term arising from the requirement of antisymmetry. The fourth and fifth terms are the interference or cross term and the purely nuclear scattering, respectively.

It will be noted that η_0 depends only on energy and not on angle. The observations (*8*) show that the angular distributions can be fitted with one parameter η_0 which has the same energy dependence for all angles observed. Including the recent measurements by Wilson, *et al.*, (*9*) these results have now been extended up to a proton energy of 14.5 Mev. The next point is to see whether the energy dependence of the phase shift η_0 can be accounted for by a single two-parameter well. That this can be done was shown by Breit and co-workers (*10*) who found the following parameters for the square well:

$$r_0 = 2.8 \times 10^{-13}\ \text{cm}, \qquad V_0 = 10.5\ \text{Mev} \qquad (24)$$

and the ^1S proton well is attractive.

If the Coulomb potential is continued into the nucleus so that $V = e^2/r - V_0$ for $r < r_0$, the singlet well depth becomes 11.6 Mev, which is essentially the same as the ^1S neutron-proton interaction *at the same range*. In view of preceding remarks it is not at all certain that one may conclude equality of forces except between pairs of nucleons in the ^1S state.

The experiments of Wilson, *et al.*, for proton energies up to 14.5 Mev have failed to give any clear indication of P-wave scattering. With the potential hole given by (24), it can be shown, in the manner of the Appendix, that two protons (He^2) do not form a stable combination. The well is too shallow to accommodate even one level.

VII. Interaction with Electromagnetic Radiation

(a) Photodisintegration. The binding energy of the deuteron was originally measured by Chadwick and Goldhaber using the photodisintegration with the ThC′ γ-rays of 2.62-Mev energy. The reaction is

$$H^2 + \hbar\omega = H^1 + n^1 + E$$

where $\hbar\omega$ is the γ-ray energy and E is the total kinetic energy of the emitted proton and neutron. Since the γ-ray momentum is negligible, the proton and neutron have opposite momenta and share the energy E equally.

$$\epsilon_1 = H^1 + n^1 - H^2 = \hbar\omega - E \qquad (25)$$

which can be evaluated by measuring the proton energy.

Our interest here is in the cross section for this process. The mechanism of the effect is as follows: The incoming radiation is composed of oscillating

electric and magnetic field components. The electric field $\mathcal{E}$ can interact with the proton charge, the interaction being simply $-e\,\mathcal{E}\cdot\mathbf{r}_p$ where $\mathbf{r}_p$ is the proton coordinate vector. The magnetic field H interacts with the magnetic moment of both proton and neutron. If these are denoted by $\boldsymbol{\mu}_p$ and $\boldsymbol{\mu}_n$, respectively, the interaction energies are $-(\boldsymbol{\mu}_p+\boldsymbol{\mu}_n)\cdot\mathbf{H}$. The photo effects due to electric and magnetic interactions are referred to as the photoelectric and photomagnetic effects, respectively. Due to the presence of the factor $\mathbf{r}_p$ (which is angle-dependent), the photoelectric transition leads from the ^3S ground state to an excited ^3P state. The presence of the magnetic moments, $\boldsymbol{\mu}_p$ and $\boldsymbol{\mu}_n$, which are intimately connected with the spins of the proton and neutron, implies that the photomagnetic interaction is spin-dependent and permits transitions with a spin change. In fact the transition here is from ^3S to the excited ^1S state. Since the final states for the two processes are different, there is no interference effect between them and the total cross section is simply the sum of the photoelectric and photomagnetic cross sections.

The calculation of the photoelectric cross section is based on the approximation that nuclear forces in the final ^3P state may be neglected. This assumption is certainly valid for γ-rays less than 15 Mev since in this case the emerging particles do not have sufficient energy to overcome the centrifugal force in the P state and hence cannot approach sufficiently close to each other to interact.

Omitting details, we find that the cross section for the process in which the proton is ejected into unit solid angle in a direction making an angle θ with the direction of the incident γ-radiation is

$$\sigma_e(\theta)=\frac{\hbar e^2}{Mc}\frac{\sqrt{\epsilon_1}\,E^{3/2}}{(\hbar\omega)^3}(1+\alpha r_0)\sin^2\theta \quad (26)$$

where $\alpha=\sqrt{M\epsilon_1}/\hbar$.

The protons therefore emerge mostly at right angles to the incident beam. This is easy to understand since the direction of the force on the protons is the direction of the electric field which is always perpendicular to the propagation direction of the radiation.

The total photoelectric cross section is, then,

$$\sigma_e=\frac{8\pi}{3}\frac{\hbar e^2}{Mc}\frac{\sqrt{\epsilon_1}\,E^{3/2}(1+\alpha r_0)}{(\hbar\omega)^3} \quad (27)$$

The photoelectric cross section vanishes at the threshold ($E=0$) and reaches a maximum of 26.6×10^{-4} barn at $\hbar\omega=2\epsilon_1=4.36$ Mev. Thereafter it decreases rather rapidly.

The angular distribution of the nucleons emitted in the photomagnetic disintegration is isotropic.* The total magnetic cross section, calculated with nuclear forces taken into account in both initial and final S states, is

$$\sigma_m=\frac{2\pi}{3}(\mu_p-\mu_n)^2\frac{e^2\hbar}{M^2c^3}\frac{\sqrt{E\epsilon_1}\,(\sqrt{\epsilon_1}+\sqrt{|\epsilon_0|})^2}{\hbar\omega(E+|\epsilon_0|)} \quad (28)$$

where μ_p and μ_n are the magnetic moments in units of the nuclear magneton $e\hbar/2Mc$: $\mu_p=2.7896$ and $\mu_n=-1.9103$. Except very near the threshold σ_m is smaller than σ_e.

The total angular distribution is

$$\sigma(\theta)=\frac{\sigma_e}{4\pi}\left(\frac{\sigma_m}{\sigma_e}+\frac{3}{2}\sin^2\theta\right) \quad (29)$$

and the total cross section is

$$\sigma=\sigma_m+\sigma_e \quad (30)$$

For 2.62-Mev γ-rays, the calculated cross sections are $\sigma_e=12.3\times10^{-4}$ barn and $\sigma_m=3.3\times10^{-4}$ barn, giving a calculated total $\sigma=15.6\times10^{-4}$ barn. The theoretical value given by the noncentral force theory (Section *VIII*) is 15.3×10^{-4} barn. This is to be compared with the measured value of 10×10^{-4} barn (*11*). In addition, the

* For the photo processes in the energy range considered, there is no distinction between the L and C coordinate systems.

theoretical value of σ_m/σ_e from the above is 0.53, whereas the best data for the angular distribution (*12*) in which $\sigma(0)/\sigma(\pi/2)$ was measured, gives $\sigma_m/\sigma_e = 0.39$. It is difficult to say whether these discrepancies are real, because of the great difficulty involved in obtaining accurate data for these rather weak effects. An important source of error is the uncertainty in the measurement of γ-ray intensity, although this affects only the measured values of the cross section and not the shape of the angular distribution (see also *VIII*).

(b) Capture of Neutrons by Protons. The photomagnetic disintegration was predicted by Fermi on the basis of the existence of the inverse process: the (magnetic) capture of neutrons in hydrogen with the emission of magnetic dipole radiation. The inverse photoelectric effect is extremely improbable. The main capture process, therefore, involves neutron and proton with initially antiparallel spins, and in the transition (^1S to ^3S) the total spin changes.

It is easy to show that, for the $^1S \rightarrow {}^3S$ capture, the ratio of cross section to that for the inverse process is

$$\frac{\sigma_{cap}}{\sigma_m} = \frac{3}{2}\left(\frac{p_\gamma}{p_n}\right)^2$$

where p_γ and p_n are the momenta of the emitted photon in the capture and of the emitted neutron in the disintegration, respectively. This gives

$$\sigma_{cap} = \pi(\mu_p - \mu_n)^2 \frac{e^2\hbar}{M^2c^2} \sqrt{\frac{2\epsilon_1}{E_0}} \frac{(\sqrt{\epsilon_1} + |\epsilon_0|)^3(\epsilon_1 + \frac{1}{2}E_0)}{(|\epsilon_0| + \frac{1}{2}E_0)} \quad (31)$$

and again E_0 is the energy of the incident neutrons. It is clear that the capture cross section is largest for slow neutrons. For slow neutrons $E_0 \ll \epsilon_1$ and $\ll |\epsilon_0|$ and $\sigma_{cap} \sim 1/\sqrt{E_0} \sim 1/v$, as is the case with capture cross sections in more complicated nuclei at sufficient low energies.

For thermal neutrons, $E_0 \sim 0.026$ ev, the calculated cross section is 0.31 barn which is practically identical with the measured value 0.30 barn. If in (31) it were assumed that the ^1S state was real, the factor $\sqrt{\epsilon_1} + \sqrt{|\epsilon_0|}$ would be replaced by $\sqrt{\epsilon_1} - \sqrt{\epsilon_0}$ and the calculated cross section would be only 0.14 barn. Thus, the conclusion that the ^1S state is virtual receives further confirmation.

VIII. Noncentral Forces

As was emphasized in the foregoing, the existence of the quadrupole moment of the deuteron requires noncentral forces which depend on the angle between the deuteron spin and the line joining neutron and proton. On general grounds of invariance with respect to displacement, rotation, and inversion of the observer's coordinate system, it can be shown that the most general interaction must have the form (*13*)

$$V(r) = V_1(r) + V_2(r)\, \boldsymbol{s}_1 \cdot \boldsymbol{s}_2 + V_3(r) S_{12} \quad (32)$$

where V_1, V_2 and V_3 are ordinary functions of r, $\boldsymbol{s}_1$ and $\boldsymbol{s}_2$ are the spin vectors of the two nucleons and the scalar product $\boldsymbol{s}_1 \cdot \boldsymbol{s}_2$ is a number which has the value 1 for the triplet state and -3 for the singlet state. The noncentral character of the interaction is contained in the S_{12} term and

$$S_{12} = \frac{3(\boldsymbol{s}_1 \cdot \boldsymbol{r})(\boldsymbol{s}_2 \cdot \boldsymbol{r})}{r^2} - (\boldsymbol{s}_1 \cdot \boldsymbol{s}_2) \quad (33)$$

is, in form, equal to the classical interaction between two magnetic dipoles.

The immediate consequences of the interaction (32) are:

1. The S_{12} term vanishes for a singlet state. Therefore for the ^1S state the remaining terms, $V_1 - 3V_2$,

must have the same form as before. In particular, the scattering of low-energy protons by protons is unaffected by noncentral forces.

2. The noncentral term implies that the orbital angular momentum is no longer a constant of the motion, and a unique value of L cannot be assigned to the ground state of the deuteron. Instead the ground state corresponds to an admixture of S and D states, the latter corresponding to $L = 2$:

$$\Psi = \Psi_S + \Psi_D$$

(There is no P state admixture because S_{12} is invariant to a change of sign of r). Stated otherwise, the relative motion of neutron and proton is a combination of a motion in which the line joining the nucleons has a random orientation and a motion in which there is a preference for the angle θ between this line and the spin direction to be small. This follows since Ψ_D is proportional to $3\cos^2\theta - 1$. This gives rise to the quadrupole moment, and the magnitude of V_3 and hence of Ψ_D must be adjusted to give the observed value for Q. Since Ψ_S amd Ψ_D are unchanged for θ replaced by $\pi - \theta$, so that neither direction along the spin axis is preferred, the electric dipole moment, proportional to $(r\cos\theta)_{av}$, still vanishes.

3. The total angular momentum is still a constant of the motion and must have the measured value 1 (deuteron spin). Thus, the ground state is a mixture of $^3S_1$ and $^3D_1$.

Calculations of the properties of two particle systems with noncentral forces were carried out by Rarita and Schwinger (*14*). They chose a force model corresponding to a square-well potential for each term in (32), that is, for $r < r_0$.

$$\begin{aligned} V_1 &= -(1 - \tfrac{1}{2}g)V \\ V_2 &= -\tfrac{1}{2}gV \\ V_3 &= -\gamma V \end{aligned} \qquad (34)$$

and for $r > r_0$ all interactions are zero. This is a model with four parameters, the constant V involved in the well depths, the *common* range r_0, and the constants g and γ measuring the relative strengths of triplet central, singlet and triplet noncentral interactions. Actually Rarita and Schwinger chose a value of the range (2.8×10^{-13} cm) and fixed the other three constants from the data: binding energy and quadrupole moment of the deuteron (fixing γ and V), and neutron-proton scattering (fixing g). The values found were

$$V = 13.9 \text{ Mev}, \quad \gamma = 0.775, \quad g = 0.0715 \qquad (35)$$

It may be noted that γ, which is a measure of the strength of the noncentral force, is not particularly small. Nevertheless, the noncentral force generally produces small effects because Ψ_D is small compared to Ψ_S corresponding to the centrifugal repulsion in the D state.

A particularly important effect of the noncentral forces is to produce a small change in the calculated value of the magnetic moment μ_D of the deuteron. This will be the sum of magnetic moments of neutron and proton $\mu_n + \mu_p$ plus a contribution due to the orbital motion of the charged proton arising from Ψ_D. The latter effect is that of a current loop and therefore contributes to the magnetic moment. It can be shown that

$$\mu_D = \mu_n + \mu_p - \tfrac{3}{2}(\mu_n + \mu_p - \tfrac{1}{2})\int \Psi_D^2 d\tau \qquad (36)$$

where $d\tau$ is the volume element for the relative coordinates between neutron and proton. The value of the integral (taken over all space) which is referred to as the percentage of D state, is calculated to be*

$$\int \Psi_D^2 d\tau = 0.039 \qquad (36a)$$

The magnetic moments can be measured very accurately. Highly precise values found by Arnold and Roberts (*15*)

* This is actually the value of $\int \Psi_D^2 d\tau / \int (\Psi_S^2 + \Psi_D^2) d\tau$. However, the functions can be normalized so that the denominator is 1.

are

$$\mu_n = -1.9103 \pm 0.0013 \text{ nuclear magnetons}$$

$$\mu_n/\mu_p = 0.68479 \pm 0.0004$$

$$\mu_D = 0.85647 \pm 0.0004 \text{ nuclear magnetons}$$

This gives a percentage D state equal to 0.040 in excellent agreement with the calculated value (36a). However, there are other small corrections to the magnetic moment arising from relativistic effects. These are of order T/Mc^2 nuclear magnetons, T being the kinetic energy in the ground state of the deuteron. These corrections cannot be calculated unambiguously at the present time but their order of magnitude is probably 10^{-2} nuclear magneton which is in the limit of experimental error. It remains to be seen whether or not the nice agreement quoted above will be maintained.

The remaining processes are very little affected by the noncentral forces. The results of the calculations by Rarita and Schwinger, using the constants (35), may be summarized as follows:

1. The scattering cross section for slow neutrons ($E_0 \approx 0$) is reduced by 0.07 barn which is a trivial change from the point of view of present experimental error.

2. The scattering cross section for high-energy neutrons ($E_0 = 2.8$ Mev) is reduced from the central value of 2.56 barn to 2.53 barn. Both values agree, well within the experimental error, with the measured value. A small anisotropy is introduced into the angular distribution of neutrons in the C system of coordinates, but again this is far too small to be observed.

3. The calculated capture cross section for thermal neutrons is reduced from 0.31 to 0.30 barn, the latter coinciding with the measured value.

4. The photoelectric cross section is reduced slightly (by 0.3×10^{-4} barn) and the angular dependence acquires a very small isotropic part. The angular distribution in the photomagnetic process is slightly anisotropic. Altogether the value of σ_m/σ_e [*cf.* (29)] is, for 2.62 Mev γ-rays, equal to 0.272. The observed value is 0.39 ± 0.12.

It seems fair to conclude that, on the whole, the theory is able to account for the experimental results sufficiently well to justify the feeling that one is on the right track. There is, of course, much that remains to be done.

APPENDIX

The problem of determining the parameters of the potential well from the given binding energy is roughly analogous to the classical problem of determining the distribution of loading on a string with a given fundamental frequency. In place of the wave equation of the string, one starts with the quantum-mechanical Schrödinger equation

$$\left\{\frac{\hbar^2}{2M_p}\nabla_p^2 + \frac{\hbar^2}{2M_n}\nabla_n^2 + W - V\right\}\Psi = 0$$

where ∇_p^2 and ∇_n^2 are the Laplace operators in the proton and neutron coordinates respectively, M_p and M_n are the proton and neutron masses, W is the total energy, and Ψ, which is a function of all coordinates, designated by $\mathbf{r}_p$ and $\mathbf{r}_n$, is the wave function. $|\Psi|^2$ is the probability of finding a proton in unit volume at $\mathbf{r}_p$ and a neutron in unit volume at $\mathbf{r}_n$. Ψ must be finite, single-valued, continuous, and smooth.

Neglecting the neutron-proton mass difference and separating the center of gravity motion from the relative motion by introducing

$$\mathbf{R} = \tfrac{1}{2}(\mathbf{r}_p + \mathbf{r}_n)$$
$$\mathbf{r} = \mathbf{r}_p - \mathbf{r}_n$$

We obtain with $\Psi = u(r)/r$,

$$\frac{d^2u}{dr^2} + \frac{M}{\hbar^2}(E - V)\,u = 0$$

where E is the energy exclusive of that associated with center of gravity motion.

Using (2) for V, setting $E = -\epsilon_1$ and introducing the notation

$$k^2 = \frac{M}{\hbar^2}(V_1 - \epsilon_1), \qquad \alpha^2 = \frac{M\epsilon_1}{\hbar^2}$$

we find

$$u = A \sin kr \qquad r < r_0$$
$$u = Be^{-\alpha r} \qquad r > r_0$$

where A and B are constants. The condition of continuity of u and du/dr at r_0 gives

$$k \cot kr_0 = -\alpha$$

which is identical with (6).

BIBLIOGRAPHY

7. M. Hamermesh, J. Schwinger, *Phys. Rev.* **71,** 678 (1947)
8. R. E. Herb, D. W. Kerst, D. B. Parkinson, E. J. Plain, *Phys. Rev.* **55,** 998 (1939)
9. R. R. Wilson, E. J. Lofgren, J. R. Richardson, B. T. Wright, R. S. Shankland, *Phys. Rev.* **73,** 1131 (1947)
10. G. Breit, H. M. Thaxton, L. Eisenbud, *Phys. Rev.* **55,** 1018 (1939)
11. H. Halban, *Compt. rend.* **206,** 1170 (1938)
12. G. A. R. Graham, H. Halban, *Revs. Mod. Phys.* **17,** 297 (1945)
13. E. P. Wigner, *Proc. Nat. Acad. Sci.* **27,** 282 (1941)
14. W. Rarita, J. Schwinger, *Phys. Rev.* **59,** 436, 556 (1941)
15. W. R. Arnold, A. Roberts, *Phys. Rev.* **71,** 878 (1947)

NUCLEONIC EVENTS

KARL COHEN NAMED DIRECTOR OF ATOMIC WORK AT FERGUSON

Karl Cohen, one of the leading contributors to the design of the K-25 (gaseous diffusion) plant at Oak Ridge, Tennessee, and former atomic consultant to the Standard Oil Company (N. J.), has joined the H. K. Ferguson Company, industrial engineers and builders, as technical director for atomic activities.

The announcement was made by Wells N. Thompson, vice president in charge of engineering at Ferguson, which is building the first peacetime nuclear reactor at Brookhaven National Laboratory, Upton, L. I. Mr. Thompson disclosed that Dr. Cohen will be available as a consultant for the Brookhaven project and for other projects sponsored by the AEC.

Dr. Cohen is one of the few nuclear scientists who has had broad experience in the development of atomic energy at both the theoretical and industrial levels. His entire association with the atomic program has been in the little understood field of translating scientific theory and laboratory results into actual production facilities.

Dr. Cohen's most recent assignment has been as head of the Theoretical Physics Group of the Standard Oil Development Company. The prime responsibility for this group the past four years was to investigate potential applications and economic effects of atomic energy on the petroleum industry.

He was extremely active in the wartime program that produced the atomic bomb and the billion dollar manufacturing facilities at Oak Ridge and Hanford, Wash., and prior to that, he made various important studies in the field of nucleonics, particularly in the field of isotope separation.

Dr. Cohen's participation in this field started shortly after he received the degree of Doctor of Philosophy in physical chemistry from Columbia University in 1937. Following the work leading to his degree, he studied theoretical physics at the University of Paris. After his return to this country, he served as assistant to Harold C. Urey at Columbia for two years.

In 1940, he began his research on uranium isotope separation. These studies led to his appointment as director of the Theoretical Division of the Manhattan Project laboratory at Columbia. In this capacity, Dr. Cohen was one of the principal contributors to the design of the K-25 plant at Oak Ridge.

The solution of the unprecedented problem of connecting thousands of separating units into a single "cascade" for producing uranium-235 depended in a large part on the cascade theory developed by him and his co-workers. Besides this work on the gaseous diffusion plant, he made fundamental contributions to the centrifugal method of separation, and to heavy-water production.

During the war, Dr. Cohen also served as a liaison between Columbia and the Metallurgical Laboratory in Chicago in the abortive heavy-water pile project. He was also a consultant for the development of the thermal diffusion plant at Oak Ridge.

While forming a technical group to investigate industrial applications of atomic energy for Standard Oil, Dr. Cohen also served as consultant to the Physics Division at Clinton Laboratories and on special problems for the AEC at Hanford and elsewhere.

CONGRESSIONAL GROUP REPORTS ON AEC BUDGET

The following is taken from the report of the Appropriations Committee of the House of Representatives on the Supplemental Independent Offices Appropriation Bill of 1949:

The committee is not satisfied with its relations to date with the Atomic Energy Commission. The committee is fully aware of the vital importance, particularly under present world conditions, of the work of the commission and of the technical aspects connected with it, and is desirous of making every provision for its adequate support. However, the commission's refusal to furnish the committee with information and appraisals of its various budgeted items, based on technical information which can be available only to the commission because of the scientific and secret character of the work involved, leaves much to be desired in establishing the confidence which the committee must have if it is to continue to supply these large grants of funds under conditions of secrecy which prevent full disclosure of the details.

As a matter of fact, there is some feeling among the membership of the committee that the commission has taken advantage of its strategic position in modern military defense to avoid facing the practical realities on less important and subsidiary elements of its budget. The impression left

with the committee is one of general extravagance.

The committee recommends $501,850,000, which is a reduction of $48,150,000 in the budget estimate but is an increase of $326,850,000 over the appropriation for the fiscal year 1948. In addition to the cash appropriation, contract authority in the amount of $400,000,000 is recommended.

The committee specifically recommends a reduction of $6,400,000 in the item "administrative expenses." Such a reduction will leave a total of $26,473,213 available, which is slightly above the amount provided in 1948. Careful check by the committee of the administrative structure of the commission, as compared with other agencies of the government, leads to the conclusion that the commission has indulged itself lavishly in this regard. The commission is exempt from many requirements imposed on other agencies of the government and the commission's work is simplified on that account. The Congress, in allowing a single item budget, with few limitations and restrictions, has conferred on the commission a degree of authority and autonomy which normally does not obtain and which should be so administered by the commission as to assure a stewardship above reproach. The establishment of a lavish administrative structure does not impress the committee as comporting with the appropriate use of these broad authorities.

A reduction of $2,700,000 in town operations is recommended. A scrutiny of the information submitted to the committee indicates that the commission has not achieved any real comparability between the three communities operated either in their accounting or financial reporting and that it has not apparently achieved any satisfactory common denominator for the various types of expenses involved to regulate the actual outlays of the three communities. By comparison with statistics compiled by the Department of Commerce, relating to comparable per capita cost for 200 cities of from 25,000 to 50,000 population, the costs of the three communities are very much out of line.

The estimated obligation for fiscal year 1949 for construction of housing and community facilities is $70,709,673. Cost figures under this project are also out of line with costs in other similar projects. It is the opinion of the committee that a substantial reduction can be made in this item. The committee also believes that an adjustment can be made in the item for research in the nonweapon, nonbiological, and nonmedical phases of the research and development program.

For the fiscal year 1948, the commission received contract authorizations totaling $400,000,000, of which $150,000,000 was included in the First Deficiency Appropriation Bill which became law on May 10, 1948. For the fiscal year 1949, the budget recommends, and the committee has approved, an additional contract authorization of $400,000,000. On the direct cash appropriation for 1949, $250,000,000 was intended to liquidate a part of the contract authorization granted for the fiscal year 1948. In the original budget this figure was $325,000,000 but was subsequently reduced by the commission itself to $250,000,000 inasmuch as it had become obvious that the full amount of cash would not be required. A recheck of the matter currently leads the committee to the conclusion that the full amount of $250,000,000 may not be required for these purposes during 1949, and a substantial portion of the reduction imposed by the committee may be absorbed in this item.

The reductions imposed by the committee are to be absorbed in other items without affecting the military phases.

POLAND STEPS UP RESEARCH

The size of Poland's atomic research group will be doubled by a decision made at Warsaw recently to put 50 additional scientists to work on atomic energy research. Most of these researchers will work at a special atomic institute in Warsaw. Others will conduct their experiments at the Universities of Kracow and Wroclaw. The decision to increase the atomic research staff was taken at a conference attended by several hundred scientists from all over Poland.

TO GIVE COURSE ON NUCLEAR PHYSICS IN LIFE SCIENCES

The University of California will give a course from August 2–20 in the application of nuclear physics to the biological and medical sciences. An instructional staff of 20 specialists from various parts of the country will include Stafford L. Warren, professor of biophysics and dean of the School of Medicine at UCLA, as general chairman, and Fred A. Bryan, associate clinical professor of medicine, School of Medicine, UCLA, as director of the course.

Tuition fee for the complete course, including laboratory training, is $350, Tuition fee for the lecture series alone is $100. Enrollment in the course is limited and applicants must present biographical data for approval by an official committee.

TO BUILD 12-MEV ACCELERATOR

Approval of construction at the University of California Los Alamos Scientific Laboratory of an electrostatic accelerator designed to yield positive ions with energies up to 12 million electron volts has been announced by the Atomic Energy Commission. Together with the associated laboratory buildings, it will cost approximately $2,000,000 and will take some two years to build.

BETHE TO TEACH AT COLUMBIA

Hans A. Bethe, professor of physics at Cornell University, will be a visiting professor at Columbia University this winter. Former chief of the theoretical physics division at Los Alamos, Dr. Bethe will give a course in advanced nuclear physics and a seminar on the theory of mesons.

OAK RIDGE SPONSORS NUCLEAR PHYSICS CONFERENCE

The Physics Division of Oak Ridge National Laboratory will sponsor a conference on "Nuclear Physics and Low Temperatures" to be held on the weekend of August 7–8. This conference, the first of a projected series of physics conferences, was organized in response to the increasing interest in nuclear problems involving low-temperature phenomena. The formal program has been arranged so as to appeal to the interests of a wide group of physicists.

The sessions devoted to the scientific part of the program will be held on Saturday, August 7, in a morning and afternoon session. The papers to be presented at the morning session are: "Alignment of Nuclear Spins," by M. E. Rose, principal physicist at Oak Ridge National Laboratory, and "Nuclear Relaxation Phenomena at Low Temperatures," by E. M. Purcell, professor of physics at Harvard University. The papers to be presented at the afternoon session are: "Thermal Equilibrium at Low Temperatures," by H. B. G. Casimir, Physics Director at the Philips Works in Eindhoven, The Netherlands, and "The Superfluid State," by F. London, professor of chemistry at Duke University.

Housing accommodations will be arranged by the Laboratory. Inquiries regarding general conference matters should be addressed to H. C. Maggart, Physics Division, Oak Ridge National Laboratory, P. O. Box P, Oak Ridge, Tennessee.

ABSTRACTS

CHEMICAL PUBLICATIONS

The synthesis of palmitic acid and tripalmitin labeled with carbon fourteen, W. G. Dauben (Univ. of California, Berkeley), *J. Am. Chem. Soc.* **70,** 1376–1378 (1948). Palmitic acid labeled in the carboxyl group with C^{14} was obtained in 72% yield by the carbonation of *n*-pentadecylmagnesium bromide with radioactive carbon dioxide. Carboxyl-labeled tripalmitin was prepared from this acid by the acid chloride method.

Search for elements 94 and 93 in nature. Presence of 94^{239} in pitchblende, G. T. Seaborg, M. L. Perlman (Univ. of California, Berkeley), *J. Am. Chem. Soc.* **70,** 1571–1573 (1948). A chemical analysis of a Canadian pitchblende concentrate showed that elements 94 and 93 were present in less than 1 part in 10^8 to 10^9. The amount of 30,000-yr 94^{239} in the concentrate was estimated as 1 part in 10^{14}.

A study of the distribution of arsine in impregnated charcoal by means of radioactive tracers, J. W. Hickey, E. O. Wiig (Univ. of Rochester, N. Y.), *J. Am. Chem. Soc.* **70,** 1574–1579 (1948). The distribution of arsine in charcoal beds was studied using As^{74} as a tracer. The distribution curves show that small amounts of water accelerate, and larger amounts inhibit, the absorption of arsine. Effects of concentration of arsine, time of exposure, and cooling were studied.

Recoil-activated and thermal exchange reactions between sulfur-35 and carbon disulfide, R. R. Edwards, F. B. Nesbett, A. K. Solomon (Massachusetts Inst. of Tech. and Harvard Med. School, Cambridge), *J. Am. Chem. Soc.* **70,** 1670 (1948). Two exchange reactions involving the exchange of a free sulfur atom or ion with one bound in the CS_2 molecule have been observed. When CS_2 dissolved in CCl_4 was bombarded with stray neutrons from a cyclotron, about 50% of the S^{35} formed in compounds not volatile below room temperature was present as CSS^*. Similarly, a solution of C_2Cl_6 in CS_2 which was bombarded by neutrons from a pile produced CSS^* having 12% of the total activity. The second reaction being studied is the exchange of sulfide ion in aqueous solution with CS_2 as a separate phase.

Present state of knowledge of the isotopes of atomic number 85, H. Hulubei (Physical Chemistry Laboratory, Faculty of Sciences, Paris), *J. chim. phys.* **44,** 225–229 (1947). A review with 14 references.

Surface radiography with alpha rays, C. Jech (Radiotherapeutical Inst., Praha-Bulovka), *Nature* **161,** 314 (1948). The structure of a surface may be examined by subjecting the surface to radon, and then placing the specimen in contact with a photographic plate for a short period of time. The plate is selectively darkened by α-rays emitted by the radium A, C and C′ deposited on the surface by the radon treatment.

Production of helium by cosmic rays, H. E. Huntley (Univ. of Witwatersrand, Johannesburg), *Nature* **161,** 356 (1948). Ilford's nuclear research plates exposed to cosmic rays showed that a large number of nuclear disintegrations occurred in the glass bases. It is concluded from this that helium is produced in the glass at the rate of at least 10^5 atoms per cc per year, and that the age of rocks and meteorites obtained from helium analysis on the assumption that the helium is derived from radioactive minerals may be high.

The meson field and the equation of motion of a spinning particle, R. C. Majumdar, S. Gupta (Tata Inst. Fundamental Research, Bombay), *Nature* **161,** 410–411 (1948). The equation of motion of a point dipole in a meson field is obtained. It is free from singularities and does not contain any arbitrary constant except the spin angular momentum of the dipole.

Electron tracks in photographic emulsions, R. W. Berriman (Research Lab., Kodak, Ltd., Wealdstone, Middlesex), *Nature* **161,** 432 (1948). A new Kodak emulsion is sufficiently sensitive to record electron tracks. They appear as short, highly curved chains of developed grains.

Resolution testing in autoradiography, G. W. W. Stevens (Research Lab., Kodak, Ltd., Wealdstone, Middlesex), *Nature* **161,** 432–433 (1948). A method is described for preparing test charts which can be used to estimate the relative importance of emulsion and geo-

metrical factors on the resolution of autoradiographs.

A 16-Mev betatron, K. J. R. Wilkinson, J. L. Tuck, R. S. Rettie (British Thomson-Houston Co., Ltd., Rugby and Clarendon Lab., Oxford), *Nature* **161,** 472–473 (1948). The construction and a preliminary account of the properties of a newly constructed 16-Mev betatron are given.

Applications of the reflecting microscope to the nuclear plates technique, W. J. Bates, G. P. S. Occhialini (H. H. Wills Phys. Lab., Royal Fort, Bristol 8), *Nature* **161,** 473 (1948). By sandwiching two plates (emulsion inwards) with immersion oil and then exposing the sandwich, the passage of particles from one plate to another may be followed. With a known air-gap between plates, long-range particles can be studied. The use of the reflecting microscope extends the scope of the method.

A new method for the determination of the mass of mesons, C. F. Powell, S. Rosenblum (Hochalpine Forschungstation, Jungfraujoch), *Nature* **161,** 473–475 (1948). The masses and the signs of the electric charge of mesons may be determined by a photographic method as follows: Two plates in a suitable plate-holder, with their emulsions face to face and separated by an air gap of 3 mm, are placed between the poles pieces of a permanent magnet (8,600 gauss) and exposed to radiation. Mesons leaving one plate will enter the other, and from the observed change in direction of motion, their momentum can be calculated. If the mesons come to rest in the second plate, then their velocity as a function of their mass is also known.

Interaction of fast neutrons with indium, S. G. Cohen (Cavendish Lab., Cambridge), *Nature* **161,** 475–476 (1948). The cross-sections for the processes $In^{115}(n,n)In^{115*}$, $In^{115}(n,\gamma)In^{116}$ (54 min), and $In^{113}(n,n)In^{113*}$ were studied. A threshold for the first reaction probably exists at about 1 Mev, while the cross section is flat above 2.2 Mev. The cross sections for the first and third reactions were found to be of the same order of magnitude. The results are compared with theory.

Disintegration of highly excited nuclei, D. H. Perkins (Imperial College of Science Tech., London), *Nature* **161,** 486–487 (1948). Measurements were made on the angular distribution of the emitted particles in nuclear disintegration stars produced in photographic emulsions by cosmic radiation. Protons were found to be emitted almost isotropically, while α-particles have angular distributions which deviate greatly from spherical symmetry. These results are compared with what might be expected from the evaporation model of the nucleus.

30-Mev electron synchrotron, D. W. Fry, J. W. Gallop, F. K. Goward, J. Dain (Atomic Energy Research Estab., Harwell), *Nature* **161,** 504–506 (1948). A brief description is given of a 30-Mev synchrotron being used to develop synchrotron techniques and to guide the design of much larger machines.

Spin-dependence of magnetic dipole gamma radiation and the nuclear level scheme of Pb^{208}, H. O. W. Richardson (Univ. of Edinburgh), *Nature* **161,** 516–518 (1948). When estimates of the coefficient of internal conversion in the *K*-shell are available, the classification of gamma rays by the proportion of magnetic dipole radiation may be useful in assigning quantum numbers to the upper levels of nuclei. Two level schemes as well as possible sets of spin quantum numbers are given for Pb^{208}.

The mass of σ-mesons, S. Lattimore (Imperial College of Science Tech., London), *Nature* **161,** 518–519 (1948). The mean mass of σ-mesons was found to be 290 $\pm$ 80 electron masses by means of measurements of Coulomb scattering of the mesons in photographic emulsions.

Fission products of U^{233}, W. E. Grummitt, G. Wilkinson (Natl. Research Council, Chalk River, Ont.), *Nature* **161,** 520 (1948). The fission yields are tabulated for the longer-lived fission products of U^{233} along with the corresponding fission yields for U^{235}. A plot of fission yield against mass number for U^{233} shows a double-humped curve indicating a light group and a heavy group.

Mass defects of the heavy isotopes, A. H. Wapstra (Rijks-Universiteit te Utrecht), *Nature* **161,** 529–530 (1948). A table is given of the mass defects of the heavy isotopes relative to Pb^{206}. The position of the isotopes of the actinium and neptunium families was determined by means of a special diagram.

The artificial production of mesons, G. P. S. Occhialini, C. F. Powell, (Univ. of Bristol), *Nature* **161,** 551–552 (1948).

A review and discussion of the latest developments in meson research.

Apparent emission of positive electrons from β-emitters, C. B. A. McCusker (Univ. of Liverpool), *Nature* **161,** 564–565 (1948). The reported observations of positive particles emitted from β-emitters in numbers much greater than theoretically predicted can be explained on the basis that the observed tracks were from β-rays exhibiting multiple scattering.

Mass-spectrographic separation of isotopes of gaseous elements, J. Koch (Univ. of Copenhagen), *Nature* **161,** 566–567 (1948). By bombarding metallic disks with beams of ions of gaseous isotopes obtained from a high-intensity mass-spectrograph, it is possible to prepare targets containing the separated isotopes. The latter may be released from the target by means of high-frequency induction heating.

Height of meson formation, A Duperier (Imperial College of Science Tech., London), *Nature* **161,** 645 (1948). The bulk of mesons is generated at, or little above, the 7.5-cm mercury pressure-level at the height of the maximum of the Pfotzer curve for the intensity of the total radiation.

Chemical effects of ionizing radiations, G. Stein, J. Weiss (Univ. of Durham, Newcastle-upon-Tyne), *Nature* **161,** 650 (1948). By exposing aqueous solutions of benzene and benzoic acid to X-rays and neutron-γ-rays and isolating the products, it was shown that hydroxyl radicals are formed by the radiation.

NOTE: In addition to the papers abstracted above, NUCLEONICS readers may also find of interest the complete texts of the important papers presented at the Notre Dame Symposium on Radiation Chemistry and Photo Chemistry in *J. Phys. Colloid Chem.* **52,** 437–611 (1948). These papers were abstracted and briefly reported on in NUCLEONICS **1,** No. 2, 27–31 (1947).

. . . I. W. RUDERMAN

LIFE SCIENCE PUBLICATIONS

The amino acid composition of aldolase and D-glyceraldehyde phosphate dehydrogenase, S. Velick, E. Ronzoni (Dept. of Biological Chem., Washington Univ. School of Medicine, St. Louis), *J. Biol. Chem.* **173,** 627–639 (1948). A complete chemical and microbiological analysis of the amino acid composition of the two enzymes was made. The nitrogen of aldolase was accounted for within the limits of errors of the methods used by the 18 amino acids found in it. Similarly the nitrogen of D-glyceraldehyde phosphate dehydrogenase was accounted for by its amino acid and diphosphopyridine nucleotide content. The molecular weight of the dehydrogenase was calculated as a minimum of 99,000 and that of aldolase 140,000 from the five observed residue numbers.

The synthesis of fatty acids in adipose tissue in vitro, B. Shapiro, E. Wertheimer (Lab. for Pathological Physiology, The Hebrew Univ., Jerusalem), *J. Biol. Chem.* **173,** 725–728 (1948). Adipose tissue incubated *in vitro* in serum enriched with heavy water was found to introduce deuterium into its fatty acids. The introduction of deuterium in adipose tissue of rats on a diet accelerating fat synthesis in the body was greater.

The distribution and excretion of injected uranium, W. Neuman, R. Fleming, A. Dounce, J. Carlson, B. Mulryan (Div. of Pharmacology and Toxicology, Dept. of Radiology, School of Medicine and Dentistry, Univ. of Rochester, N. Y.), *J. Biol. Chem.* **173,** 737–748 (1948). The distribution and excretion of injected uranium by rabbits, rats and cats was studied. Approximately two-thirds of the dose was excreted quickly via the urine. Up to one-fifth of the dose was found in the skeleton from which it was mobilized slowly. Large initial concentrations were found in the kidney but they fell to a low level at the end of 40 days. All other tissues including blood contained very low quantities. Administration of alkali reduced the amount deposited in the kidney and increased the quantity found in the urine.

The requirements of the fatty acid oxidase complex of rat liver, A. Lehninger, E. Kennedy (Depts. of Surgery and Biochemistry, Univ. of Chicago, Ill.), *J. Biol. Chem.* **173,** 753–771 (1948). Washed particulate material separated from rat liver homogenized in isotonic salt solutions, washed with saline and suspended in water showed no activity in the oxidation of fatty acids when supplemented with ATP, Mg and phosphate buffer. However, suspending the material in saline in addition to the supplements named resulted in highly active

preparations. The fatty oxidase activity of the water suspension would be restored completely in the presence of phosphate buffer, Mg, ATP, cytochrome c, neutral salts, or certain nonelectrolytes such as sugar and small amounts of malate or oxalacetate. Using P^{32} as a tracer, the function of the inorganic phosphate was found to lay in its participation in coupled oxidative phosphorylation. The malate or oxalacetate initiated the oxidation of octanoate to the stage of the 2-carbon intermediate and caused the latter to enter into the Krebs cycle by forming tricarboxylic acid. The neutral salts are believed to reproduce an enzymatically active "flocculated" form of the enzyme from an inactive "dispersed" form.

Preparation of radioactive carbon-labeled sugars by photosynthesis, E. Putnam, W. Hassid, G. Krotkov, H. Barker (Div. of Plant Nutrition, Univ. of California, Berkeley), *J. Biol. Chem.* **173,** 785–795 (1948). A description of methods used in the isolation of starch, glucose, fructose, and sucrose containing C^{14} from plants exposed to an atmosphere of radioactive carbon dioxide in the presence of light.

The *in vitro* synthesis of heme in the human red blood cell of sickle cell anemia, I. London, D. Shemin, D. Rittenberg (Depts. of Medicine and Biochemistry, College of Physicians and Surgeons, New York), *J. Biol. Chem.* **173,** 797–798 (1948). Experiments indicate that blood from sickle cell anemia subjects synthesize hemin from glycine in vitro. No synthetic activity was found in other hematologic disorders such as hypochromic anemia, sickle cell trait, and conditions such as pernicious anemia and congenital hemolytic jaundice which have reticulocytex counts comparable to those found in sickle cell anemia. The components responsible for heme synthesis in sickle cell blood have not yet been determined.

The *in vitro* synthesis of heme from glycine by the nucleated red blood cell, D. Shemin, I. London, D. Rittenberg (Depts. of Biochemistry and Medicine, College of Physicians and Surgeons, New York), *J. Biol. Chem.* **173,** 799–800 (1948). The incubation of nucleated red blood cells of the duck in whole blood or saline with N^{15}-labeled glycine resulted in the formation of labeled heme.

Tracer experiments on the mechanism of glycine fermentation by diplococcus glycinophilus, H. Barker, B. Volcani, B. Cardon (Div. of Plant Nutrition, Univ. of California, Berkeley), *J. Biol. Chem.* **173,** 803–804 (1948). Glycine fermentations with C^{14}-labeled substrates revealed that approximately 75% of the methyl carbon and 54% of the carboxyl carbon of acetic acid are derived from the methylene carbon of glycine and from 90 to 95% of the carbon dioxide formed from the fermentation of glycine is derived from the carboxyl carbon of glycine, with the remainder coming from the methylene carbon. Possible mechanisms of the reactions are discussed.

The effect of pyruvate and insulin on fatty acid synthesis *in vitro,* K. Bloch, W. Kramer (Dept. of Biochemistry and Inst. of Radiobiology and Biophysics, Univ. of Chicago, Ill.), *J. Biol. Chem.* **173,** 811–812 (1948). The presence of pyruvate increased several fold the incorporation of acetate carbon into liver fatty acids. This was also true to a lesser extent of oxalacetate or glucose. Other dicarboxylic acids, *i.e.*, fumarate, malate and succinate, were without effect. Addition of insulin resulted in a further increase of fatty acid synthesis when the medium contained pyruvate, but had no effect when glucose was present. Insulin depressed the uptake of isotope by fatty acids when acetate was the only substrate. The experiments suggest that one of the roles of insulin involves generally the metabolism of pyruvate and more specifically the use of pyruvate in fatty acid synthesis.

Radioisotopes for local treatment of tumors, (No author given), *Lancet* **1,** 372–373 (1948). A brief review of the role of radioisotopes in the treatment of local tumors. The successful use of colloidal solutions of Au^{198} in the treatment of tumors, Hodgkins disease, lymphatic leukemia and squamous-cell carcinoma are discussed. Failures in some cases were ascribed to the lack of retention of the colloid by the tissues involved. Radioactive silver compounds are believed to be retained longer because of their cauterizing action.

Methods for labeling thyroxine with radioactive iodine, E. Frieden, M. Lipsett, R. Winzler (Depts. of Biochemistry and Nutrition, Univ. of Southern California School of Medicine, Los Angeles) *Science* **107,** 353–354 (1948). A number of syntheses of iodine-labeled

thyroxine are discussed. A convenient preparation of thyroxine with identical specific activity in all four positions is through the iodinization of certain tyrosine-containing proteins. Another method investigated by the authors, the exchange reaction, proved successful. It is not known which of the iodine atoms enter into the exchange reaction.

. . . BERNARD KANNER

PHYSICAL PUBLICATIONS

Low energy yield of $D(D,p)H^3$ and the angular distribution of the emitted protons, E. Bretscher, A. P. French, F. G. P. Seidl (Los Alamos Scientific Lab., N. Mex.), *Phys. Rev.* **73,** 815–821 (1948). A monoenergetic deuteron beam was directed onto a thick D_2O ice target, with its intensity monitored by the charge transferred to the target. The number of protons emitted from the target per unit time was counted as a function of the angle with the deuteron beam, using a proportional counter. The deuteron energy was varied from 15 to 105 kev. The distribution is found to be anisotropic even at very low energies. The total yield and cross section for the process are also measured as a function of energy. Errors vary from 4 to 8%.

Theoretical considerations concerning the $D + D$ reactions, E. J. Konopinski (Indiana Univ., Bloomington), E. Teller (Univ. of Chicago, Chicago, Ill.), *Phys. Rev.* **73,** 822–830 (1948). An explanation is proposed for the angular distribution $1 + A(E) \cos^2 \theta$ for $D + D$ reactions (θ is the angle between deuterons and protons in the center of mass system, and A, a function of energy, is the asymmetry coefficient). The large asymmetry at low energies is ascribed to the effects of P-waves (asymmetric) superposed on the isotropic effects of S-waves. The presence of a spin-orbit coupling which causes an isotropic contribution from P-waves would explain neutron emission distributions for much higher bombarding energies.

Radiations from molybdenum (99) and technetium (99), C. E. Mandeville, M. V. Scherb (Bartol Research Foundation, Franklin Inst., Swarthmore, Pa.), *Phys. Rev.* **73,** 848–852 (1948). Mo_2O_3 irradiated with Clinton pile neutrons shows a 67-hr activity. Mo^{99} emits two groups of beta rays, one of maximum energy 1.03 Mev, the other of low energy with an energy of 240 kev, and a range of 0.057 gm/cm² in Al. The low-energy betas are associated with a gamma ray. The maximum energy of the gamma radiation is 0.71 Mev. Tc^{99} has a 6-hr metastable state whose gamma radiation is highly converted, the electrons having a 0.022 gm/cm² range in Al. Disintegration schemes are proposed.

The penetration of gamma radiation through thick layers—I. Plane geometry, Klein-Nishina scattering, J. O. Hirschfelder, J. L. Magee, M. H. Hull (Los Alamos Scientific Lab., N. Mex.), *Phys. Rev.* **73,** 852–862 (1948). The Klein-Nishina (Compton) scattering of gamma rays incident perpendicularly on a thick target was calculated. The total intensity of penetrating radiation is given by the sum of the unscattered, singly scattered, and multiply scattered beams. The first two terms are exactly treated, the multiple scattering being approximated by assuming small angles of scattering and averaging the angles. Intensity of penetrating gamma-radiation as a function of target thickness for various incident energies (1, 3, and 5 Mev) is given.

The penetration of gamma radiation through thick layers—II. Plane geometry, iron and lead, J. O. Hirschfelder, E. N. Adams (Univ. of Wisconsin, Madison), *Phys. Rev.* **73,** 863–868 (1948). Pair formation and photoelectric effect calculations are included in the equations for multiple scattering of gamma rays. Calculations are made for passage through iron and lead of gamma-ray beams of 1, 3, and 5-Mev energy, and thicknesses corresponding to attenuation by 0.5, 0.1, 0.01, 0.001, and 10^{-6} for Fe, Pb, air, water, and concrete (for the last three, pair formation and photoelectric effects may be ignored). The distinction between the roentgen and the unit of flux is discussed with regard to shielding from gamma-ray dosages.

Sensitivity of proton-proton scattering to potentials at different distances, G. Breit, A. A. Broyles, M. H. Hull (Yale Univ., New Haven, Conn.), *Phys. Rev.* **73,** 869–876 (1948). Estimates are given concerning the relative usefulness of measurements at different energies for determining the proton-proton force in nonrelativistic approximation. They indicate it would be possible to detect interaction energies located at distances of the order of 10^{-13} cm by observations in the 200–500 kev range. The sensitivity is enhanced in this region by the

interference between the Coulomb and other potentials. The calculations were made on the basis of first-order perturbation theory for phase shifts.

A study of the breakup of Li^8, T. W. Bonner, J. E. Evans, C. W. Malich, J. R. Risser (Rice Inst., Houston, Texas), *Phys. Rev.* **73,** 885–890 (1948). Radioactive Li^8 atoms are introduced into a cloud chamber, and the breakup (into two α particles, an electron, and neutrino) studied by means of photographs in 426 cases. The α particles were emitted in directions ranging from opposite to each other to a 10 deg separation. The combined ranges were divided by two in order to obtain the range of one α particle; this was then converted into an energy distribution. No very-short-range α particles were found corresponding to a disintegration of Be^8 in the ground state; this agreed with the prediction, on the basis of selection rules, that such a nucleus would not be formed in this reaction. The energy of greatest probability is 3.3 Mev, and the half-width is about 1 Mev. Attempts are made to fit the data with various theoretical distributions.

The identification of the surplus gamma radiation from granite, V. F. Hess, J. D. Roll (Fordham Univ., New York), *Phys. Rev.* **73,** 916–918 (1948). A redetermination of the intensity of gamma radiation, as evidenced in the ionization produced, is described, and a new value of Eve's constant given. This is used to explain the excess radiation from granite.

Excitation function for proton-neutron reaction in lithium [$Li^7(p,n)$], J. E. Hill, W. E. Shoupp (Westinghouse Electric Corp., Pittsburgh, Pa.), *Phys. Rev.* **73,** 931–933 (1948). The yield of neutrons from thin films of lithium was measured as a function of the energy of bombarding protons. A BF_3 ionization chamber was used as neutron detector, and an electrostatic generator was used to provide protons of energies up to 3.2 Mev, with magnetic deflection used to avoid deuteron contamination. The excitation curve shows a definite threshold at 1.85 Mev, with resonances at 1.92, 2.28, and 3.06-Mev bombarding energy. The various competing reactions are discussed, and [$Li^7(p,n)$] is explained by excited energy levels in $_4Be^{8*}$ at 18.8, 19.1, 19.8 Mev, from which decomposition by neutron emission is possible. The reaction of decomposition has a Q value of -1.62 Mev.

Note on second Born approximation and proton-neutron and proton-proton scattering, Ta-You Wu (Columbia Univ., New York), *Phys. Rev.* **73,** 934–939 (1948). The scattered amplitude $f(\vartheta)$ is expressed as a series in powers of the interaction potential V, and carried out to the fourth power of V. The scattering at 100 Mev for n-p and p-p is calculated on the basis of a Gaussian well without tensor forces, for symmetrical, charged, and neutral theories. For symmetrical theory, these cross sections are 0.96×10^{-25} and 0.22×10^{-25} cm^2 (n-p and p-p). Their sum is 1.18, much closer to the observed deuteron scattering of protons (1.17) than the result given by either of the other theories.

Nuclear properties of 93^{237}, A. C. Wahl, G. T. Seaborg (Univ. of California, Berkeley), *Phys. Rev.* **73,** 940–941 (1948). U^{238} irradiated with fast neutrons undergoes a n, $2n$ reaction, producing U^{237}, which is beta-emitting with 6.8-day half-life. The daughter substance Np^{237} was chemically separated after a period of several months following the bombardment of U^{238} with the fast neutrons of a 15,000 microampere-hour deuteron bombardment of beryllium in a cyclotron, all U^{237} having decayed. Np^{237} decays with the emission of alpha particles (half-life about 3×10^6 years), and its cross section for slow neutron fission is less than 1% of that of U^{235}.

Shapes of nuclear induction signals, B. Jacobsohn, R. K. Wangsness (Stanford Univ., Stanford, Cal.), *Phys. Rev.* **73,** 942–946 (1948). For the case of weak r-f field, the analysis of signal shape is given, which allows the resonance value to be known to a limit of error smaller than the line width. For the case where the strong magnetic field is swept sinusoidally back and forth about resonance, numerical results are given for various sweep rates and relaxation times.

A photographic study of the neutron spectra from Al(αn) and Si(dn), R. A. Peck (Yale Univ., New Haven, Conn.), *Phys. Rev.* **73,** 947–955 (1948). Four neutron-yielding reactions were studied by the photographic-microscopic method of observation of recoil hydrogen nuclei originating within the photographic emulsion. Their range allows the calculation of their energy and hence of the energy of the neutrons. Histograms were plotted to show the energy distribution of the neutrons. Corrections must be made for the greater probability of a long track passing

out of the emulsion and being rejected, and for the energy dependence of the n-p cross section. The various groups of neutrons allow the identification of energy levels in the compound nuclei.

Search for a resonance absorption of neutrons in graphite, S. Bernstein (Clinton National Lab., Oak Ridge, Tenn.), *Phys. Rev.* **73,** 956–962 (1948). A Ra-Be photo-neutron source was surrounded by a graphite sphere, and this in turn by paraffin. The activities of thin indium foils were measured as a function of distance from the source with the graphite sphere removed and in place. From these distributions and the relative thermal neutron capture cross sections of paraffin and graphite, the number of neutrons absorbed by the graphite sphere was calculated. Results indicate that at most 5% of neutrons passing through a resonance level were absorbed by the 11-inch radius graphite sphere.

Slow neutron velocity spectrometer studies of Cu, Ni, Bi, Fe, Sn, and calcite, W. W. Havens, Jr., L. J. Rainwater, C. S. Wu, J. R. Dunning, (Columbia Univ., New York), *Phys. Rev.* **73,** 963–972 (1948). The cross sections of various substances were investigated. Resonance levels and $1/v$ lines were established. Bismuth was found to have a constant cross section (where crystal effects are unimportant) to within the accuracy of the experiment. The Tyndall Nicol Prism was used to measure the transmission of calcite. The cross section decreases from 20 barns in the energy region where the nuclei should scatter independently to about 3.5 in the region of 0.01 ev. The free Ca cross section is calculated as 4.1 barns. The transparency of crystalline materials to low-energy neutrons is explained, by application of the Bragg condition. The residual cross section is due to Ca capture (1.0 barns) and incoherent scattering (isotope, crystal, and most important, temperature effects).

Neutron-proton and proton-proton scattering at high energies, J. Ashkin (Univ. of Rochester, N. Y.), Ta-You Wu (Univ. of Michigan, Ann Arbor), *Phys. Rev.* **73,** 973–985 (1948). Using a square-well potential adjusted to fit the ground state of the deuteron and the low-energy n-p scattering, and taking account of tensor forces, calculations were made of the n-p and p-p scattering at 100 and 200 Mev. The Born approximation was used for ordinary, spatial exchange, and symmetric exchange forces. Exact calculation was also made for the latter. This shows that the Born approximation is poor at 100 Mev but not bad at 200. For symmetric forces, the n-p cross section disagrees with experimental results by a factor of 1.6, while the angular distribution ratio is in error by 3.

Elastic and inelastic scattering of 100- to 200-Mev protons or neutrons by deuterons, Ta-You Wu (Univ. of Michigan, Ann Arbor), J. Ashkin (Univ. of Rochester, N. Y.), *Phys. Rev.* **73,** 986–1001 (1948). Elastic and total cross sections were calculated on the basis of the Born approximation, including tensor forces but using a Gaussian potential well. The nucleon potentials used were ordinary, exchange, and symmetrical forces, which give, for p-d total cross sections at 100 Mev, 0.424, 0.212, 0.089×10^{-24} cm^2, as compared with an experimental value of 0.117×10^{-24} cm^2. Angular distribution of scattering at 100, 150, and 200 Mev was also calculated.

On the behavior of cross sections near thresholds, E. P. Wigner (Princeton Univ., Princeton, N. J.), *Phys. Rev.* **73,** 1002–1009 (1948). The energy dependence of the cross section for the formation of a product, in the vicinity of the threshold, is considered in general. The cross section is shown to be the same function of energy, regardless of the reaction mechanism and provided that the long-range interaction of product or reacting particles is the same. Energy dependence is derived for no interaction, Coulomb attraction, and Coulomb repulsion. Long-range interaction is found to mean one that does not go to zero faster than $1/r^2$. The general effect of small perturbations in the long-range interactions is discussed.

The production of nucleons by the cosmic radiation—II, S. A. Korff (New York Univ.), A. Cobas (Univ. of Puerto Rico, Rio Piedras), *Phys. Rev.* **73,** 1010–1014 (1948). Flights were made by balloons carrying BF_3 proportional counters to high altitudes (2-cm Hg). No maximum was found in the neutron counting rate. Surrounding the counters with lead produced little change; therefore neutrons do not depend for their production on heavy nuclei. Surrounding them with water increased neutron count only slightly because most of the neutrons were already slow. Use of cadmium shields showed that the neutrons reached the counter approximately isotropically. There was no pronounced diurnal effect.

Particle and quantum counters, D. R. Corson, R. R. Wilson (Cornell Univ., Ithaca, N. Y.), *Rev. Sci. Instr.* **19,** 207–233 (1948). A review is given of the operating mechanism and special properties of various types of counter in common use. The theory of operation, time resolution, methods of amplification, and construction and operation details are given for the ionization chamber. The inherent limit in gain because of noise is discussed. Proportional counters are introduced with a discussion of gas multiplication. The theory of Geiger counters is given in some detail, including the problems of random time lags, recovery time, and lifetime. Electron multipliers and the possible use of photo-multiplier with phosphors are discussed. Crystal counters are also reviewed, including pulse size and gamma-ray counting efficiency.

A magnetic-lens beta- and gamma-ray spectrometer, E. A. Quade, D. Halliday (Univ. of Pittsburgh, Pa.), *Rev. Sci. Instr.* **19,** 234–238 (1948). A magnetic lens spectrometer designed for the study of beta and gamma spectra is described. The construction of the chamber, lens coils, baffles, source, and detection system is given. The whole system can be aligned so as to reduce the effect of the earth's magnetic field. Measurements were made using an electron gun as source in order to determine the spherical aberration of the lens, which was minimized by proper coil arrangement. The effect of self-absorption in and local scattering near the source was tested with the internally converted gamma (0.67 Mev) from Cs^{137}. The effect on the resolution curve was noted. The ratio of the "pass band" interval of momentum to the electron momentum was about 0.8% at high resolution.

Directional counter for the determination of the complete azimuthal effect of primary cosmic radiation, A. Bafios, M. L. Perusquia (Univ. of California, Los Angeles, and National Univ. of Mexico, Mexico City), *Rev. Sci. Instr.* **19,** 239–243 (1948). An apparatus was constructed to record automatically the cosmic-ray intensity as a function of zenith and azimuthal angles. It consists of four sets of triple-coincidence counters mounted as telescopes at zenith angles of 0, 20, 40, and 60 deg, all of which are rotated through an azimuthal angle of 22.5 deg every 32 min. The coincidence circuit connects the Geiger counters in series, with a single amplifier. This decreases the circuit complexity but reduces the resolution of the instrument and decreases the stability. Three times the voltage is required. The automatic periodic rotation of the system is governed by sequence relays, and photographic units record the number of counts registered at various times.

A high resolution nuclear spectrometer, L. M. Langer, C. S. Cook (Indiana Univ., Bloomington), *Revs. Mod. Phys.* **19,** 257–262 (1948). By giving the magnetic field specified radial inhomogeneity, a double-focusing effect is achieved which makes the resolution 0.5% with a transmission of 0.1%, at a mean radius of curvature of 40 cm. Background and scattering effects from the instrument are negligible. The iron-core magnet is of annular ring type with the exciting coil wound on the central core. The sources are mounted on 0.02 mg/cm² of Zapon laid over a hole in a thin mica sheet, and are covered with another layer of Zapon. An end window G-M counter is used as the detector. The windows consist of five layers of 0.01 mg/cm² Zapon, supported on lucite and metal supporting grids. The counters are filled in place on the system, and the windows have stopping powers as low as 2.5 kev. Acceleration through the window may be used.
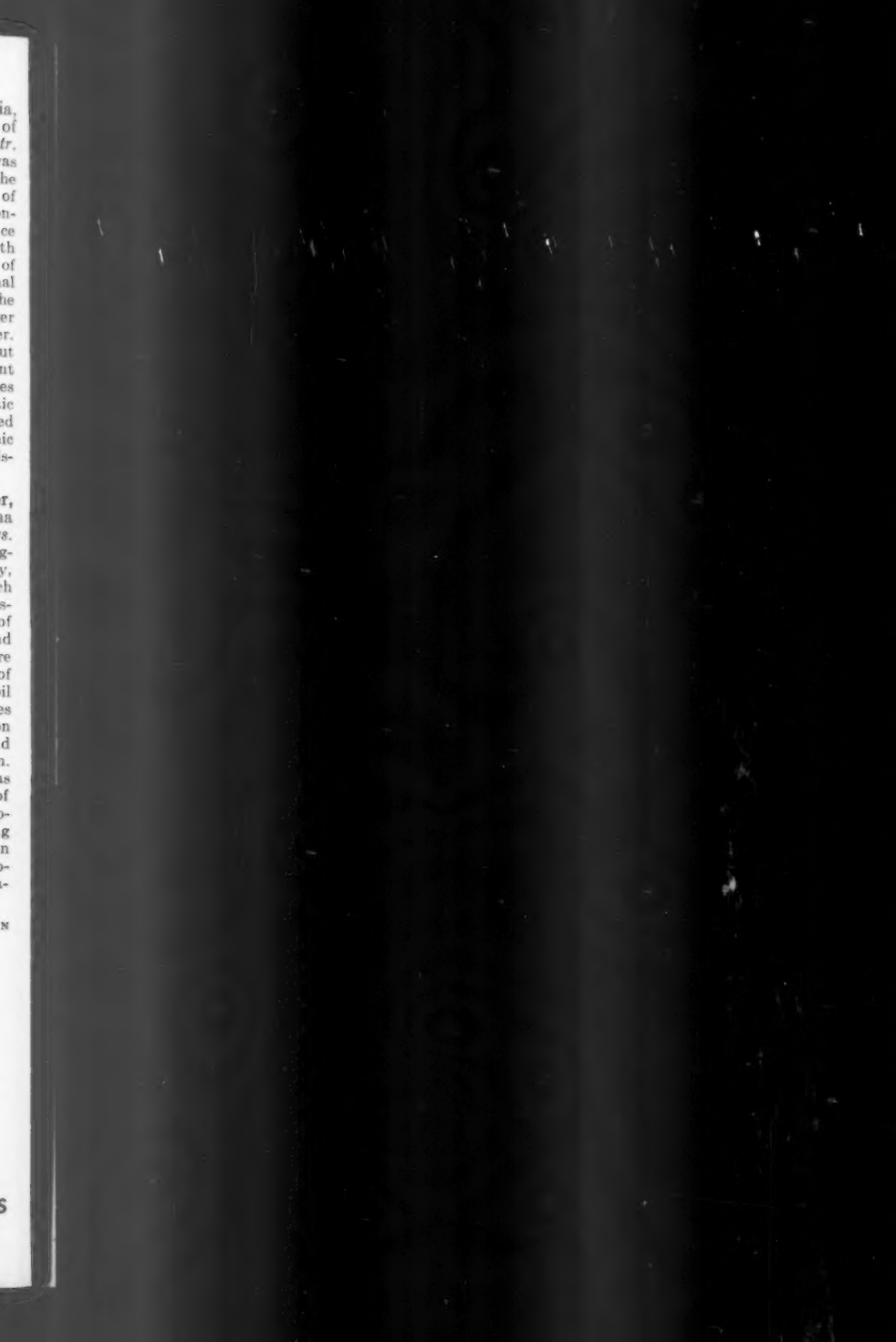
. . . HAROLD BROWN